DISCLAIMER

This report was prepared as an account of work sponsored by an agency of the United States Government. Neither the United States Government nor any agency thereof, nor any of their employees, makes any warranty, express or implied, or assumes any legal liability or responsibility for the accuracy, completeness, or usefulness of any information, apparatus, product, or process disclosed, or represents that its use would not infringe privately owned rights. Reference herein to any specific commercial product, process, or service by trade name, trademark, manufacturer, or otherwise does not necessarily constitute or imply its endorsement, recommendation, or favoring by the United States Government or any agency thereof. The views and opinions of authors expressed herein do not necessarily state or reflect those of the United States Government or any agency thereof. Reference herein to any social initiative (including but not limited to Diversity, Equity, and Inclusion (DEI); Community Benefits Plans (CBP); Justice 40; etc.) is made by the Author independent of any current requirement by the United States Government and does not constitute or imply endorsement, recommendation, or support by the United States Government or any agency thereof.

INL/RPT-23-72884-Revision-0

Engineering Scale Pyroprocessing Activities in the United States

December 2023

Guy L Fredrickson, Tae-Sic Yoo

Changing the World's Energy Future

Idaho National Laboratory

INL is a U.S. Department of Energy National Laboratory operated by Battelle Energy Alliance, LLC

INL/RPT-23-72884-Revision-0

Engineering Scale Pyroprocessing Activities in the United States

Guy L Fredrickson, Tae-Sic Yoo

December 2023

Idaho National Laboratory
Idaho Falls, Idaho 83415

http://www.inl.gov

Prepared for the
U.S. Department of Energy
Under DOE Idaho Operations Office
Contract DE-AC07-05ID14517

Technical Letter Report

[TLR-RES/DE/REB-2023-10]

Engineering Scale Pyroprocessing Activities in the United States

Date: December 2023

Prepared in response to Task 1 in the Research Assistance Request NMSS-2022-003, by:

Guy L. Fredrickson
INL

Tae-Sic Yoo
INL

NRC Project Managers:

W. Reed, R. Iyengar
Reactor Engineering Branch

Division of Engineering
Office of Nuclear Regulatory Research
U.S. Nuclear Regulatory Commission
Washington, DC 20555–0001

This report does not contain or imply legally binding requirements. Nor does this report establish or modify any regulatory guidance or positions of the U.S. Nuclear Regulatory Commission and is not binding on the Commission.

INL/RPT-23-03365

Engineering Scale Pyroprocessing Activities in the United States

December 2023

Task Order 31310022F0031 Report

Guy L. Fredrickson
Tae-Sic Yoo

Idaho National Laboratory

INL is a U.S. Department of Energy National Laboratory operated by Battelle Energy Alliance, LLC

Technical Letter Report

[TLR-RES/DE/REB-2023-10]

Engineering Scale Pyroprocessing Activities in the United States

Task Order 31310022F0031 Report

Guy L. Fredrickson
Tae-Sic Yoo

December 2023

Idaho National Laboratory
Idaho Falls, Idaho 83415

http://www.inl.gov

Prepared for the
Office of Nuclear Regulatory Research
U.S. Nuclear Regulatory Commission
Under U.S. Department of Energy Idaho Operations Office
Contract DE-AC07-05ID14517

Page intentionally left blank

ABSTRACT

This report summarizes the present state of pyroprocessing technologies for nuclear materials applications. The goal of pyroprocessing in this context is to reject fission products to waste streams, and retain actinides in product streams, as dictated by the requirements of the fuel cycle application. Pyroprocessing includes unit operations such as molten salt electrochemical cells for the conversion of oxides to metals, uranium electrorefining, and the recovery of transuranics. Flowsheets are included for pyroprocessing as applied to the Integral Fast Reactor (IFR), Spent Fuel Treatment (SFT), and Joint Fuel Cycle Study (JFCS) Programs performed at the INL. The flowsheets for covered pyroprocessing technologies included in this report may include steps such as salt distillation and metal casting operations.

Important distinctions between pyroprocessing and conventional aqueous reprocessing (such as the Plutonium Uranium Reduction Extraction process known as PUREX) have to do with the characteristics of the feed streams and recovered actinide products, in addition to practical considerations. Aqueous reprocessing recovers oxide products and has inherent advantages for the oxide-to-oxide fuel cycle. In contrast, pyroprocessing has inherent advantages for the metal-to-metal fuel cycle, and generates a smaller volume of waste. Some additional distinctions that separate pyroprocessing from aqueous processing that are discussed in this report include: lower technological maturity, greater importance for materials accountancy, the necessity to use hot cells, greater radiation accumulation, and different corrosion considerations.

There are unique safety considerations for pyroprocessing of irradiated nuclear materials in molten salt electrochemical cells, distillation furnaces, and casting furnaces. This report identifies and discusses pertinent safety topics, including materials control and accounting. Salt management is a key issue: salts must be processed to encapsulate the fission products, which accumulate over time, into acceptable waste forms.

This report also encompasses information about the status of pyroprocessing knowledge and the challenges that are currently being investigated for pyroprocessing commercialization, especially with regards to scaleup, automation, salt management, waste management, and nuclear materials accountancy. The report ends with a summary that includes recommendations for further assessment

Page intentionally left blank

EXECUTIVE SUMMARY

This report was prepared for the United States Nuclear Regulatory Commission (NRC) by the Idaho National Laboratory (INL). This report summarizes the present state of pyroprocessing technologies which include a family of different high-temperature unit operations that are selected, engineered, and organized into flowsheets that are designed for specific types of spent fuels and for specific fuel cycle requirements. Pyroprocessing is not one technology nor is it a technology that can be represented by a single flowsheet. The technologies and the flowsheets that can be brought to bear as pyroprocessing solutions for fuel cycle applications have many variants.

This report focuses on the technologies and flowsheets that have been realized at an engineering level in the United States. These include pyroprocessing as applied to the Integral Fast Reactor (IFR), Spent Fuel Treatment (SFT), and Joint Fuel Cycle Study (JFCS) Programs performed at the INL. The IFR Program was intended to demonstrate reprocessing using Experimental Breeder Reactor-II (EBR-II), but after much development was never realized. The SFT Program applies pyroprocessing to the recovery of uranium from EBR-II spent fuel (sodium-bonded metallic fast reactor fuel) for the purpose of dispositioning the spent fuel inventory and converting the high enriched uranium (HEU) into high assay low enriched uranium (HALEU). The JFCS Program applies pyroprocessing to the recovery of uranium/transuranic (U/TRU) alloys from light water reactor oxide fuels for the purpose of making sodium-bonded metallic fast reactor fuels. The IFR Program began in the mid-1980s and was terminated in 1994 coinciding with the closure of EBR-II. The SFT Program effectively began in 1996 and continues. The JFCS Program began in 2011 and continues.

After a brief introduction, this report provides technical descriptions of the flowsheets used for the IFR, SFT, and JFCS Programs. Subsequent sections provide information on technical fundamentals related to process chemistries, process challenges encountered through direct experience with pyroprocessing operations, and summaries of recent research literature on pyroprocessing technologies and facility safeguards.

In pyroprocessing, chemical separations largely take place in high-temperature molten salts. The oxide reduction (OR) cell is used to chemically convert oxide fuels to metals. The OR cell uses a salt that is lithium chloride (LiCl) with a nominal concentration of lithium oxide (Li_2O) at approximately 650°C. The electrorefining (ER) cell is used to electrorefine uranium metal and allow TRUs to accumulate in the ER salt. The ER cell uses a salt that is a eutectic mixture of LiCl and potassium chloride (KCl) with a nominal concentration of uranium trichloride (UCl_3) at approximately 500°C. In the OR cell, the alkali and alkaline earth fission products such as cesium and strontium accumulate in the salt as cesium chloride (CsCl) and strontium chloride ($SrCl_2$). In the ER cell, fission products that are alkali, alkaline earth, lanthanides, and TRUs accumulate in the salt as their metal chlorides. Because salt systems are used for chemical separations, salt management is the most important aspect of pyroprocessing because it dictates the management of actinides, fission products, and most of the process wastes.

The goal of pyroprocessing is to reject fission products to waste streams, and retain actinides in product streams, as dictated by the requirements of the fuel cycle application. Therefore, the management and recovery of TRUs from ER salts is another important aspect of pyroprocessing. TRUs can be recovered from the ER salts by chemical techniques that rely on selective reduction of the actinide cations from the salts. TRUs are generally recovered as U/TRU alloys with compositions that are desired for the fabrication of fast reactor metallic fuels, although many other fuel cycle applications are possible. By selective chemistry, it is possible to recover actinides from ER salts while leaving most of the alkali, alkaline earth, and lanthanide fission products in the salts. With the actinides effectively removed from the ER salts and with further selective chemistry, it is possible to recover most of the remaining fission products from ER salts for the purpose of concentrating the fission products into a waste stream. There are many technical approaches to salt management strategies for recovering TRUs from salt, drawing

down actinides from the salt, and drawing down fission products from the salt. Much of the current research is focused on these strategies.

Unique safety considerations of pyroprocessing stem from factors associated with processing of irradiated nuclear materials in high-temperature operations that include molten salt electrochemical cells, distillation furnaces, and casting furnaces. This report identifies and discusses pertinent safety issues. Brief highlights are provided below.

Technology Maturity: Aqueous reprocessing technologies are vastly more developed than pyroprocessing technologies. Pyroprocessing has not been developed past the engineering scale as exemplified in the SFT Program. In comparison, aqueous reprocessing has been used for military applications in the United States and for military and commercial applications in several other countries.

Materials Accountancy: Inventory tracking of nuclear materials is important with respect to safeguards but is also important with respect to operations control and criticality safety. This is achieved through a combination of facility design and process monitoring techniques that are unlike those involved in aqueous reprocessing. Pyroprocessing is required to track nuclear materials in many forms, including spent fuels, molten salts, molten metals, casting drosses, anode residue, and holdup in process equipment.

Deliquescence and Pyrophoricity: A generally accepted design feature for pyroprocessing facilities is that the high-temperature processes are contained within hot cells with dry argon atmospheres. This is because the salts and metals used by the process are reactive with the oxygen and moisture in the air. The hot cell facilities provide the necessary radiation containment and shielding required to work with spent nuclear fuels.

Radiation Accumulation: Most of the radiation emanating from spent fuel comes from the decay of fission products. A consequence of minimizing the volume of waste streams is that these fission products are concentrated into small volumes of metal and salt wastes. Very high radiation and decay heat levels can develop in the OR and ER vessels as fission products accumulate in these salts.

Corrosion Damage: Pyroprocessing as explained here uses chloride salts. Oxygen gas, $O_2(g)$, and chlorine gas, $Cl_2(g)$, are highly reactive gases. The OR cell liberates $O_2(g)$ at the anode, which will cause corrosion of the metal components if not managed properly. The chlorine chemical potential, related to the presence of $Cl_2(g)$, is very low in the OR and ER cells and corrosion of the metal components is mitigated. Some of the proposed means of managing salt wastes include dehalogenization of the salt to liberate the chlorine as $Cl_2(g)$ or hydrogen chloride, HCl(g), and to chemically convert the fission product metals into geologically stable mineral forms. In these processes, the management of the liberated $Cl_2(g)$ and HCl(g) will present engineering challenges with respect to corrosion and the fate of these materials. Similar challenges are related to the chlorination processes that are proposed for salt management.

Process Interruptions: Loss of electrical power to the process equipment is inevitable. The high temperature operations involving molten salts and molten metals must be able to withstand and recover from power outages. In an industrial reprocessing application, OR and ER cells can each potentially contain on the order of 1 MT of salt or more. The equipment must be designed to withstand the mechanical stresses caused by salt solidification and remelting. Similar design considerations will need to be made for the distillation and casting furnace operations.

Studies on molten salt chemistries for nuclear applications date back to the 1940s with work on Molten Salt Aircraft Reactors at Oak Ridge National Laboratory (ORNL), the 1950s with work on the Salt Cycle Process at Hanford, the 1960s with work on the Molten Salt Reactor Experiment at ORNL, and the 1980s with work on the IFR Program at Argonne National Laboratory and Argonne National Laboratory – West (now INL). Pyroprocessing research has been ongoing since the inception of the IFR Program in the United States and other countries including Republic of Korea, Japan, France, United Kingdom, India, China, and Russia.

The most recent pyroprocessing research includes studies related to the many aspects of salt management because this is a key issue for pyroprocessing. As fission products accumulate in the OR and ER salts, the salts must be processed to place the fission products into acceptable waste forms. These processes include actinide drawdown to retain the actinides in the fuel cycle, fission product drawdown to minimize the volume of waste, and chemical conversions of the fission product chlorides into forms that are geologically more stable such as oxides, phosphates, carbonates, and sulfides. Other research includes engineering operations, safeguards, and process monitoring.

Page intentionally left blank

CONTENTS

ABSTRACT iii
EXECUTIVE SUMMARY v
ACRONYMS xiii
1. INTRODUCTION 1
1.1 Scale of Pyroprocessing Operations 2
1.2 Sensitive Nuclear Technology 2
2. DESCRIPTION OF PYROPROCESSING 3
2.1 Fuel Characteristics 3
2.2 SFR Fuels Processing (EBR-II Example) 5
2.3 LWR Fuels Processing (JFCS Example) 11
2.4 Product and Waste Materials Characterizations 13
2.5 Process Flowsheets 17
3. TECHNICAL FUNDAMENTALS 21
3.1 Separations Chemistries 21
3.2 Thermodynamic Limitations to Separations Chemistries 22
3.3 Exchange Current Density 22
3.4 Chlorination Chemistry 23
3.5 Distillation Chemistry 23
3.6 Cadmium Pool in the EBR-II Driver Fuel Electrorefiner 23
3.7 Fission Product Radiochemistry 24
3.8 Consequences of Process Efficiency 27
4. PYROPROCESSING PROCESS CHALLENGES AND ATTRIBUTES 32
4.1 Input Accountancy 32
4.2 Materials Control and Accountancy 32
4.3 Salt Homogeneity and Sampling 32
4.4 Oxide Reduction 33
4.5 Different Fuel Types 33
4.6 Process Wastes 34
4.7 Corrosion 34
4.8 Reference Electrodes 35
4.9 Process Equipment Scaleup 35
4.10 Planar Electrode and Scraped Cathode Designs 36
4.11 Manual versus Automated Process Operations 38

4.12 Process Equipment Holdup 38
4.13 Material At Risk 38
4.14 Hydrogen Release 40
4.15 Decay Heat Load 40
4.16 Criticality Limits 41
4.17 Service Life of OR and ER Salts 41
4.18 Loss of Power Event 42
4.19 Exposure of Salts to Oxygen and Moisture 42
4.20 Casting Crucible Failure 44
4.21 Furnace Overtemperature 44
4.22 Loss of Process Signals 45
4.23 Radiation Damage and Dry Argon 46
4.24 Excessing Equipment from Hot Cells 46
4.25 Emissions from Hot Cells 47
4.26 Fuel Fabrication 47
4.27 Molten Salt Reactors 47
4.28 Resources Required for Pyroprocessing Research 48
5. SUMMARY OF RECENT R&D PUBLISHED IN THE OPEN LITERATURE 49
5.1 Review Papers 49
5.2 Salt Management 49
5.3 Oxide Reduction 57
5.4 Chemical Decladding 58
5.5 Uranium Electrorefining 58
5.6 Chlorination Chemistries 59
5.7 Reprocessing Facility Investigations 59
6. PYROPROCESSING FACILITY SAFEGUARDS 60
6.1 Safeguards Challenges and Opportunities 60
6.2 Input Accountancy 63
6.3 Output Accountancy 64
6.4 In-Process Material Accountancy 65
6.5 Accountancy Tools 65
6.6 Inventory Resetting 66
6.7 Applicable Measurement Technologies Review 67
6.7.1 Low Latency Measurement Technologies 67
6.7.2 High Latency Measurement Technologies 70

6.8 Summary and Recommendations 72
7. ACKNOWLEDGEMENTS 77
8. AUTHORS 78
9. REFERENCES 79

FIGURES

Figure 1. Schematic flowsheet of the IFR Program driver fuel processing. 17
Figure 2. Schematic flowsheet of the IFR Program blanket processing. 17
Figure 3. Schematic flowsheet of the IFR Program TRU recovery from blanket processing. 18
Figure 4. Schematic flowsheet of the IFR Program TRU recovery from driver fuel processing. 18
Figure 5. Schematic flowsheet of the SFT Program. 19
Figure 6. Schematic flowsheet of the JFCS Program. 19
Figure 7. Illustration of an integrated fuel reprocessing scheme. 27
Figure 8. Process model for actinide retention. 28
Figure 9. Relationship between burnup, reprocessing recovery, and fissile losses 29
Figure 10. Process model for lanthanide rejection. 29
Figure 11. Conceptual electrorefiner with planar anode baskets and scaped cathodes. 37
Figure 12. From left to right, photographs of an anode basket, bare cathode mandrel, and cathode mandrel with electrorefined uranium deposit. 37
Figure 13. EBR-II driver fuel cooling curve. 41
Figure 14. Photographs of LiCl-KCl-UCl_3 salt before (left) and after (right) exposure to air at 500°C. 43
Figure 15. Photographs of LiCl-KCl salt before (left) and after (right) exposure to air at 32°C. 44

TABLES

Table 1. Comparison Between Characteristics of SFR and LWR Fuels. 4
Table 2. Comparison Between Pyroprocessing Unit Operations of SFR and LWR Fuels. 7
Table 3. Comparison Between Pyroprocessing Wastes of SFR and LWR Fuels. 16
Table 4. Primary Fission Fragments Pairs of Uranium 25
Table 5. Results of Actinide Model 29
Table 6. Results of lanthanide model. 30
Table 7. Summary of the Materials Contributing to “Material at Risk.” 38
Table 10. Summary of Recent Review Papers 49
Table 11. Summary of Research on Reactive Metal Electrodes. 50

Table 12. Summary of Research on Reactive Metal Drawdown. 53
Table 13. Summary of Research on Precipitation-Based Drawdown for Salt Wastes..... 53
Table 14. Summary of Research on Salt Purification by Crystallization..... 56
Table 15. Summary of Research on Oxide Reduction..... 57
Table 16. Summary of Research on Chemical Decladding of Zirconium-Clad Fuels..... 58
Table 17. Summary of Research on Uranium Electrorefining..... 58
Table 18. Summary of Research on Chlorination of Actinides 59
Table 19. Summary of Research on Reprocessing Facility Considerations 59
Table 20. List of prospective measurement technologies applicable to pyroprocessing facilities..... 65
Table 21. Summary of low latency measurement technologies..... 69
Table 22. Summary of high (hour or more) latency measurement technologies. 72

ACRONYMS

A	Ampere
A	Mass Number, Number of Protons and Neutrons in Nucleus
ANI	Active Neutron Interrogation
ANL	Argonne National Laboratory
ANL-W	Argonne National Laboratory – West
ATR	Advanced Test Reactor
BEA	Battelle Energy Alliance
BWR	Boiling Water Reactor
CFR	Code of Federal Regulations
CMC	Closed Metal Confinement
CRADA	Cooperative Research and Development Agreement
d	Day
DC	Direct Current
DOE	Department of Energy
DU	Depleted Uranium
EBR-II	Experimental Breeder Reactor II
ER	Electrorefiner
FCF	Fuel Conditioning Facility (later name)
FCF	Fuel Cycle Facility (earlier name)
FFTF	Fast Flux Test Facility
g	Gram
HEPA	High Efficiency Particulate Air
HEU	High Enriched Uranium
HFEF	Hot Fuel Examination Facility
HKED	Hybrid K-Edge Densitometry
HP	Health Physicist
hr	Hour
HRA	Hot Repair Area
IAEA	International Atomic Energy Agency
ICP	Inductively Coupled Plasma
IFR	Integral Fast Reactor
INL	Idaho National Laboratory
IR	Infrared

JFCS	Joint Fuel Cycle Study
KED	K-Edge Densitometry
kg	Kilogram
kJ	Kilojoules
kV	Kilovolts
LCC	Liquid Cadmium Cathode
LIBS	Laser-Induced Breakdown Spectroscopy
LWR	Light Water Reactor
MC&A	Materials Control and Accountancy
m	Meter
mm	Millimeter
MOX	Mixed Oxide
MPACT	Materials Protection, Accountancy, and Control Technologies
MS	Mass Spectroscopy
MT	Metric Ton
MTG System	Mass Tracking System
MWe	Megawatt Electrical
MWt	Megawatt Thermal
NRC	Nuclear Regulatory Commission
NTT	Nuclear Technology Transfer
OES	Optical Emission Spectroscopy
OR	Oxide Reduction
ORNL	Oak Ridge National Laboratory
PIE	Post Irradiation Examination
ppm	Parts Per Million
PWR	Pressurized Water Reactor
RCRA	Resource Conservation and Recovery Act
RE	Reference Electrode
RIAR	Russian Institute of Atomic Reactors
ROK	Republic of Korea
SERA	Suited Entry Repair Area
SFR	Sodium Fast Reactor
wt%	Weight Percent
SFT	Spent Fuel Treatment
TES	Transition-Edge Sensor

TIMS	Thermal Ionization Mass Spectrometry
TRU	Transuranic
UV	Ultraviolet
V	Volts
Vis	Visible
W	Watts
WWS	Water Wash Station
XRF	X-Ray Fluorescence
y	Year
Z	Atomic Number, Number of Protons in Nucleus

Page intentionally left blank

Engineering Scale Pyroprocessing Activities in the United States

1. INTRODUCTION

This report discusses pyroprocessing technologies as applied to two types of spent nuclear fuel for the purpose of reprocessing. The two types of fuel are sodium-bonded, metallic, uranium fuel for sodium-cooled fast reactors (SFRs) and uranium oxide fuel for light water reactors (LWRs). These two fuel types were chosen because they are likely to be among the first applications of pyroprocessing, and significant research has been performed in these areas in the US. The prior Experimental Breeder Reactor II (EBR-II) Integral Fast Reactor (IFR) Program and the present EBR-II Spent Fuel Treatment (SFT) Program will serve as case studies to describe pyroprocessing of SFR fuels. The recent collaborative project between the US and the Republic of Korea (ROK) on the Joint Fuel Cycle Study (JFCS) Program will serve as the case study to describe pyroprocessing of LWR fuels.

The goal of the IFR Program was to demonstrate a closed fuel cycle around EBR-II using electrometallurgical methods. In anticipation of the IFR Program, EBR-II fuel was converted from an alloy of high enriched uranium (HEU) with 5 wt% fissium, to an alloy of HEU with 10 wt% zirconium (Zr). Fissium itself was an alloy of transition metals between yttrium (Y) and palladium (Pd) that was developed for an earlier reprocessing technology called the "*Melt Refining Process"* that was demonstrated on EBR-II in the 1960s. Under the IFR Program, the spent U-10Zr fuel was to be reprocessed to make fresh U-10Zr fuel. However, as reprocessing continued, transuranics (TRU) would have accumulated in the electrorefiner salt. Ultimately, the TRU would have been recovered to make an alloy of depleted uranium (DU) with 20 wt% TRU and 10 wt% Zr (example nominal fuel composition), which would have been tested in EBR-II. However, EBR-II was shut down while the equipment and hot cell for the IFR Program were still being prepared. Shut down occurred in 1994 about a year before the IFR Program could begin the reprocessing efforts. Consequently, the IFR Program was terminated, and the mission transitioned into the SFT Program to deal with the entire EBR-II spent fuel inventory including driver fuels (containing HEU) and blanket materials (containing DU). Therefore, the pyroprocessing technologies described here were never used to reprocess fuels while EBR-II was operational. However, these technologies have been extensively used to treat spent EBR-II fuels for disposition. The differences between pyroprocessing as applied to reprocessing, and pyroprocessing as applied to disposition will be discussed.

Under the JFCS, the purpose of reprocessing was to recover TRU from LWR fuels to make SFR fuels. Pyroprocessing technologies to this end were demonstrated at the kilogram-scale, and the recovered plutonium was used to fabricate fuel test specimens that were irradiated in the INL Advanced Test Reactor (ATR) and subsequently subject to post irradiation examination and characterization. The fuel test specimens were comprised of sodium-bonded DU/TRU/Zr ternary alloys. In this application of pyroprocessing, the spent LWR fuel was simply the source of TRU available to the ROK to make these SFR ternary fuels. Presently, the ROK has about 24 LWRs in service. The implementation of SFRs in the ROK is a future prospect.

The IFR Program and the subsequent SFT Program were initiated at ANL-W, which became INL MFC after a site-wide contract change in 2005. ANL-W was managed by the University of Chicago, while INL Materials and Fuels Complex (MFC) is now managed by Battelle Energy Alliance (BEA). Following the termination of the IFR Program in 1994, the mission entered a technology assessment period that lasted until 1996, at which time electrometallurgical processing was demonstrated and ultimately selected as the spent fuel treatment technology as recorded by a Federal Registry Record of Decision in 2000. That marked the beginning of the SFT Program which continues today. Likewise, the JFCS began in 2011. In the discussions that follow, the IFR Program is described in past tense, and the SFT and JFCS Programs are described in the present tense.

1.1 Scale of Pyroprocessing Operations

By commercial standards, EBR-II was a small experimental reactor that operated at 62 MWt and 20 MWe. As already explained, no EBR-II fuel was reprocessed under the IFR Program. When EBR-II was shut down in 1994, the spent fuel inventory included about 3 MT of driver fuel and 22 MT of blanket. To date, between 1996 and 2023, the SFT Program has treated about 1.6 MT of EBR-II driver fuel, 0.2 MT of Fast Flux Test Facility (FFTF) Reactor driver fuel, and 3.7 MT of EBR-II blanket. In comparison, the JFCS Program processed a total of about 26 kg of spent oxide fuel in nine experimental runs. Out of necessity JFCS Program used oxide fuels that were available for the program, which included mixed oxide (MOX) fuel from the FFTF Reactor, and some LWR oxide fuels from the Belgian Reactor 3 and the Dresden Unit 1 Reactor.

Aqueous processing technologies have been deployed at enormous industrial scales in support of plutonium production and commercial fuel reprocessing. By comparison, the body of work performed on pyroprocessing development is dwarfed by what has been accomplished on aqueous reprocessing.

1.2 Sensitive Nuclear Technology

Nuclear fuel reprocessing technologies are considered sensitive nuclear technologies by the Department of Energy (DOE). Pyroprocessing is clearly a reprocessing technology as it involves the separation, concentration, and purification of actinide metals from spent nuclear fuels. Much has been published in the open literature on pyroprocessing for the IFR and SFT Programs. Much of what has been published on these programs would, by today's standards of export control and nonproliferation, not be permitted to be published. This is particularly the case with regard to technical descriptions of the engineering-scale equipment and operating parameters. The collaboration between the US and the ROK on the JFCS Program was performed under a Cooperative Research and Development Agreement (CRADA) and a Bilateral Nuclear Technology Transfer (NTT) Agreement. Within the JFCS Program, in general terms, information related to oxide reduction operations is considered less sensitive than information related to electrorefining operations. Consequently, few publications related to the JFCS Program appear in the open literature.

2. DESCRIPTION OF PYROPROCESSING

All reprocessing flowsheets are concerned with chemical separations between what is desired to be retained in the fuel cycle, and what is desired to be rejected from the fuel cycle. Reprocessing deals only with chemical and physical separations, not isotopic separations. The most fundamental way to understand the behavior of a particular reprocessing flowsheet is to understand the mass and energy balance throughout the entire process. The guiding principles of mass and energy balances are straight forward, in that the masses of all materials into and out of the flowsheet, along with the thermal energies associated with chemical reactions and thermal management, must be accounted for and balance. In addition, radiochemical processes that alter the isotopic compositions and introduce energy must also be accounted for and balanced. However, in practice performing a detailed mass and energy balance is a complex task.

A fictitious perfect reprocessing technology would be able to accept any spent nuclear fuel and break it down into its individual elements with perfect separations. These elements could then be binned into three categories: non-radiological elements that are easily disposed of or recycled, radiological elements whose disposition must be managed, and actinide elements retained in the fuel cycle. The second category is the actual nuclear waste, and this perfect reprocessing technology would produce the absolute minimum amount of nuclear waste. However, such perfect separations are never possible in practice. In practice, all three categories become partitioned throughout the process and waste volumes increase as chemical reagents and equipment are consumed and radiological contaminations are spread.

A way of considering separation efficiencies during reprocessing is to determine, for each element present in the spent nuclear fuel, what fractions report to the refined actinide products and what fractions report to each individual waste streams. In this context, it is desired to have a high retention of actinides in to, and a high rejection of fission products out of, the refined actinide products. However, a general rule of separations is that purity decreases as recovery increases. A consequence of this rule is, for example, as higher fractions of the actinides are retained in the refined products, so too are higher fractions of the unwanted fission products. A balance must be struck between the competing factors influencing the practicality and economics of the process.

A reprocessing facility based on pyroprocessing technologies will be comprised of several unit operations that are scaled and duplicated as needed to meet the throughput requirements of the facility. The number and engineering details of the unit operations are based on the performance requirements of the facility. For the moment, the performance requirements will be limited to the type of spent fuel to be processed (LEU oxide fuel and HEU metallic fuel), the throughput rate of the facility (equipment scaling and duplication), and the specifications of the refined nuclear materials (electrorefined, metallic uranium and uranium/TRU alloy).

2.1 Fuel Characteristics

A comparison of the characteristics of metallic SFR and oxide LWR fuels is summarized in Table 1. The SFR fuel is comprised of a metallic alloy clad in stainless steel, along with bond sodium which provides improved thermal conductivity between the fuel alloy, where the heat is generated, and the cladding. The core of the reactor is comprised of an array of hexagonal assemblies containing individual fuel elements, blanket elements (in breeder reactors), and control elements (neutron absorbers). As a fast reactor, the neutrons are unmoderated as there is no water or graphite in the core. The hexagonal assemblies are made of stainless steel and, in addition to containing the elements, act as fluid ducts to channel the flow of sodium through the inside and outside of the assemblies. In a pool-type SFR, a large reservoir of primary sodium is circulated through the core. The primary sodium loop then flows through heat exchangers with the secondary sodium loop that is used to make the steam. Assemblies removed from the SFR are removed from a pool of primary sodium and must be washed prior to disassembly. Washing is performed with steam or a mixture of water and alcohol to control what is otherwise a vigorous reaction between water and sodium. Because both the bond sodium and the fuel alloys are highly reactive with water, spent SFR fuels are typically not stored in water pools for cooldown.

Table 1. Comparison Between Characteristics of SFR and LWR Fuels.

Feature	Fuel Type	
	SFR	LWR
Fuel Composition	HEU/Zr or DU/Pu/Zr metallic alloy. Bond sodium present.	$LEUO_2$ or $LEUO_2/PuO_2$ ceramic pellets.
Fuel Element Cladding	Stainless steel alloy.	Zirconium alloy.
Fuel Geometry	Fuel elements are loaded into enclosed-duct hexagonal assemblies made for sodium circulation.	Fuel elements are loaded into open square assemblies made for water circulation.
Fuel Assembly Hardware	Stainless steel alloy.	Stainless steel alloy.
Fuel Assembly Exposure	Submerged in a pool of sodium.	Submerged in a pool of water.
Spent Fuel Cleaning	Upon removal from the reactor the fuel assemblies are washed to remove external sodium.	N/A
Spent Fuel Storage	Dry storage only. Risk of bond sodium exposure too great for wet storage.	Wet or dry storage possible.

The LWR fuel is comprised of ceramic fuel pellets clad in a zirconium alloy, along with stainless steel hardware, such as springs and plates, to maintain compaction of the fuel pellets. There is no bond sodium in LWR oxide fuel elements, and thermal conduction is reliant on a tight fit between the fuel pellets and the cladding. The core of the reactor is comprised of an array of square assemblies containing individual fuel elements or control elements. As a thermal reactor, the neutrons are moderated by the cooling water circulating through the core. The assemblies are made of stainless steel and, in addition to containing the elements, are open to allow the flow of water around the fuel elements. In both the pressurized water reactor (PWR) and the boiling water reactor (BWR) a reservoir of water is circulated through the core. The PWR design has three water systems: primary, secondary (which makes the steam), and condenser coolant (which cools the steam). The BWR design has two water systems: primary (which makes the steam) and condenser coolant (which cools the steam). In the case of a PWR design, there are two heat exchanges between the primary and secondary, and secondary and coolant waters. In the case of a BWR, there is one heat exchanger between the primary and the coolant waters. Assemblies removed from the LWR are removed from a pool of water and no washing is required prior to disassembly. Spent LWR fuels are stored in water pools (when the decay heat is high), or dry storage (when the decay heat is low).

A comparison of the unit operations and materials handling characteristics of pyroprocessing SFR and LWR fuels is summarized in Table 11. In aqueous reprocessing, the entire fuel assemblies (including the stainless-steel hardware, cladding, and spent fuel) are mechanically shredded and digested in concentrated nitric acid and the solution is transferred into an input accountancy tank. Input accountancies of the various metals are determined based on the volume, density, and concentrations of the solution in the tank. This type of input accountancy is not possible with pyroprocessing, and this topic is discussed in greater detail later in Sections 4.2 and 6.2.

Pyroprocessing flowsheets begin with the recovery of the fuel elements by mechanical disassembly of the fuel assemblies. This involves cutting operations to free the fuel elements from the assemblies. Care is taken to not breach the cladding of the fuel elements during disassembly operations. The assembly hardware is mostly stainless steel that has become activated in the reactor core. Assembly hardware is advanced to waste processing (see Table 2, *Waste Metals Consolidation of Assembly Hardware*). Since bond sodium and metal fuels are highly reactive in air, all subsequent operations involving the metallic SFR fuels are performed in a dry argon atmosphere. The processes for metallic SFR fuels and LWR fuels are discussed in subsequent subsections.

2.2 SFR Fuels Processing (EBR-II Example)

Each fuel element is chopped through the length of the fuel region. The lengths of the chopped pieces are approximately equal to the diameter of the fuel element, about 6 to 7 mm. The purpose of chopping is to expose the bond sodium and metallic fuel for the subsequent uranium electrorefining operation. The bond sodium and fuel must be exposed to the electrolyte for the separations chemistry to occur. The chopped fuel is loaded into an anode basket that is advanced to electrorefining (see Table 3, *Uranium Electrorefining*). Pyroprocessing unit operations and materials handling operations are inherently batch operations. The batch sizes may be limited by criticality constraints related to the fissile materials inventories, which are largely uranium and plutonium. In the case of EBR-II fuels, where the ^{235}U enrichment is around 65%, the total actinide mass loaded into the anode basket is limited to 15 kg.

Under the current practice, the plenum regions of the fuel elements are not chopped and are segregated separately. These plenums contain some fraction of the bond sodium, and some fraction of the alkali (Group 1) and alkaline earth (Group 2) fission products that have solubilities in the bond sodium. Plenums are advanced to waste processing (see Table 4, *Waste Metal Consolidation of SFR Plenums*).

The electrorefiner (ER) is an electrochemical cell with an electrolyte comprised of LiCl-KCl eutectic (55.8 wt% KCl and 44.2 wt% LiCl), with a nominal concentration of 5 wt% UCl_3. The operating temperature is 500°C, ensuring a molten salt phase with a negligible vapor pressure. The formation of high valence uranium chloride such as UCl_4 is chemically suppressed because the salt is continuously exposed to uranium metal. The refining of uranium is driven electrochemically by an external DC power supply. Uranium is oxidized from the "impure" spent fuel in the anode basket, and "purified" uranium is reduced onto a cathode mandrel. The purified uranium deposits with a highly dendritic morphology exhibiting a high surface area. The rate at which uranium is transferred from the anode basket, through the salt, to the cathode mandrel is governed by the DC amperage applied to the circuit by the power supply. A current of 100 A, applied for 1 hr (100 A-hr of charge) will move approximately 300 g of uranium. This is merely an expression of Faraday's Law.

In an electrochemical cell, oxidation always occurs at the anode, and reduction always occurs at the cathode. In a Galvanic cell, e.g., a common battery, the electrochemical reactions are spontaneous, and the anode has a lower potential than the cathode. In an electrolytic cell, e.g., uranium electrorefining, the electrochemical reactions are driven by an external power supply, and the cathode has a lower potential than the anode. Nevertheless, oxidation always occurs at the anode and reduction always occurs at the cathode.

$$Oxidation\ occurs\ at\ the\ anode: U = U^{3+} + 3e^-$$

$$The\ cations\ (U^{3+})\ migrate\ through\ the\ salt\ from\ the\ anode\ to\ the\ cathode.$$

$$The\ electrons\ (e^-)\ flow\ through\ the\ electrical\ circuit\ from\ the\ anode\ to\ the\ cathode.$$

$$Reduction\ occurs\ at\ the\ cathode: U^{3+} + 3e^- = U$$

Significant chemical separations occur in the ER. The spent fuels processed in the ER must be metallic. Uranium oxide does not electrorefine to uranium metal in the ER. Oxide fuels are first reduced to metals in the oxide reduction (OR) cell. All metals in spent fuel can form metal chlorides. However, each metal has a different affinity to form its chloride. In the ER salt, UCl_3 is the least stable metal chloride present under most normal operating conditions. Therefore, metals in the spent fuel that have higher affinities than uranium to form chlorides will accumulate in the molten salt at the expense of the UCl_3 concentration. The uranium thus lost from the salt will mostly deposit as a metal on the anode basket. The Group 1, Group 2, lanthanide, and transuranic metals have higher affinities than uranium to form chlorides and consequently accumulate in the ER salt. Conversely, the transition metals have lower affinities than uranium to form chlorides and consequently remain in the anode basket as metals.

To summarize, the metallic spent fuel in the anode basket is partitioned three ways. The uranium reports to the cathode as electrorefined uranium. The reactive metals with affinities greater than uranium to form chlorides accumulate in the ER salt, and the noble metals with affinities lower than uranium to form chlorides remain in the anode basket. As discussed earlier, these chemical separations are not perfect. For example, metals cannot be oxidized into the ER salt unless they are in contact with the ER salt. Simply stated, reactants must come together to react; the electrolyte cannot oxidize from the electrode what it cannot reach, and the electrode cannot reduce from the salt what it cannot reach. As pyroprocessing does not attempt to oxidize all anode materials, the result is incomplete recovery of actinides from the chopped fuel in the anode basket. Separations in the ER and the consequences of different fuel types are discussed in greater detail in Section 3.

In the present ER operations, about 14 kg of chopped fuel is loaded into the anode basket. To electrorefine this amount of uranium approximately five cathodes are harvested. The volume of 14 kg of chopped fuel is much less than the volume of 14 kg of dendritic electrorefined uranium. To harvest uranium, the cathode mandrel is removed from the ER, allowed to cool to ambient temperature, and the dendritic uranium is scraped off the mandrel into a process crucible. Meanwhile, a clean cathode mandrel is returned to the ER so electrorefining operations can continue. The electrorefined uranium is comprised of high surface area dendritic uranium deposits and adhering salt. Due to the high surface area of the dendritic uranium, typical recovered uranium deposits are about 11 wt% adhering ER salt. This composite material is then advanced to distillation (see Table 5, *ER Salt Distillation from Electrorefined Uranium*).

When no further uranium can reasonably be recovered from the anode basket, the anode basket is removed from the ER and the contents are emptied into a process crucible. When the fuel elements are chopped, the cladding pieces are called *"segments."* When an anode basket is emptied, the cladding pieces are called *"hulls."* The hulls are comprised of stainless-steel cladding, fuel residue (unoxidized metals from the spent fuel), and adhering salt. This material is then advanced to waste processing (see Table 6, *Waste Metal Consolidation of ER Anode Residue*).

Distillation furnaces for pyroprocessing are designed to distill salt from metal under vacuum conditions. The furnace may also be designed to melt the metal into a consolidated ingot. The process crucibles in distillation furnaces are held under a vacuum as the temperature is raised. The vapor pressure of ER salts becomes significant at temperatures above 800 to 1,000°C. Uranium melts at approximately 1,130°C, and stainless-steel alloys melt at approximately 1,550°C. The process crucible in the distillation furnace must be compatible with molten salt and, in the case of metal consolidation, must also be compatible with molten metal. For distillation furnaces with induction heating, successful process crucibles designs include graphite crucibles as the induction coupler, which are coated on the inside with castable liners. In the case of salt distillation and uranium consolidation, the crucible liner is zirconia. In the case of uranium consolidation without salt present, the crucible liner is yttria. And in the case of salt distillation in the presence of stainless-steel, the crucible liner is alumina. Eventually, these process crucibles reach the end of their service lives and become waste that is contaminated with remnants of the materials they processed. These types of process waste are discussed in greater detail in Sections 2.4 and 4.5. Alternatives to graphite crucibles lined with zirconia, yttria, and alumina is an ongoing research area.

The electrorefined uranium harvested from the cathode mandrel is loaded into a process crucible and advanced to distillation (see Table 7, *ER Salt Distillation from Electrorefined Uranium*) to distill the salt, which is returned to the ER, and the uranium dendrites are consolidated into an ingot. The uranium ingot from this distillation furnace is advanced to a casting furnace (see Table 8, *Uranium Metal Casting*) for remelting and sampling. Sampling is performed by drawing a sample of the well-mixed, molten uranium into a quartz tube where it solidifies. These *"pin samples"* are sent for destructive analysis where they are used to verify the enrichment of the electrorefined uranium ingots. The ingots produced by this second casting furnace are too large (>25 kg) to be accommodated by the presently anticipated downstream processing. Therefore, the ingots from the second casting furnace are advanced to a third casting furnace (see Table 9, *Uranium Metal Casting*) to recast the uranium into smaller shapes called "*reguli*" which are about 3 kg each. The anode residue harvested from the anode basket is loaded into a process crucible and advanced to waste processing (see Table 10, *Waste Metal Consolidation of ER Anode Residue*).

Table 11. Comparison Between Pyroprocessing Unit Operations of SFR and LWR Fuels.

Unit Operations and Materials Handling	Fuel Type	
	SFR (EBR-II Example)	LWR (JFCS Example)
Headend Fuel Preparation for Electrochemical Operations	Fuel elements are removed from assemblies. Assemblies are advanced to waste metal consolidation.	Fuel elements are removed from assemblies. Assemblies are advanced to waste metal consolidation.
	Inert atmosphere required for all subsequent operations.	N/A
	N/A	Fuel is declad, and oxide fuel and cladding are separated from each other.
	N/A	Cladding is advanced to waste metal consolidation.
	Cladding and fuel alloy are chopped and loaded into the ER anode basket.	Oxide fuel is prepared as powder or pellets and loaded into the OR cathode basket.
	Plenums are advanced to waste metal consolidation.	N/A
	N/A	Inert atmosphere required for all subsequent operations described below.
Oxide Reduction (OR)	N/A	OR cathode basket is electrochemically processed in LiCl-Li_2O salt.
	N/A	Oxide is converted to metal while O_2(g) is liberated at semi-inert anode.
	N/A	Most of the Group 1 fission products accumulate in the OR salt.
	N/A	OR cathode basket is advanced to OR salt distillation.

Unit Operations and Materials Handling	Fuel Type	
	SFR (EBR-II Example)	LWR (JFCS Example)
OR Salt Distillation	N/A	Salt is distilled and returned to OR.
	N/A	Materials in the OR cathode basket are advanced to the ER as materials in the ER anode basket.
Uranium Electrorefining	ER anode basket is electrochemically processed in LiCl-KCl-UCl_3 salt.	ER anode basket is electrochemically processed in LiCl-KCl-UCl_3 salt.
	Uranium in the fuel is oxidized from the anode basket, while purified uranium is reduced on the cathode.	Uranium in the fuel is oxidized from the anode basket, while purified uranium is reduced on the cathode.
	Group 1, Group 2, lanthanides, and transuranics fission products accumulate in the ER salt. Transition metals remain in the anode basket.	Group 1, Group 2, lanthanides, and transuranics fission products accumulate in the ER salt. Transition metals remain in the anode basket, except most of the Group 1 fission products accumulate in the OR salt.
	Choose uranium downblending strategy.	N/A
	Electrorefined uranium is harvested from the cathode and advance to ER salt distillation.	Electrorefined uranium is harvested from the cathode and advance to ER salt distillation.
	Anode residue is harvested from the anode basket and advanced to waste metal consolidation.	Anode residue is harvested from the anode basket and advanced to waste metal consolidation.
ER Salt Distillation from Electrorefined Uranium	Salt is distillated and returned to ER. Uranium is consolidated into an ingot.	Salt is distillated and returned to ER. Uranium is consolidated into an ingot.
	Uranium ingot is advanced to metal casting.	Uranium ingot may be waste or advanced to metal casting.
Uranium Metal Casting	Electrorefined uranium cast into desired shapes.	Electrorefined uranium may be waste or cast into desired shapes.
U/TRU Alloy Recovery from ER.	U/TRU alloy recovered from ER salt using a liquid cadmium cathode.	U/TRU alloy recovered from ER salt using a liquid cadmium cathode.
	U/TRU alloy advanced to ER salt and cadmium distillation.	U/TRU alloy advanced to ER salt and cadmium distillation.

Unit Operations and Materials Handling	Fuel Type	
	SFR (EBR-II Example)	LWR (JFCS Example)
ER Salt and Cadmium Distillation from U/TRU Alloy	Salt is distilled and returned to ER. U/TRU alloy consolidated into ingot. Cadmium becomes waste.	Salt is distilled and returned to ER. U/TRU alloy consolidated into ingot. Cadmium becomes waste.
U/TRU Alloy Casting	Recovered U/TRU alloy cast into desired shapes.	Recovered U/TRU alloy cast into desired shapes.
Fuel Fabrication	HEU and HEU/TRU alloy, or DU and DU/TRU alloy, available for fuel fabrication.	LEU/TRU alloy available for fuel fabrication. LEU may be waste.
Waste Metal Consolidation of Assembly Hardware	Assemblies are consolidated into compact or waste metal ingot.	Assemblies are consolidated into compact or waste metal ingot.
Waste Metal Consolidation of SFR Plenums	Bond-sodium is distilled and neutralized. Plenums are consolidated into compact or waste metal ingot.	N/A
Waste Metal Consolidation of LWR Cladding	N/A	Cladding is consolidated into compact or waste metal ingot.
Waste Metal Consolidation of ER Anode Residue	Salt is distilled and returned to ER. Anode residue is consolidated into waste metal ingot.	Salt is distilled and returned to ER. Oxide fraction is returned to OR for processing. Metal fraction is consolidated into waste metal ingot.

The box in Table 11, "Choose uranium downblending strategy," has to do with the difference between the enrichment of the fuel being processed versus the desired enrichment of the electrorefined uranium product. For example, under the IFR Program, no downblending would have occurred because the desire was to reprocess HEU EBR-II fuels. However, the SFT Program requires that the electrorefined HEU is downblended to LEU (<20% ^{235}U). Presently, downblending occurs at three locations. First, by simultaneously electrorefining HEU from an anode basket containing the chopped fuel, and DU from an anode basket containing a DU ingot. The two sources of HEU and DU are collected on a common cathode mandrel. Second, by adding DU to the uranium ingot in the ER salt distillation furnace. Third, by adding DU to the uranium ingot in the first casting furnace, the one that collects the pin sample described earlier.

U/TRU alloy recovery from the ER salt is also dependent on the objectives of the reprocessing strategy. The SFT Program requires that the plutonium and other TRUs remain in the ER salt, which is the present practice. However, under the IFR Program the destination of TRUs may have been different. For example, plutonium could have been recovered to make ternary fuels for testing in EBR-II. Nevertheless, during the SFT Program the liquid cadmium cathode (LCC) technology was demonstrated for recovering plutonium from the ER salt as U/TRU metallic alloys. The LCC operates under the following thermodynamic principles. Under normal uranium electrorefining conditions, plutonium deposits on the cathode mandrel at potentials about 400 mV more negative than uranium. Therefore, under normal uranium electrorefining conditions, plutonium remains in the salt and is not co-deposited with uranium. Using a molten pool of cadmium as the cathode allows plutonium and uranium to deposit together as an alloy at the same cathode potential. This is because the chemical potential of plutonium is

greatly reduced in the cadmium, compared to the cathode mandrel, thereby allowing the plutonium to be reduced at the same potential as uranium. The result is that the pool of cadmium becomes saturated with plutonium and uranium to a degree governed by the concentrations of plutonium and uranium in the salt. The resulting cadmium alloy is harvested, loaded into a process crucible, and advanced to distillation (see Table 12, *ER Salt and Cadmium Distillation from U/TRU Alloy*). The cadmium distills at a lower temperature than the salt. In principle, the cadmium could be reused, but the reuse of cadmium has not been demonstrated. The remaining U/TRU alloy is consolidated into an ingot. Like electrorefined uranium, the U/TRU alloy is advanced to casting (see Table 13, *U/TRU Alloy Casting*) to recast the alloy into shapes more suitable for fuel fabrication. The LCC technology was demonstrated in the blanket ER four times. Afterward, the U/TRU alloy ingots were re-electrorefined in the blanket ER to return the TRU to the salt.

The products from the casting operations (see Table 14, *Uranium Metal Casting and U/TRU Alloy Casting*) are advanced to fuel manufacturing (see Table 15, *Fuel Fabrication*), where further alloying and casting takes place to make the desired fuel alloy compositions and shapes. The alloys required for fuel fabrication have a significant effect on the operation of the ER. For example, EBR-II had driver fuel assemblies containing HEU and blanket assemblies containing DU. The operating EBR-II core contained about 50 driver fuel assemblies, each with approximately 3 kg of HEU-10Zr in 61 fuel elements. The driver core was surrounded by about 590 blanket assemblies, each with approximately 47 kg of DU in 19 blanket elements. Both spent driver and blanket contained TRU. Under the IFR Program, the primary objective of electrorefining the HEU-10Zr fuel would have been to recover a HEU/Zr alloy to make HEU-10Zr binary fuel, and the primary objective of electrorefining the DU blanket would have been to recover a DU/TRU alloy from the salt to make DU/TRU/Zr ternary fuel. However, the IFR Program was terminated before this happened and the fuel cycle management of uranium, TRU, and zirconium was never experienced. Under the SFT Program, the objective of electrorefining the HEU-10Zr fuel is to recover the HEU and downblend it to LEU and to put the bond sodium and TRU into the salt. While the objective of electrorefining the DU blanket is to recover the DU and to put the bond sodium and TRU into the salt. These distinctions between the objectives of the IFR Program and the SFT Program have significant impacts on flowsheet design and operations.

The SFR fuels involve three types of materials for "*Waste Metal Consolidation*": "*Assembly Hardware*," "*SFR Plenums*," and "*ER Anode Residue*." There are multiple process options for each that depend on many factors, not the least of which is the acceptance criteria of the destination waste repository. The "*Assembly Hardware*" is comprised of activated stainless-steel that can be either compacted or melted into an ingot. This waste is generally not associated with actinide or fission product contamination. The "*SFR Plenums*" pose more of a challenge because they contain bond sodium that was exposed directly to the fuel and consequently contain dissolved Group 1 and Group 2 fission products. It is possible to change the flowsheet strategy and rather than segregate the plenums, to chop and load the entire lengths of fuel elements into the anode baskets. However, this would result in greater bond sodium and fission product loading to the ER salt, and minimizing this accumulation is generally considered the best practice. Therefore, the path suggested here is to distill the bond sodium from the plenums and to neutralize and stabilize the sodium by chemical conversion from a highly reactive metal to, for example, a hydroxide, carbonate, or chloride form. The cladding, once free of metallic sodium, can be either compacted or melted into an ingot. Treatment of the "*ER Anode Residue*" is necessarily a distillation operation to allow return of the salt to the ER. The remaining fraction is consolidated into a waste metal ingot that contains cladding, and residual quantities of fission products and actinides.

2.3 LWR Fuels Processing (JFCS Example)

There are differences and similarities between the flowsheets for SFR and LWR fuels. In both cases, the fuel elements are removed from the assembly hardware. The LWR fuel is then mechanically declad and the zirconium alloy cladding is separated from the oxide fuel. Because the separations are incomplete, the zirconium cladding is expected to be significantly contaminated with adhering fuel and fuel powder.

The recovered oxide fuel is then prepared for oxide reduction. There are many options available, but ultimately the fuel must be loaded into the cathode baskets for oxide reduction. Increasing the surface area of the fuel aids in oxide reduction by exposing a greater surface area of the fuel to the electrolyte in the oxide reduction (OR) cell. The recovered fuel can be calcined at high temperature in the presence of oxygen to convert the UO_2 to U_3O_8. Calcination results in a form of chemical decrepitation that converts the granular fuel into a fine powder. In other words, there is a volume expansion when going from UO_2 to U_3O_8 that breaks the fuel into a fine powder. Calcination of UO_2 to U_3O_8 can also be utilized to improve the efficiency of mechanical decladding of LWR fuels by helping to disengage the fuel from the cladding. Alternatively, without calcination, standard comminution (size reduction) techniques can be applied by the operations of crushing, grinding, and sizing to produce a fine powder. And finally, the fine powder can be loaded directly into the cathode basket, or pelletized and loaded into the cathode basket. There are significant material handling challenges related to recovering the oxide fuel from the cladding and loading it into a cathode basket. The challenges associated with remote handling fine powders include the efficient separation of the oxide fuel from the cladding and containment during size reduction, representative sampling for input accountancy, and loading into the OR cathode baskets. The loaded cathode basket is then advanced to the OR cell (see Table 16, *Oxide Reduction*).

The OR cell is an electrochemical cell with an electrolyte comprised of LiCl with a nominal concentration of a few weight percent Li_2O. The operating temperature is 650°C, considerably higher than the ER cell operating temperature of 500°C. The reduction of the oxide fuel to metal is driven electrochemically by an external DC power supply. There are two predominant mechanisms for the reduction. Uranium oxide is used as an example below.

The Li_2O is dissolved in the electrolyte as lithium cations (Li^+) and oxygen anions (O^-). By applying a negative potential to the cathode and a positive potential to the anode, the lithium cations are reduced to metallic lithium at the cathode, while the oxygen anions are oxidized to oxygen gas at the anode. The cathode and anode "half-cell" reactions are shown below, respectively.

$$8Li_2O + 16e^- = 16Li(l) + 8O^{2-}$$

$$8O^{2-} = 4O_2(g) + 16e^-$$

The net reaction is the conversion of Li_2O to lithium metal and oxygen.

$$8Li_2O = 16Li(l) + 4O_2(g)$$

Since lithium forms a more stable oxide than uranium, the lithium metal can reduce the uranium oxide to uranium metal. The uranium oxide has little solubility in the electrolyte and remains in the cathode basket. By comparison, lithium oxide has a high solubility in the electrolyte and dissolves into the electrolyte as described above. The net reaction is the reduction of fuel oxides to metals.

$$U_3O_8(s) + 16Li(l) = 8Li_2O + 3U(s)$$

In addition, there is a mechanism of direct electrochemical reduction of the UO_2 or U_3O_8. This is possible because the fuel oxides have some degree of electrical conductivity. The cathode and anode "half-cell" reactions are shown below, respectively.

$$U_3O_8(s) + 16e^- = 3U(s) + 8O^{2-}$$

$$2O^{2-} = O_2(g) + 4e^-$$

The anode is made of a semi-inert material. Choices include platinum and iridium. However, each of these materials exhibit degradation over time from chemical interactions with various fission products that report to the electrolyte. Degradation occurs when the surface of the metallic anode becomes passivated by the buildup of an electrically resistive layer (for iridium), or the metallic anode loses mass as the corrosion products spall off the surface of the metals (for platinum). Both of these anode materials are high-cost and there is an active search for alternative materials. The anode can be made of a low-cost consumable material such as carbon, but this introduces carbon to the salt, which may have other deleterious effects. In a similar manner as described earlier, chemical partitioning of fission products into the salt is possible for metals that have a greater affinity to form a chloride than lithium. These include cesium and strontium. Another consequence of oxide reduction is that any noble gas fission products remaining in the fuel loaded into the cathode basket are released as the oxides are reduced to metals.

Carryover of salt from the OR cell to the ER cell was avoided by advancing the reduced metals to distillation (see Table 17, *OR Salt Distillation*). The reason is primarily to prevent excess LiCl and Li_2O from entering the ER salt where it can form uranium oxide. As discussed earlier, oxides are not electrorefined in the ER cell. A potential mechanism for the oxidation of UCl_3 to UO_2 by the action of Li_2O is shown below.

$$6Li_2O + 4UCl_3 = 12LiCl + 3UO_2 + U$$

There are many options available for salt distillation. The conversion efficiency of oxides to metals during OR operations was, at best, around 95%. The contents of the cathode basket could have been removed and loaded into a process crucible for salt distillation, and then loaded into an anode basket for electrorefining (see Table 18, *Uranium Electrorefining*). Salt distillation could have included metal consolidation, which has the advantage of separating all oxides from the metal product advanced to electrorefining (see Table 19, *Uranium Electrorefining*). However, during the JFCS Program the cathode basket itself was advanced to distillation and then to electrorefining. In other words, the same basket served as the cathode basket during oxide reduction, the process crucible during distillation, and the anode basket during electrorefining.

The chemical separations during electrorefining are essentially the same between the metallic SFR and oxide LWR fuels, with the exception that the LWR fuels will have lost most of the Group 1 and Group 2 fission products to the OR salt. A consequence of incomplete reduction during OR cell operations was that the anode residue from electrorefining contained un-reduced oxides, which required a disposition path. During the JFCS Program, the anode residue was a waste. In the context of a closed fuel cycle, the oxides in the anode residue would be returned to OR cell operations for another pass through the OR cell. This can be achieved by advancing the anode residue to distillation (see Table 20, *Waste Metal Consolidation of ER Anode Residue*) to remove the ER salt before advancing the material to the headend of OR cell operations.

The electrorefined uranium recovered from LWR fuels is LEU, which may or may not have value to the fuel cycle strategy being deployed. For LWR fuels, the only product of value may be the U/TRU alloys recovered from the ER salt. This was the case during the JFCS Program. However, the electrorefiner is operated the same way for LWR fuels as SFR fuels with regards to uranium electrorefining, U/TRU alloy recovery, salt distillation, and casting operations. Of course, due to mass limits imposed by criticality considerations, batch sizes are influenced by the enrichment level of the uranium and the concentration of TRU.

The LWR fuels involve three types of materials for "*Waste Metal Consolidation*": "*Assembly Hardware*," "*LWR Cladding*," and "*ER Anode Residue*." As with SFR fuels, the "*Assembly Hardware*" is comprised of activated stainless-steel that can be either compacted or melted into an ingot. This waste is generally not associated with actinide or fission product contamination. LWR fuels will also have a plenum section, but because there is no bond sodium present, the plenum sections are treated in the same manner as the cladding. The "*LWR Cladding*" is a challenge for two reasons. First, it is a zirconium alloy that has a higher melting temperature than stainless steels, 1,850°C for the zirconium alloys versus

1,550°C for stainless-steel alloys. Consequently, the zirconium cladding is blended with stainless-steel to reduce the melting temperature to below 1,550°C. Second, it is contaminated with oxide fuel that remains from the decladding operations. Therefore, compaction into a waste form appears to be a reasonable path. Treatment of the "*ER Anode Residue*" is necessarily a distillation operation to allow return of the salt to the ER. However, the anode residue is a mixture of un-reduced oxides and metallic fission products and actinides. Metal consolidation by casting is an option to form a metal ingot for disposal, while the dross could be returned to the headend of OR cell operations.

2.4 Product and Waste Materials Characterizations

Spent nuclear fuels contain an array of radioactive fission products and actinides. As described earlier, the objective of a reprocessing strategy is to make separations between the elements to be retained in the fuel cycle and the elements to be rejected from the fuel cycle. These two streams report on fuel fabrication and waste management, respectively. However, incomplete separations, chemical processing, and materials handling always results in the spread of radioactive elements from the spent fuel, which increases the mass of materials requiring waste management. The result is two competing goals of maximizing actinide recovery while minimizing waste generation. Reprocessing is feasible only if an acceptable balance is struck between the two attainable ranges of actinide recovery and waste generation. Everything associated with the process requires an accepted disposition path that is governed by the criteria established for product specifications, waste acceptance, environmental release, etc. A comparison of waste streams produced by pyroprocessing SFR and LWR fuels is summarized in Table 21. Each waste stream is discussed below.

"Reactor Primary Sodium Residue" is the sodium adhering to the fuel assemblies removed from the SFR. This sodium will contain activated sodium and potentially radionuclides from the fuel in cases where cladding breached in the reactor core and contaminated the primary sodium. Naturally occurring sodium is 100% ^{23}Na. Some amount of ^{23}Na is activated by the (n, 2n) mechanism (capture of a neutron and ejection of two neutrons) to ^{22}Na (2.6 y). Therefore, the sodium wash operation will produce radiological waste.

"Assembly Hardware" includes all the stainless-steel components associated with the fuel assemblies. Stainless-steel alloys contain nickel and cobalt. Naturally occurring nickel is 68% ^{58}Ni. Some amount of ^{58}Ni is activated by neutron capture with proton ejection to ^{58}Co (71 d). Naturally occurring cobalt is 100% ^{59}Co. Likewise, some amount of ^{59}Co is activated by neutron capture to ^{60}Co (5.27 y). Therefore, the assembly hardware is radiological waste.

"Fission Product Gases" include the volatile radionuclides in the spent fuel that are highly mobile in the atmosphere. The long-lived radionuclides of greatest importance include ^{85}Kr (10.8 y), ^{3}H (12.3 y), ^{14}C (5700 y), ^{129}I (15.7 My), and, if present, ^{131}I (8.02 d) and ^{127}Xe (36.3 d). Volatile fission products are potentially released during decladding operations and electrochemical processing. With regards to chemical pathways leading to atmospheric release, in some cases there are distinct differences between aqueous reprocessing and pyroprocessing. For example, iodine is a halide fission product and pyroprocessing uses molten chloride salts, the majority of iodine is expected to report to the OR and ER salts. Otherwise, the management of fission product gases is essentially the same between aqueous reprocessing and pyroprocessing.

"Groups 16 (chalcogen) and 17 (halogen) Fission Products" include selenium, tellurium, bromine, and iodine. Much attention has been paid to the fate of Group 1, Group 2, lanthanides, transuranics, and noble gases. However, these fission products also accumulate in the OR and ER salts and can interfere with the performance of the oxygen evolving anodes in the OR.

"Fuel Element Cladding" includes stainless-steel alloys from SFR fuels and zirconium alloys from LWR fuels. The SFR cladding is split between two process streams. The section of the fuel elements containing fuel are chopped and loaded into the electrorefiner anode baskets. This portion of the cladding ultimately reports to the waste metal ingots along with the ER anode residues. The "*Fuel Element Plenums"* report directly to a sodium distillation furnace. After sodium distillation, the cladding can either be consolidated by compaction or melted into a waste metal ingot. The LWR cladding was separated from the oxide fuel and is contaminated with the remnants of adhering fuel particles. Due to the high melting temperature of the zirconium alloy, remelting is not a preferred processing option. The cladding can be consolidated by compaction.

"Anode Residues" are different between processing metallic fuels and oxide fuels. When processing metallic fuels, anode residue is primarily cladding and the transition metal fission products that do not get dissolved into the salt during uranium electrorefining in the ER cell. When processing oxide fuels, if there is incomplete conversion of the oxide fuel to metal in the OR cell, then the anode residue includes the residual oxide fuel as well as the transition metal fission products. The residual oxide fuel can be returned to the headend for processing again in the OR cell. Ultimately, the transition metal fission products report to the waste metal ingots.

"Bond Sodium" is associated only with the SFR fuels, where it is directly exposed to the fuel alloy. Sodium has a high solubility for Group 1 and Group 2 fission products. The normal melting temperature of sodium is 98°C. Alloying with fission products such as cesium and strontium, drops the melting temperature significantly. Liquid sodium alloys have been observed in plenum sections at ambient temperatures near 25°C, indicating that significant alloying has occurred. The bond sodium follows along with the cladding that is segregated between the electrorefiner (the chopped cladding) and the sodium distillation furnace (the plenum sections). "*Bond Sodium in the Fuel Element Cladding"* reports to the electrorefiner where it partitions into the salt as NaCl. "*Bond Sodium in the Fuel Element Plenums"* that reports to sodium distillation must be stabilized into a waste form. The management of bond sodium is not trivial. If it reports to the ER salt, it significantly increases the volume of salt waste. If collected by distillation, it must be converted into a stable waste form accommodating not only the sodium, but also the fission products accompanying the sodium.

"Fission products" that report to the OR salt are those that can exchange with the LiCl in the salt. The candidates are select elements from Group 1 and Group 2 that include Cs, K, Na, Rb, Ba, and Sr. The thermodynamic driving forces to partitioning of these elements from the fuel and into the salt by displacing LiCl are marginal. Therefore, the separation efficiencies may be low. Conditions relative to the ER salt are markedly different because partitioning into the ER salt requires displacing UCl_3, which is a much less stable chloride than LiCl. "*Group 1 and Group 2 Fission Products*" in SFR fuels report to the bond sodium and the ER salt, and in LWR fuels report to the OR salt and the ER salt. "*Lanthanide and Transuranic Fission Products*" tend to form chlorides that are less stable than LiCl, but more stable than UCl_3. Therefore, these fission products in both SFR and LWR fuels report to the ER salt. Conversely, "*Transition Metal Fission Products*" tend to form chlorides that are less stable than LiCl and UCl_3. Therefore, these fission products in both SFR and LWR fuels remain as undissolved solids in the ER anode baskets. These separations chemistries are discussed in greater detail in Section 3.1.

"Process Casting Drosses" are generated to a greater or lesser degree in every operation that melts metal. For example, when electrorefined uranium is processed in a distillation furnace that both distills salt and consolidates the uranium into an ingot, the graphite process crucible is lined with a castable zirconia (ZrO_2). The selection of zirconia is a compromise because it must be compatible with both molten salt and molten metal. The result is that the molten uranium reacts with the zirconia to form some uranium oxide, which is the casting dross. In the case of the LWR flowsheet, oxide casting drosses can potentially be processed in the OR cell. However, an OR cell is not available in the SFR flowsheet. Alternatively, there are chemical means to chlorinate the casting drosses into a salt similar to the ER salt. These chlorination chemistries are discussed in greater detail in Section 3.4.

"OR Salts" become laden with Group 1 and Group 2 fission products, and "*ER Salts"* become laden with Group 1, Group 2, and lanthanide fission products along with transuranics. There are several consequences of the changing salt compositions. Consider the ER. The LiCl-KCl eutectic salt has a liquidus temperature of about 350°C. If the cell is operating at 500°C and the liquidus temperature is 350°C, then the cell is operating with 150°C of "superheat." As UCl_3 and other metal chlorides accumulate in the salt the liquidus temperature increases. After the accumulation of a significant loading of fission products in the salt, the liquidus temperature could increase to 450°C, at which point the cell would be operating with only 50°C superheat. At some point there is too little superheat to operate the cell and the salt must be managed. Another consideration is the thermal load in the salt generated from the decay heat released by the fission products in the salt. The OR and ER salts are held in a steel vessel surrounded by electrical resistance heaters and thermal insulation. As the thermal load in the salt increases, less power is needed from the electrical heaters to maintain the operating temperature. At some point, it may be possible that the thermal load is sufficient to keep the salt molten without any support from the heaters. This too is a condition to be avoided. Another consideration is the fissile inventory in the salt, and the consequences of this on criticality control and safety control limits.

"Cadmium" was used in both the SFT Program and the JFCS Program in the LCC runs to recover U/TRU alloys from the ER salts. Cadmium in the form of $CdCl_2$ is currently used in the SFT Program to replenish the UCl_3 concentration in the ER salt that is lost as fission products and transuranics accumulate in the salt. This is achieved by the following reaction.

$$3CdCl_2 + 2U(s) = 2UCl_3 + 3Cd(l)$$

$CdCl_2$ is added directly to the ER salt where it reacts with uranium metal to form UCl_3 in the salt and cadmium metal. At 500°C, the cadmium metal reports to a pool of molten cadmium on the bottom of the ER vessel. Although this is an easy and effective way of replenishing the UCl_3, the high vapor pressure of cadmium does cause some operational difficulties. For example, cadmium metal condenses in the headspace of the ER vessel resulting in the occasional electrical shorting between the anode and cathode leads and the vessel.

As a chemical reagent, UCl_3 is referred to as an "oxidant" because it is consumed as the more reactive metals in the fuel are oxidized in the ER salt. Depending on the details of the fuel cycle application, the enrichment of the uranium in the UCl_3 oxidant may be an issue. In the example given above, the $CdCl_2$ will react with any uranium it contacts in the ER vessel. Alternatively, UCl_3 can be produced in a laboratory glovebox using DU, natural uranium, or HEU, according to the requirements. Experience has shown that compared to making purified UCl_3, it is easier to make UCl_3 as LiCl-KCl-UCl_3 ternary salt mixture that is about 12, 8, 80 wt%, respectively. However, this excess LiCl and KCl does add to the salt volume.

"Fuel Fabrication Scraps" includes casting drosses, machining scraps, out of specification fuel elements, etc. It is technically easier to recover the actinides from these materials, than it is to recover actinides from spent fuels.

"Process Equipment Scraps" include all forms of contaminated process equipment that becomes waste. A significant source of process waste are the crucibles used for distillation and casting operations. Additional items include electrodes, heat shields, motors, vacuum pumps, electrical cables, fixturing, containers, etc.

"Hot Cell Equipment Scraps" include those items specifically related to hot cell operations. These items tend not to be as highly contaminated as "*Process Equipment Scraps*," but as with all other wastes, a disposition path is required. There are many mechanical and electrical systems related to hot cell operations. A hot cell facility is essentially a large machine staffed with an operations crew that include operators, mechanical engineers, electrical engineers, criticality safety engineers, health physicists (HPs), etc.

Table 21. Comparison Between Pyroprocessing Wastes of SFR and LWR Fuels.

Waste Material	Fuel Type	
	SFR	LWR
Reactor Primary Sodium Residue	Reports to sodium wash operation. Suspect contamination from breeched fuel in the reactor and sodium activation in the core.	N/A
Assembly Hardware	Reports to disassembly operation, then to metal waste consolidation.	Reports to disassembly operation, then to metal waste consolidation.
Fission Product Gases	Released during fuel element chopping and uranium electrorefining.	Released during decladding and oxide reduction.
Fuel Element Cladding	Reports to ER anode residue, then to waste metal consolidation.	Reports to decladding operation, then to waste metal consolidation.
Bond Sodium in Fuel Element Cladding	Reports to ER salt.	N/A
Fuel Element Plenums	Reports to fuel element chopping operation, then to waste metal consolidation.	N/A
Bond Sodium in Fuel Element Plenums	Distilled and neutralized during waste metal consolidation.	N/A
Group 1 and Group 2 Fission Products	Reports to ER salt and bond sodium in plenums.	Reports to OR salt.
Lanthanide Fission Products	Reports to ER salt.	Reports to ER salt.
Transuranic Fission Products	Reports to ER salt.	Reports to ER salt.
Transition Metal Fission Products	Reports to ER anode residue.	Reports to ER anode residue.
Process Casting Drosses	From casting of plenums, electrorefined uranium, U/TRU alloy, and anode residue.	From casting of zirconium cladding, electrorefined uranium, U/TRU alloy, and anode residue.
OR Salt	N/A	Requires fission product management and/or direct disposal.
ER Salt	Requires fission product and actinide management and/or direct disposal.	Requires fission product and actinide management and/or direct disposal.
Cadmium	Requires fission product management and/or direct disposal.	Requires fission product management and/or direct disposal.
Fuel Fabrication Scraps	Includes casting drosses and heals.	Includes casting drosses and heals.
Process Equipment Scraps	Includes excessed casting crucibles and process equipment.	Includes excessed casting crucibles and process equipment, plus, OR anode materials.
Hot Cell Equipment Scraps	Includes all items associated with hot cell operations.	Includes all items associated with hot cell operations.

2.5 Process Flowsheets

Schematic flowsheets of the IFR Program, SFT Program, and JFCS Program are shown in Figure 1 through Figure 6. These figures illustrate the processes that were described previously. Each figure is a simple flowsheet and in no way illustrates the complexity required of a large-scale commercial reprocessing facility.

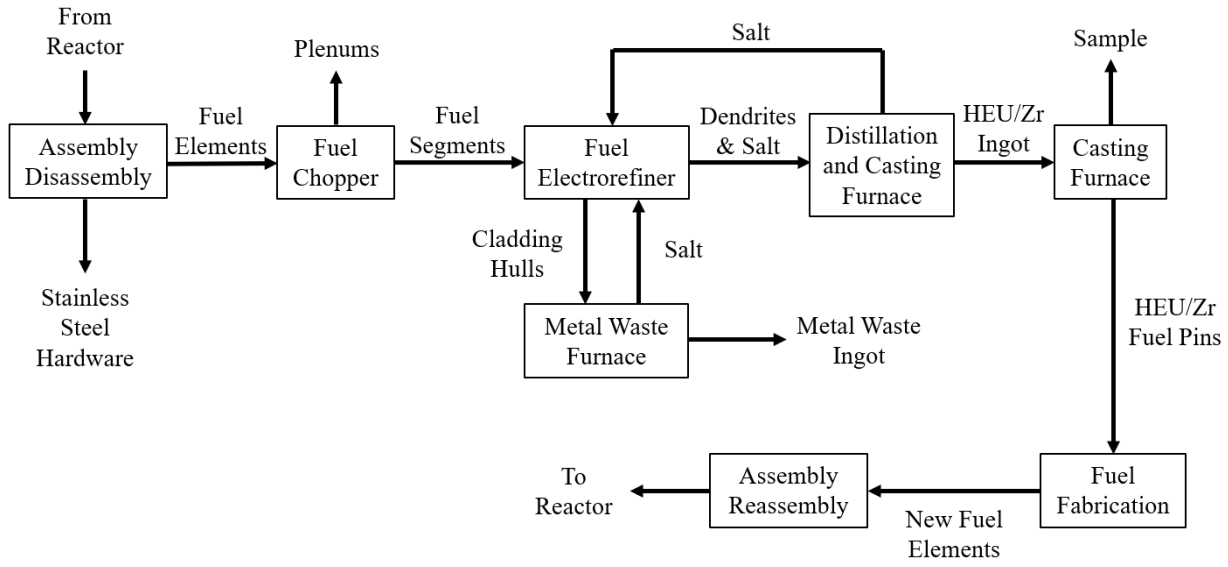

Figure 1. Schematic flowsheet of the IFR Program driver fuel processing.

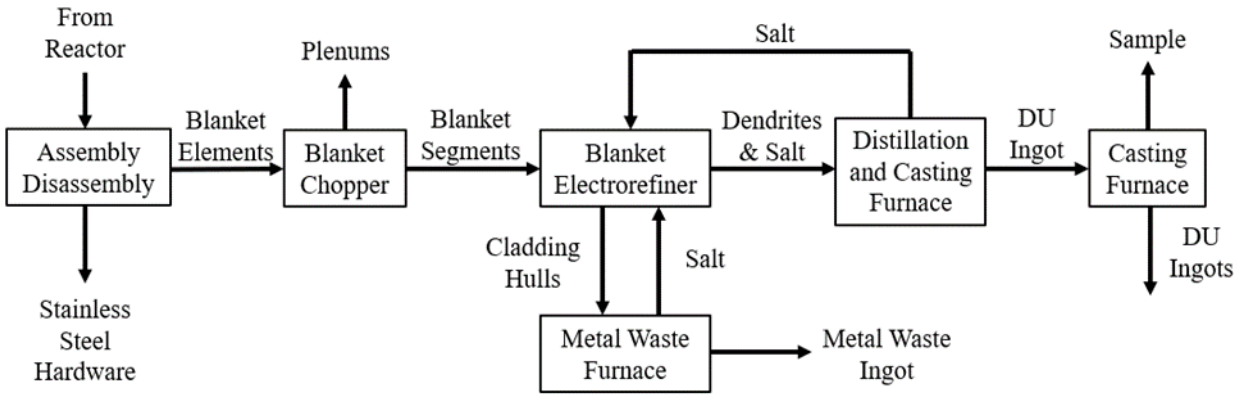

Figure 2. Schematic flowsheet of the IFR Program blanket processing.

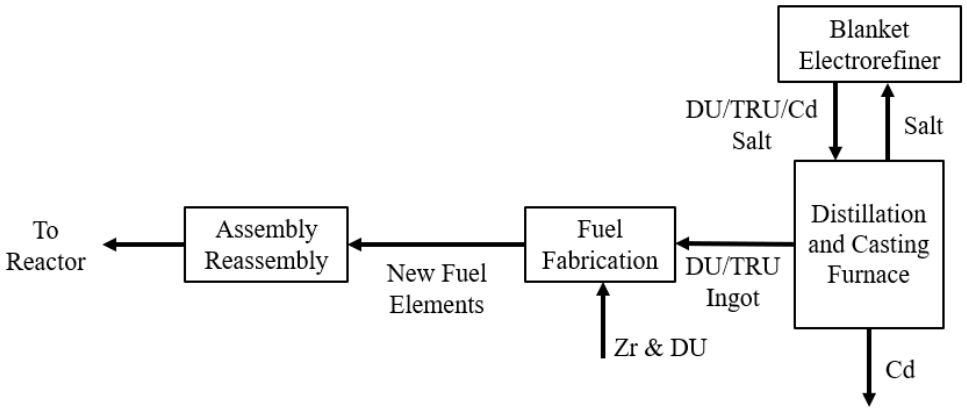

Figure 3. Schematic flowsheet of the IFR Program TRU recovery from blanket processing.

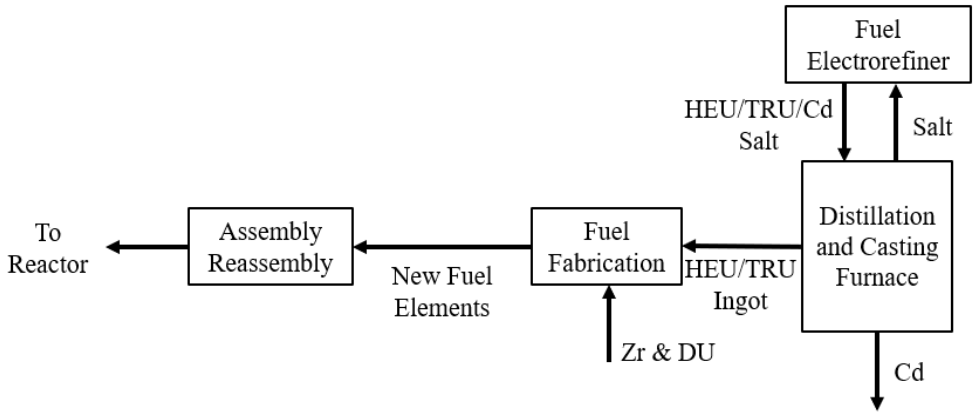

Figure 4. Schematic flowsheet of the IFR Program TRU recovery from driver fuel processing.

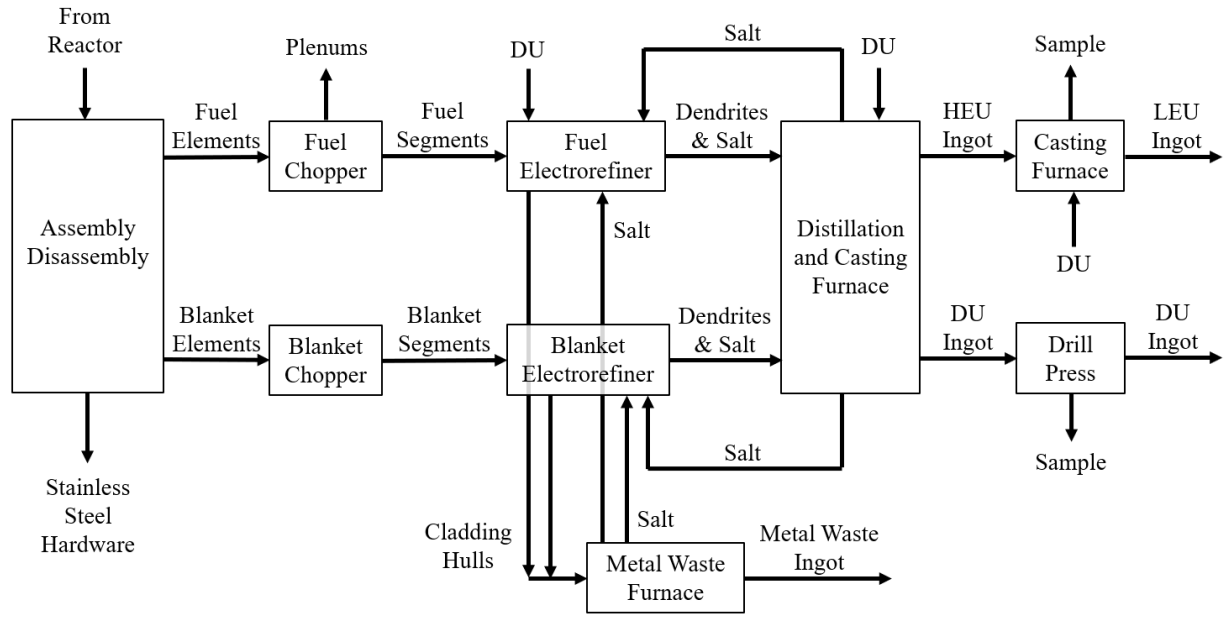

Figure 5. Schematic flowsheet of the SFT Program.

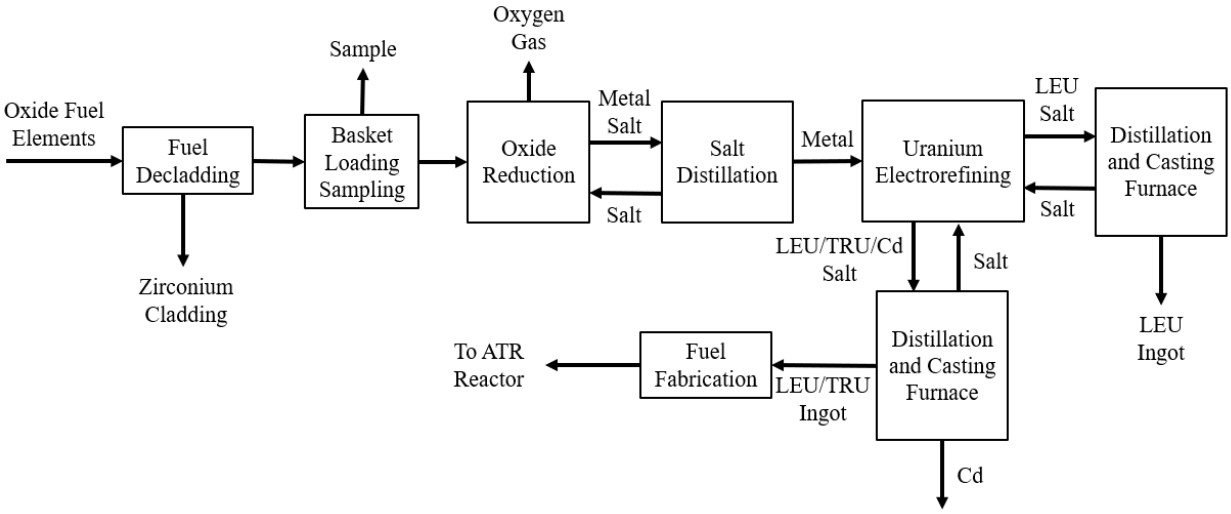

Figure 6. Schematic flowsheet of the JFCS Program.

Flowsheets related to the IFR Program are shown in Figure 1 to Figure 4. Figure 1 illustrates how EBR-II driver fuel can be processed to recover electrorefined HEU/Zr alloy for fuel fabrication and allow TRU to accumulate in the driver ER salt. Figure 2 illustrates how EBR-II blanket can be processed to recover electrorefined DU ingots and allow TRU to accumulate in the blanket ER salt. Figure 3 illustrates how TRU can be recovered from the blanket ER salt using the LCC technology and in this example, the TRU is recovered as a DU/TRU alloy. Figure 4 illustrates how TRU can be recovered from the driver ER salt using the LCC technology and in this example, the TRU is recovered as a HEU/TRU alloy. The requirements of ternary fuel fabrication are different when the TRU is provided as a DU/TRU alloy versus a HEU/TRU alloy.

Conceptual flowsheet modeling is an integral part of the engineering design process. However, flowsheet modeling does not prove a process, only pilot studies and successful deployment prove a process. Flowsheet modeling can be of little value when not backed-up by direct engineering experience, and when one or more of the following negative attributes apply:

- Include unit operations that have not been demonstrated.
- Include unit operations that have not been demonstrated at the scales shown.
- Include unit operations that have not been demonstrated integrated as shown.
- Assume technical readiness levels that have not been demonstrated.
- Assume separations characteristics that have not been demonstrated.
- Assume chemical behaviors that have not been demonstrated.
- Assume equipment performance characteristics that have not been demonstrated.
- Do not consider corrosion, holdup, and cross contamination.
- Do not consider process upsets and recovery strategies.
- Do not consider detailed mass and energy balances.
- Do not consider decay heat management.
- Do not consider criticality engineering.
- Do not consider a materials control and accountancy strategy.
- Do not consider a safeguard strategy.
- Do not consider facility safety requirements.
- Do not consider remotely operated system designs.
- Do not consider equipment repair and replacement.
- Do not consider disposition paths for each waste.
- Do not consider government regulations.
- Do not specify the exact fuel cycle application.

On the other hand, when done well and with objectivity, flowsheet modeling can provide useful information that helps identify the most critical areas needing attention and resource allocation.

3. TECHNICAL FUNDAMENTALS

A pyroprocessing flowsheet utilizes several different chemical operations including molten salt chemistry, molten salt electrochemistry, salt distillation, metal distillation, melting, and casting. This section outlines some of the basic considerations.

3.1 Separations Chemistries

The separation chemistries in pyroprocessing generally involve high-temperature materials exchanges between several phases including molten salt, solid salt, molten metal, solid metal, salt vapor, metal vapor, oxides, and other gases. The partitioning of elements between these phases is governed by thermodynamic and kinetic considerations. Thermodynamically, the elements partition themselves according to their relative chemical stabilities between the phases as the system seeks its most stable configurations. Kinetically, the rates of the reactions are governed by amperage, voltage, surface area, concentration, temperature, diffusion, mixing, and other rate-controlling factors. Many of the most important reactions are interfacial, occurring in narrow regions along the interface between two or more phases.

For example, electrorefining uranium requires two electrodes: an anode and a cathode. The anode and cathode are submerged in a common electrolyte, and they are electrically connected to a DC power supply. The anode is connected to the positive terminal and the cathode is connected to the negative terminal. In the external electrical circuit, electrons flow from the anode to the cathode. In the internal ionic circuit, uranium cations flow from the anode to the cathode. The two circuits, electrical and ionic, are balanced with respect to charge. As one uranium cation (U^{3+}) completes the ionic circuit from the anode to the cathode, three electrons (e^-) complete the electrical circuit from the anode to the cathode. Impure uranium (spent fuel) is loaded into the anode and purified uranium deposits on the cathode. Ampere is a unit of rate: coulombs per second. And a coulomb is a quantity of electrons: 6.24E18 e^-. The greater the amperage in the external circuit, the greater the rate uranium is electrorefined.

The ER salt is LiCl-KCl eutectic with about 5 wt% UCl_3 with a liquidus temperature of approximately 350°C. The ER operating temperature is approximately 500°C. The OR salt is LiCl with a few wt% Li_2O with a liquidus temperature of approximately 605°C. The OR operating temperature is approximately 650°C. These salts are essentially clear liquids with densities and viscosities only a little greater than water. As fission products and transuranics accumulate in the OR and ER salts, the liquidus temperatures rise, the salts become opaque, and the densities and viscosities increase.

In OR operations, salt is distilled from the cathode product and returned to the OR cell. In ER operations, salt is distilled from the cathode product and the anode residue and returned to the ER cell. Under these idealized conditions, the salts are contained in the cells, baring small inventories of in-process salts contained in the materials heading to distillation, the salts within the distillation furnaces, and the salts being returned to the cells from distillation. As fission products accumulate in the OR salt at the expense of LiCl, the salt volume and density are affected, but to a lesser extent than what occurs in the ER salt. As fission products and transuranics accumulate in the ER salt, they do so at the expense of the UCl_3 concentration. However, unlike the OR cell where LiCl is the bulk of the salt, in the ER cell, the UCl_3 concentration must be maintained at approximately 5 wt%. This means that additional UCl_3 must be added to the salt at the same rate it is displaced from the salt. This results in a significant increase in salt volume over time. The mass balance can be thought of in terms of a chlorine balance. As metal cations accumulate in the salt, chlorine must be provided in stoichiometric ratios proportional to the cumulative valence increases of the cations.

3.2 Thermodynamic Limitations to Separations Chemistries

Chemical potential, or activity, is a thermodynamic construct related to the "*strength-of-presence"* (a term made-up here to illustrate a concept) of a species or element in a chemical system. The greater its activity, the greater its strength-of-presence, and the greater its reactivity with regards to its participating in chemical reactions. By definition, the activity of a pure species is numerically equal to 1. For example, in a process crucible containing molten LiCl at 650°C, the activity of LiCl is 1 because the species is pure. Similarly, in a process crucible containing molten LiCl-KCl eutectic at 500°C, the activities of LiCl and KCl are each something less than 1 because neither species is pure. In the first example, the phase is molten LiCl, and in the second example, the phase is a molten mixture of LiCl and KCl. Mathematically, activity of a species can be expressed as its concentration multiplied by a correction term, the activity coefficient, which is an empirical construct. Arguably, all chemical thermodynamics is an empirical construct used to describe the behaviors of chemical systems. The value of an activity coefficient for a particular species is influenced by temperature, concentration of the paired species, and the concentrations of all other species in the chemical system. In the field of molten salt electrochemistry, it is not often that activity coefficients are known with much accuracy and precision. And when they are known, it is often for limited conditions of salt composition and temperature range.

The OR salt is LiCl with a nominal concentration of Li_2O, and the ER salt is LiCl-KCl eutectic with a nominal concentration of UCl_3. For the moment, assume the salts are otherwise free of fission product chlorides. It is almost intuitive that as the concentration of Li_2O in the OR salt is decreased, its strength-of-presence decreases, meaning its activity decreases. The same is true of UCl_3 in the ER salt. The consequence is that the chemical behaviors of Li_2O and UCl_3 change as their concentrations change. By such mechanisms, the performance of the OR cell is influenced by the concentration of Li_2O in the OR salt, and the performance of the ER cell is influenced by the concentration of UCl_3 in the ER salt.

Many separation processes in pyroprocessing rely on the partitioning of elements between two phases that are in pseudo-equilibrium with each other. For two (or more) phases to be in true thermodynamic equilibrium, the activities of all species are equal across each of the phase boundaries. But this says nothing about concentrations of the species in each phase. It is possible for two phases to be in equilibrium, sharing common activities for a given species, while exhibiting vastly different concentrations of that species in each phase. This observation suggests that the activity coefficient behavior of this species is different in each phase. It is by such chemical driving forces that separations are possible where an element is driven into one phase at the expense of the other phase. The driving force goes away as the activity differential approaches zero.

The consequence of separations is that as the concentration of a species decreases, so too does its strength-of-presence, rendering it less likely to participate in the desired reactions. To force it to participate at lower concentrations more chemical driving force can be applied, but then other species will begin to respond in an undesirable way thwarting the desired separations outcome. This is the more fundamental explanation of why product purity decreases as recovery increases.

3.3 Exchange Current Density

Exchange current density is a well-known electrochemical phenomenon. It involves mass transfer initiated by the exchange of atoms between an electrode and electrolyte. Atoms on the electrode are being oxidized into the salt as cations in the salt are being reduced onto the electrode. The rate of oxidation is balanced by the rate of reduction; therefore, the net mass transfer is effectively zero. For example, uranium metal and uranium cations in ER salts exhibit this behavior. Since cations are charged particles, the rate of exchange is measured by current density.

Exchange current density is an interfacial phenomenon. Even when the system is otherwise at pseudo-equilibrium, at least with respect to the bulk compositions of the salt and metal, mass transport can be active in the interfacial region. The surface morphology of the metal can be affected as the process is not necessarily uniform and can occur at preferred sites. The effect is a form of corrosion in that it can alter the surface condition of the metal. For any particular metal, the effect is enhanced or inhibited by the composition of the salt.

3.4 Chlorination Chemistry

Chlorination is the chemical process of converting metals into metal chlorides. Chlorination has already been discussed in the context of fission product accumulation in the OR salt at the expense of LiCl, fission product accumulation in the ER salt at the expense of UCl_3, and UCl_3 production by the reaction of uranium metal with $CdCl_2$. The function of the OR cell is to convert spent oxide fuels to metals. The function of the ER cell is to collect electrorefined uranium from spent metal fuels, or from spent oxide fuels that have been converted to metals in the OR cell.

Casting drosses and corroded metallic fuels are not candidate materials for electrorefining in the ER cell; and they are not necessarily good candidate materials for oxide reduction in the OR cell, particularly if bond sodium is present. However, these oxidized, or partially oxidized, materials can be chlorinated. For example, $ZrCl_4$ is a good chlorinating reagent for actinide oxides because it forms a weak chloride and a strong oxide. The reactions below tend to be thermodynamically favorable in ER salts:

$$4UO_2(s) + 3ZrCl_4 + Zr(s) = 4UCl_3 + 4ZrO_2(s)$$

$$4PuO_2(s) + 3ZrCl_4 + Zr(s) = 4PuCl_3 + 4ZrO_2(s)$$

The stoichiometry shown is only conceptual as these metals can exhibit multiple valence states in the salt depending on the chlorine chemical potential. Such chlorination chemistry provides opportunities to recover actinides from process streams that otherwise would have less favorable disposition paths.

3.5 Distillation Chemistry

Distillation exploits differences in vapor pressures between materials to affect separations. In the case of uranium dendrites and adhering salt, as the materials are heated under a vacuum, the vapor pressure of the constituents in the salt are much higher than the vapor pressure of the uranium metal, or the U/TRU alloy in the case of actinide recovery. Consequently, the salt transitions from a solid, to a liquid, to a vapor. The vapor pressure of the salt becomes significant at temperatures of approximately 800°C and above, and mass transfer is noticeably accelerated. The salt vapors migrate to a cooler part of the distillation furnace where the salt vapors condense back to a liquid and are collected. Meanwhile, the uranium metal melts at approximately 1,130°C, but even at that high temperature the vapor pressure of uranium is low. A noticeable exception is cadmium used for the LCC. Cadmium melts at approximately 320°C and has a high vapor pressure, meaning that the cadmium will melt and distill before the salt.

3.6 Cadmium Pool in the EBR-II Driver Fuel Electrorefiner

The ER used to process EBR-II driver fuels for the SFT Program contains both cadmium and salt. As described earlier, the ER vessel is approximately 1-m in diameter and 1-m tall. The densities of molten cadmium and salt are approximately 7.5 and 1.7 g cm^{-3}, respectively. The salt floats on top of the cadmium as these phases are particularly immiscible.

The purpose of the cadmium pool has a historical origin. The early electrorefiner design concepts for the IFR Program included a deep cadmium pool beneath the salt. The intention was to submerge the basket containing the chopped fuel into the cadmium pool. The cadmium would dissolve metallic fuel and act as the anode. The uranium would transport from the cadmium pool, through the salt, and collect on the cathode mandrel as a refined metal product.

Such an electrorefiner may very well have been constructed for the IFR Program, except for the constraint that the FCF hot cell did not have enough overhead height to accommodate the envisioned design feature requiring a deep molten cadmium pool. As a compromise, the electrorefiner was designed with a shallow cadmium pool. The intention was to transport uranium from the anode basket, through the salt to the cadmium pool, then from the cadmium pool, through the salt to the cathode mandrel. The process was demonstrated at ANL in equipment that was about $1/4^{th}$ the scale of the equipment installed at ANL-W (now INL) in the FCF. However, operations during the SFT Program demonstrated that uranium could be transported from the anode basket, through the salt, to the cathode mandrel.

Today the ER is operated in four modes. Direct transport moves the uranium from the anode basket to the cathode mandrel. Anodic dissolution moves the residual anode materials, primarily uranium and zirconium, from the anode basket to the cadmium pool. Deposition moves the uranium from the cadmium pool to the cathode mandrel. And cathode stripping moves the uranium from the cathode mandrel to the cadmium pool.

There are pros and cons to having the cadmium pool in the ER vessel. The pros include the following.

- As described earlier, adding $CdCl_2$ to the ER salt is a very easy and convenient way of replenishing the UCl_3 concentration.
- Uranium that falls from the anode basket and cathode mandrel are dissolved in the cadmium pool and are easily recovered by the deposition operation described above.
- Electrochemical measurement or direct sampling of the cadmium pool provides a tool to assess fissile materials inventory in the ER.

The cons include the following.

- Cadmium has a noticeable vapor pressure at 500°C. Consequently, the cadmium permeates the salt and forms a cadmium vapor pressure in the headspace above the salt. Over time, this cadmium vapor condenses on the cooler parts of the lid assembly and causes electrical shoring between the anode and vessel, and cathode and vessel. This problem is mitigated by manually cleaning the affected areas.
- Cadmium is a Resource Conservation and Recovery Act (RCRA) metal, which complicates waste management and disposal. Adding $CdCl_2$ increases the overall cadmium inventory in the hot cell facility.

The cadmium pool in the ER vessel has nothing to do with the LCC technology described earlier. The cadmium pool is not used to recover TRU from the salt, although it is conceptually feasible.

3.7 Fission Product Radiochemistry

A reactor operating at 1,000 MW thermal consumes approximately 1 kg d^{-1} of fissile metals such as ^{235}U. A uranium nucleus contains 92 protons (Z = 92). The moment this nucleus splits into two daughters (primary fission fragments), there remain 92 protons between the daughters. The possible combinations of two daughters are listed in Table 22 along each row. These 36 daughters represent about 39% of the elements of the Periodic Table up to uranium.

However, there are about 383 possible daughter nuclide types as each daughter can be born as one of several isotopes. Many of these isotopes are ephemeral as the processes of radioactive decay begin immediately upon formation. There are many different modes of radioactive decay, some of the major modes are shown below:

Alpha Decay	${}^{A}_{Z}X \rightarrow {}^{A-4}_{Z-2}X' + {}^{4}_{2}\alpha$
Beta Electron Decay	${}^{A}_{Z}X \rightarrow {}_{Z+1}{}^{A}X' + {}^{0}_{-1}\beta + \nu'$
Beta Positron Decay	${}^{A}_{Z}X \rightarrow {}_{Z-1}{}^{A}X' + {}^{0}_{+1}\beta + \nu$
Electron Capture	${}^{A}_{Z}X + {}^{0}_{-1}e \rightarrow {}_{Z-1}{}^{A}X' + X\ ray$
Gamma Emission	${}^{A}_{Z}X^{*} \rightarrow {}^{A}_{Z}X' + \gamma\ ray$
Spontaneous Fission	${}^{A+B+C}_{Z+Y}X \rightarrow {}^{A}_{Z}X' + {}^{B}_{Y}X'' + Cn$

Here, Z is the atomic number (number of protons), A is the mass number (number of protons and neutrons), α is a helium nucleus, β is an electron (-) or a positron (+), ν is a neutrino, ν' is an antineutrino, X-ray and γ-ray are forms of high energy electromagnetic radiation, and n is a neutron.

Table 22. Primary Fission Fragments Pairs of Uranium

Daughter A	Z	Daughter B	Z
Copper	29	Europium	63
Zinc	30	Samarium	62
Gallium	31	Promethium	61
Germanium	32	Neodymium	60
Arsenic	33	Praseodymium	59
Selenium	34	Cerium	58
Bromine	35	Lanthanum	57
Krypton	36	Barium	56
Rubidium	37	Cesium	55
Strontium	38	Xenon	54
Yttrium	39	Iodine	53
Zirconium	40	Tellurium	52
Niobium	41	Antimony	51
Molybdenum	42	Tin	50
Technetium	43	Indium	49
Ruthenium	44	Cadmium	48
Rhodium	45	Silver	47
Palladium	46	Palladium	46

As an example, uranium can fission into ^{140}Xe and ^{94}Sr, and decay according to the following modes for ^{140}Xe:

$$^{140}_{54}Xe \rightarrow {}^{140}_{55}Cs + {}^{0}_{-1}\beta \ (13.6\ s)$$

$$^{140}_{55}Cs \rightarrow {}^{140}_{56}Ba + {}^{0}_{-1}\beta \ (1.06\ min)$$

$$^{140}_{56}Ba \rightarrow {}^{140}_{57}La + {}^{0}_{-1}\beta \ (12.75\ d)$$

$$^{140}_{57}La \rightarrow {}^{140}_{58}Ce\ (stable) + {}^{0}_{-1}\beta \ (1.678\ d)$$

and for ^{94}Sr:

$$^{94}_{38}Sr \rightarrow {}^{94}_{39}Y + {}^{0}_{-1}\beta \ (1.25\ min)$$

$$^{94}_{39}Y \rightarrow {}^{94}_{40}Zr\ (stable) + {}^{0}_{-1}\beta \ (18.7\ min)$$

Alternately, uranium can fission into ^{137}Xe and ^{95}Sr, and decay according to the following modes for ^{137}Xe:

$$^{137}_{54}Xe \rightarrow {}^{137}_{55}Cs + {}^{0}_{-1}\beta \ (3.82\ min)$$

$$^{137}_{55}Cs \rightarrow {}^{137}_{56}Ba\ (stable) + {}^{0}_{-1}\beta \ (30.07\ yr)$$

and for ^{95}Sr:

$$^{95}_{38}Sr \rightarrow {}^{95}_{39}Y + {}^{0}_{-1}\beta \ (25.1\ s)$$

$$^{95}_{39}Y \rightarrow {}^{95}_{40}Zr + {}^{0}_{-1}\beta \ (10.3\ min)$$

$$^{95}_{40}Zr \rightarrow {}^{95}_{41}Nb + {}^{0}_{-1}\beta \ (64.02\ d)$$

$$^{95}_{41}Nb \rightarrow {}^{95}_{42}Mo\ (stable) + {}^{0}_{-1}\beta \ (34.99\ d)$$

Notice that the decay chains of ^{140}Xe and ^{94}Sr lead to stable Ce and Zr, while those of ^{137}Xe and ^{95}Sr lead to stable Ba and Mo. Each of these decay paths are occurring simultaneously along with all other possible fission product pairs and isotopes, and their respective decay paths. Computer modeling of these phenomena for a specific reactor application can be done using burnup code as previously described, which predicts the composition of the fuel as a function of all the parameters associated with reactor operations. There are significant variations in fission product yield that are dependent on the neutron spectrum in the core, the fuel type, and the degree of burnup.

A consequence of these decay processes is that the compositions, decay heats, and radiation signatures of spent fuels are constantly changing. Presently, the SFT Program is processing EBR-II Mk-II generation driver fuels that are at least 50 years old. The JFCS Program processed oxide fuels that were at least 30 years old. The radiation signatures and decay heat load of these aged fuels are much lower than what would be experienced in the application of a nuclear reactor with a co-located pyroprocessing facility, as was envisioned for the IFR Program.

3.8 Consequences of Process Efficiency

This section presents two simple models of an integrated fuel reprocessing scheme that illustrate the importance of 1) maximizing the retention of actinides, and 2) maximizing the rejection of lanthanides, during reprocessing. This analysis applies generally to any reprocessing scheme be it aqueous reprocessing or pyroprocessing. The integrated fuel reprocessing scheme is illustrated in Figure 7.

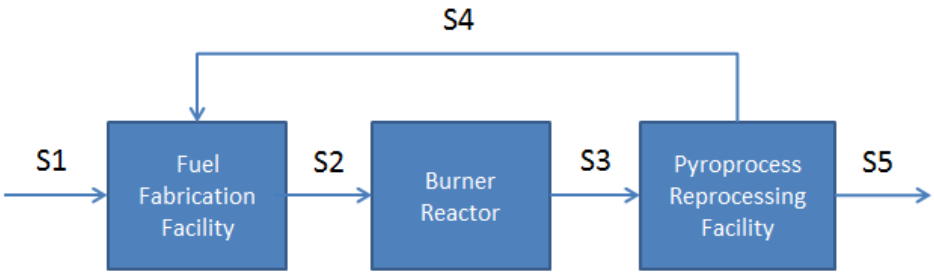

Figure 7. Illustration of an integrated fuel reprocessing scheme.

As is the case with an integrated recycle system, the composition of any process stream is affected, to one degree or another, by the performances and efficiencies of all the integrated processes. The process streams shown in Figure 7 are identified as follows.

- S1: Incoming stream to fuel fabrication. This stream is needed to sustain the fuel cycle. For example, it could contain HEU from an enrichment plant, or plutonium from weapons stockpiles or TRU recovered from LWR spent fuels.
- S2: Fresh fuel stream from fuel fabrication to the reactor. This is the reprocessed "new" fuel entering the reactor, it is not virgin fuel. It contains a complex mixture of uranium, plutonium, minor actinides, and lanthanides.
- S3: Spent fuel stream from the reactor to reprocessing. This is the "spent" fuel entering the reprocessing facility. It contains less fissile inventory and greater fission product inventory than the "new" fuel.
- S4: Recovered stream from reprocessing to fuel fabrication. This stream contains actinides and lanthanides that are retained in the fuel cycle.
- S5: Discharged stream from reprocessing to waste. This stream contains actinides and lanthanides that are rejected from the fuel cycle to the waste streams.

In general terms, the goals of nuclear fuel reprocessing are to maximize the retention of actinides, and minimize the retention of lanthanides, in the fuel cycle process. However, the separations sciences embedded within these two goals do not behave independently of each other. For example, those technologies which are deployed to maximize the retention of actinides will, at the same time, tend to increase the retention of lanthanides. In other words, if the primary goal is to meet some established target threshold for the retention of actinides (e.g., 99.5 wt% of the actinides must be retained in the fuel cycle), then the secondary goal becomes optimization of rejection of lanthanides while meeting that target. This is only one of many ways in which this engineering challenge of reprocessing can be expressed.

The integrated fuel reprocessing scheme illustrated in Figure 7 is considered in regard to the retention of actinides in the fuel cycle. A simple process efficiency model for actinide retention is illustrated in Figure 11.

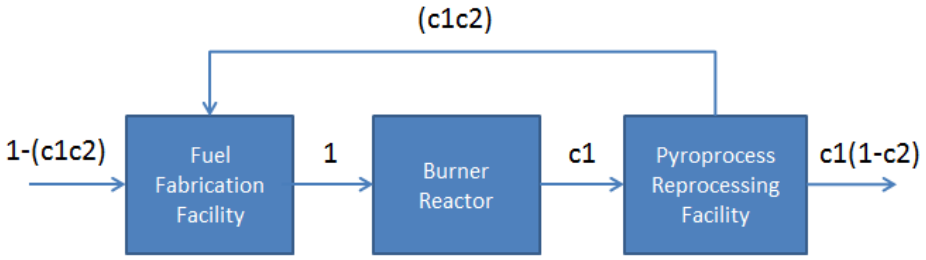

Figure 8. Process model for actinide retention.

The mass distribution parameters shown in Figure 8 are identified as follows:

- 1: Mass of Actinides in Stream S2. This value is normalized to 1, which means that the "new" fuel stream contains 1 arbitrary mass unit of actinides. In engineering units, this value would equal the actinide fuel demand of the reactor.
- c1: Mass of Actinides in Stream S3. This value is the mass of actinides in the "spent" fuel stream, expressed as a fraction of the mass of actinides in the "new" fuel stream.
- c2: Reprocessing Efficiency. This is the efficiency of the reprocessing facility to retain actinides in the fuel cycle.
- 1-c1: Reactor Efficiency. This is the efficiency of the reactor to burn actinides. This value is in terms only of comparison of the actinide loadings of the "new" and "spent" fuel streams. This is not a rigorous definition of burnup efficiency.
- c1c2: Mass of Actinides in Stream S4. This value is the mass of actinides in the recycle stream, expressed as a fraction of the mass of actinides in the "new" fuel stream.
- c1(1-c2): Mass of Actinides in Stream S5. This value is the mass of actinides in the waste stream, expressed as a fraction of the mass of actinides in the "new" fuel stream.
- 1-(c1c2): Mass of Actinides in Stream S1. This value is the mass of actinides needed to complement the mass of actinides in the recycle stream to meet the demand of the reactor.

Results of the model are presented in Table 23 and Figure 9. The loss of actinide to the waste stream (c1[1-c2]) from the reprocessing facility is shown as a percentage of the fresh actinide make-up (1-[c1c2]) to the fuel fabrication, for various values of 1-c1 and c2. This relationship is expressed in the following equation:

$$Actinide\ Loss\ (\%) = \frac{c1(1-c2)}{1-(c1c2)} \times 100$$

Typical prototype reactor designs give actinide burnup efficiencies ranging between 0.10 and 0.15. Considering this range as an achievable "near term" performance for proposed burner reactors, demonstrating actinide recycling efficiency better than 0.99 (>99%) is crucial to justifying the integrated burner/reprocessing cycle as an effective means of utilizing and minimizing actinide discharges to a long-term geological repository.

Table 23. Results of Actinide Model

Reactor Efficiency (1-c1)	Reprocessing Efficiency (c2)		
	0.98	0.99	0.999
0.05	27.54	15.97	1.86
0.10	15.25	8.26	0.89
0.15	10.18	5.36	0.56
0.20	7.41	3.85	0.40

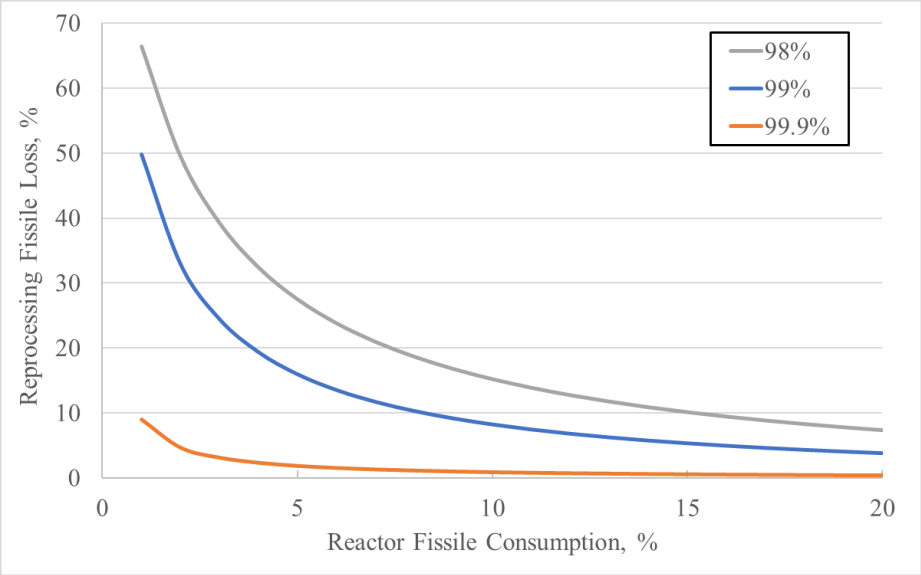

Figure 9. Relationship between burnup, reprocessing recovery, and fissile losses.

The integrated fuel reprocessing scheme illustrated in Figure 8 was considered for the rejection of lanthanides from the fuel cycle. A simple process efficiency model for lanthanide rejection is illustrated in Figure 10.

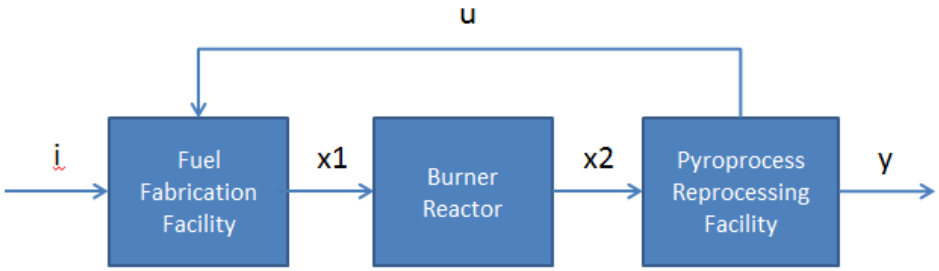

Figure 10. Process model for lanthanide rejection.

The mass distribution parameters shown in Figure 10 are identified as follows:

- i: Mass of Lanthanides in Stream S1. This value reflects a condition in which Stream S1 contains some mass fraction of lanthanides.
- x1: Mass of Lanthanides in Stream S2. This value is the mass of lanthanides in the new fuel stream.
- x2: Mass of Lanthanides in Stream S2. This value is the mass of lanthanides in the spent fuel stream.
- u: Mass of Lanthanides in Stream S4. This value is the mass of lanthanides in the recycle stream.
- y: Mass of Lanthanides in Stream S5. This value is the mass of lanthanides in the waste stream.

The model for lanthanide rejection achieves steady state values as the limit of the number of cycles (n) through the process approaches infinity. The following equations describe the model.

$$x1_n = u_{n-1} + i_n$$

$$x2_n = x1_n + b_n$$

$$y_n = c(x1_n)$$

$$u_n = (1-c)(x2_n)$$

$$x2_n = \frac{(i+b)(1-(1-c)^{n-1})}{c}$$

In the equations above, i_n is an impurity related constant associated with Stream S1, b_n is a burnup related constant associated with the reactor, and c is the rejection efficiency of lanthanides from the reprocessing facility. The model achieves steady state as the number of cycles (n) approaches infinity.

$$\lim_{n\to\infty}(x2_n) = \frac{(i+b)}{c}$$

$$\lim_{n\to\infty}(x1_n) = \frac{(i+b)}{(c-b)}$$

$$\lim_{n\to\infty}(y_n) = (i+b)$$

$$\lim_{n\to\infty}(u_n) = \frac{(1-c)(i+b)}{c}$$

Results of the model are presented in Table 24. This set of results reflects a case in which no lanthanides are present in Stream S1; which is to say, $i = 0$.

Table 24. Results of lanthanide model.

Relative Burnup in Reactor	Ln Generation in the Reactor (wt% of total fuel) (x2-x1)	Ln Rejection Fraction from Reprocessing y/x2	Ln to Fuel Fabrication (wt% of total fuel) u	Ln to Reprocessing (wt% of total fuel) x2
Low	2	0.9	0.22	2.22
	2	0.8	0.50	2.50
	2	0.7	0.86	2.86
	2	0.5	2.00	4.00
Medium	4	0.9	0.44	4.44
	4	0.8	1.00	5.00
	4	0.7	1.71	5.71
	4	0.5	4.00	8.00

Relative Burnup in Reactor	Ln Generation in the Reactor (wt% of total fuel)	Ln Rejection Fraction from Reprocessing	Ln to Fuel Fabrication (wt% of total fuel)	Ln to Reprocessing (wt% of total fuel)
	(x2-x1)	y/x2	u	x2
High	8	0.9	0.89	8.89
	8	0.8	2.00	10.00
	8	0.7	3.43	11.43
	8	0.5	8.00	16.00

Table 24 is divided into three sections representing low, medium, and high burnup in the reactor. This comparison is subjective, but for these purposes "low" burnup converts 2 wt% of the fuel mass to lanthanides; "medium" burnup converts 4 wt%; and "high" burnup converts 8 wt%. For each of the three levels of burnup, the table considered four values of reprocessing efficiencies: 0.9, 0.8, 0.7, and 0.5. A value of 0.9 means that 90 wt% of the lanthanides in Stream S3 are rejected to Stream S5. For the case in which the reactor is operated at a "medium" burnup, and the reprocessing efficiency is 80%, the "new" fuel to the reactor will contain 1 wt% lanthanides, due to the 1 wt% lanthanide return to fuel fabrication in Stream S4. And the "spent" fuel from the reactor will contain 5 wt% lanthanides, due to the additional 4 wt% lanthanide generation in the reactor. The actinide retention and lanthanide rejection models presented here are not, in the strictest sense, rigorous, but they do accurately reflect the consequences associated with these process effects.

However, what can be stated with certainty is that actinide retention and lanthanide rejection are not independent considerations, and that, generally, as we seek to increase actinide retention, lanthanide rejection will decrease. However, much remains unknown. For example, if it is deemed necessary to have 99.9% efficiency for actinide retention in the reprocessing facility, the corresponding maximum lanthanide rejection efficiency is presently unknown and there are no satisfactory tools for its estimation.

Nevertheless, much information can be gleamed from this data. The following are some of the observed relationships:

- Higher burnup improves the consumption of actinides.
- Increased actinide retention improves the consumption of actinides.
- If burnup is a limitation, then improved actinide retention can allow for higher consumption of actinides.
- Increased lanthanide rejection decreases lanthanide loading of the fuel.
- Higher burnup increases the lanthanide loading of the fuel.
- If actinides loading of the fuel is a limitation, then improved lanthanide rejection can allow for higher burnup.
- Improved purity of the actinide source material decreases the lanthanide loading of the fuel.

However, in practice each category is comprised of a family of elements with unique separations behaviors. The consequence of these unique behaviors is that each actinide will have an independent retention efficiency and each lanthanide will have an independent rejection efficiency; and, as is already understood, there will be some degree of overlap between the separation behaviors of the two families.

4. PYROPROCESSING PROCESS CHALLENGES AND ATTRIBUTES

4.1 Input Accountancy

Pyroprocessing has no analog to the input accountancy tank used for aqueous reprocessing. Pyroprocessing input accountancy requires other techniques. In the SFT Program, input accountancy is performed by a combination of burnup code and representative sampling. In the SFT Program, only EBR-II fuels, and a small inventory of Fast Flux Test Facility (FFTF) fuels have been treated. The histories of these fuels are well known and computer code for reactor physics burnup has been applied in most cases to calculate the compositions of the spent fuels. In addition, select samples of fuel segments from the chopping operations are collected for destructive analysis. These two sources of data are used for input accountancy. In the JFCS Program, the fuel elements were declad and the oxide fuels were crushed into powders. Representative samples of these powders were collected for destructive analyses. Input accountancy is addressed in much greater detail later in this report.

4.2 Materials Control and Accountancy

For both the SFT and JFCS Programs, the ER and OR vessels were volume calibrated following their fabrication. For example, the cylindrical ER vessel for the SFT Program is about 1-m in diameter and 1-m tall. The calibration procedure was to add purified water to the vessel in 2-kg increments and measure the water depth after each addition. By this method, a calibration curve was developed that relates water depth to water volume. During ER operations, a salt level probe is inserted from the top and lowered until it contacts the surface of the salt, and contact is determined by electrical continuity measurements through the probe and vessel. The probe is calibrated such that it measures the depth of the salt which, together with the calibration curve described above, provides the volume of salt in the vessel. The density of the salt is determined empirically through the chemical composition of the salt. The volume and density of the salt provide the mass of the salt in the vessel. A similar approach was used for the JFCS Program for both the ER and OR vessels.

The level measurement technique works well provided the vessel is filled with a homogenous liquid. The technique loses accuracy and precision when, for example, there are solid phases present in the vessel as well. In this instance the technique still provides the total volume occupied in the vessel, but determining the volume of liquid and solid phases individually is challenging. Examples of solid phases are oxide sludges on the bottom of the OR vessel, uranium metal on the walls of the ER vessel, and zirconium inventory accumulated in the ER vessel.

The Fuel Conditioning Facility (FCF) and Hot Fuels Examination Facility (HFEF) hot cells are divided into zones for materials control and accountancy (MC&A) purposes. These zones are administratively defined areas within the hot cells that do not necessarily have any physical barriers. The materials inventories in each zone, and that transfer of materials between zones, are tracked by computer software that is a combination of process modeling and database capabilities. FCF uses software for this purpose that was originally developed for the IFR Program called the Mass Tracking (MTG) System. MC&A is addressed in much greater detail in Section 6.

4.3 Salt Homogeneity and Sampling

During the SFT and JFCS Programs, ER and OR salt samples are routinely collected and analyzed. In conjunction with a lack of active salt mixing, temporary compositional stratification of ER salt has been observed immediately following termination of electrorefining operations. The temporary stratification effect manifests as an upper salt layer with a distinctly lower concentration of UCl_3, and a lower salt layer with a distinctly higher concentration of Ucl_3, within the ER vessel. However, the stratification dissipates shortly after electrorefining is terminated by turning off the current between the anode and cathode. It has generally been observed that when no current is flowing, OR and ER salts have homogenous compositions due to the action of mechanical agitation in the salts and/or the natural convective flow of

salts. Thus, the homogeneity of the salt should not be assumed without proper validation in any operating OR and ER cell.

It is generally the practice at INL to collect salt samples that are approximately 1-g for chemical analyses. The homogeneity of the bulk salt is important in order for the small 1-g salt sample to be representative of the composition of the bulk salt. A reoccurring problem with salt sampling is metal particulate suspended in the salt. This is true of chloride and fluoride salts. For example, when analyzing to determine the uranium concentration in an ER salt, the information most often sought is the concentration of Ucl_3. However, the currently practiced analytical techniques dissolve salt samples as a whole in an acidic solution and cannot distinguish between uranium present as Ucl_3, or uranium present as small particles of uranium metal entrained in the salt sample.

The hygroscopic nature of OR and ER salts can also contribute to analytical error stemming from sample handling. If the salt samples absorb water before the tare weights are taken prior to digestion of the samples, the concentrations determined by the chemical analyses will be biased lower than they are because the sample weights will be biased higher than they are.

4.4 Oxide Reduction

The basic chemistries of oxide reduction in the OR cell, and electrorefining in the ER cell, were discussed earlier and it was shown how the rate of electrorefining in the ER cell is controlled by the amperage supplied to the circuit by the external DC power supply. This is true up to a limit that is set by factors such as the surface areas of the electrodes and the concentration of Ucl_3 in the salt. The rate of oxide reduction in the OR cell does not behave in the same way. The rate limiting step in oxide reduction is the diffusion of reactants and products into and out of the bed of material in the cathode basket that is undergoing conversion from oxide to metal. All things being equal, oxide reduction takes considerably more time than electrorefining.

For example, consider the oxide fuel reduction sequence when lithium is the reductant. Lithium cations permeate the salt at every location. Lithium cations are reduced to metal at the electroactive surface of the cathode. The lithium metal diffuses into a bed of material in the cathode basket, which becomes a mixture of oxide fuel and metal fuel as reduction proceeds. The lithium metal reacts with oxide fuel, to oxidize the lithium, and reduce the fuel to metal. The Li_2O formed dissolves into the salt. The oxygen anions migrate through the bed of material into the bulk salt, and through the bulk salt to the anode, where they are oxidized to oxygen gas at the electroactive surface of the anode. The oxygen gas forms bubbles on the surface of the anode. The gas rises to the surface of the salt, where it is channeled away and discharged from the OR cell.

4.5 Different Fuel Types

In the IFR Program, pyroprocessing was to be applied to SFR HEU-10Zr metal fuel to recover electrorefined HEU/Zr alloys for the purpose of making reprocessed fuel for EBR-II, which was never demonstrated. In the SFT Program, pyroprocessing is applied to SFR HEU-10Zr metal fuel to recover electrorefined LEU for future uses. In the JFCS Program, pyroprocessing was applied to LWR LEU oxide fuel to recover electrorefined LEU/TRU alloys for the purpose of making SFR metal fuel specimens that were irradiated in the INL ATR. In all these applications, the fuel being processed had only the TRU that was bred into the fuel while it was in the reactor, which means the TRU concentrations in these spent fuels were low. This allows the TRU to accumulate in the ER salt slowly as uranium is electrorefined. However, in the future, pyroprocessing may be applied to SFR DU-20TRU-10Zr metal fuels to recover DU/TRU/Zr alloys for reprocessing. Pyroprocessing of high-TRU fuels will have new challenges with regards to TRU management.

Mixed oxide fuels have been developed for use in both thermal and fast reactors. A pyroprocess called the "*Salt Cycle Process"* to reprocess MOX fuels was developed at Hanford in the 1950s and 1960s. Research on the process in the U.S. was dropped after an engineering-scale demonstration. However, to support MOX fuel reprocessing, development continued in Russia under the names "*Dimitrovgrad Dry Process* and the *Russian Institute of Atomic Reactors (RIAR) Dry Process*." This process uses molten salt electrochemistry to recover purified UO_2, PuO_2, or a mixture of UO_2 and PuO_2 from spent MOX fuel, or from other uranium- and plutonium-bearing feedstocks.

4.6 Process Wastes

All process wastes require a disposition path. In some cases, the wastes are treated within the flowsheet, in other cases the wastes are shipped to a waste facility. The receiving waste facility establishes the waste acceptance criteria for the facility. Therefore, wastes to be shipped to a waste facility must meet the acceptance criteria of the receiving waste facility. Until the establishment of waste facilities and acceptance criteria, pyroprocessing waste form development is open ended. Likewise, until the establishment of pyroprocessing waste characteristics, the requirements for waste facilities and acceptance criteria are open ended. There must be mutual compatibility between the waste generators, waste shippers, and waste repositories with regards to mutually acceptable waste acceptance criteria.

Of all the waste generated by pyroprocessing, ER salts have received the most attention. The reason is that ER salts accumulate Group 1, Group 2, lanthanides, and transuranic metals as electrorefining progresses. Obviously, the ER salt requires a management strategy to deal with its ever-changing composition and ever-increasing volume. The useful life of salt can be limited by its increasing liquidus temperature, its increasing thermal load with respect to decay heat, and its increasing volume. When it is necessary to dispose of salt, several strategies have been considered. Nearly all are discussed in the open literature.

4.7 Corrosion

The SFT Program is performed in the INL FCF hot cell that is divided into air- and argon-atmosphere compartments. Similarly, the JFCS Program was performed in the INL HFEF hot cell that, likewise, is divided into air- and argon-atmosphere compartments. In the argon-atmosphere compartments, the oxygen and moisture levels are maintained by a purification system to levels nominally below approximately 50 ppm each. Generally, fuel assemblies were disassembled in the air cells, and the fuel elements were transferred into the argon cells for the chopping and decladding operations. During the pyroprocessing operations, no significant equipment corrosion has resulted from the oxygen and moisture levels in the argon-atmospheres. However, metallic fuels and bond sodium are highly reactive materials when exposed to oxygen and moisture. When exposed to the argon-atmosphere, corrosion of these materials ensues at rates governed by the metal compositions and surface areas. Uranium and plutonium alloys can experience surface oxidation. Whereas the bond sodium will eventually completely oxidize and become a powder, albeit slowly.

Pyrophoricity is generally thought of as the spontaneous ignition of a material when exposed to air, although this is an oversimplification of the condition. Pyrophoricity is not a problem in the argon-atmosphere hot cell compartments. For example, the highly dendritic high-surface-area electrorefined uranium may be pyrophoric in air under the right conditions, but not in the hot cell argon-atmospheres. However, pyrophoricity is not an unusual condition as it applies to many finely divided high-surface-area metals such as aluminum and magnesium. The pyrophoric tendencies of a material are governed by a combination of the rate of oxidation and the rate of dissipation of the resulting heat. Ignition can occur when the former is high, and the latter is low.

For the SFT Program, the materials of construction of the ER cell include plain carbon steels, Cr/Mo alloy steels, and stainless steels. The chemical condition of ER salts is reducing with respect to the chlorine and oxygen chemical potentials, largely due to the presence of uranium metal which buffers these potentials to low levels. Corrosion of the materials of construction has been negligible, especially considering that the ERs used for the SFT Program have been in operation since 1996, which is about 27 years at this time.

For the JFCS Program, the materials of construction of the ER and OR cell were stainless steel. An important exception is the oxygen-evolving anode in the OR cell. The anode in the OR cell had a rather complex engineering design. The platinum-group metals served as the anodes, ceramic shrouds contained and directed the flow of oxygen gas evolved at the anodes, and nickel alloys served as the structural housing of the anode assemblies. The chemical condition of OR salts is much more complex than that of the ER salts. Again, the chlorine and oxygen chemical potentials are low at the cathode due to the presence of lithium and uranium metals. However, the oxygen chemical potential is high at the anode due to the presence of oxygen gas. The primary mechanism for corrosion in the OR cell is high temperature oxidation resulting from the oxygen gas evolved at the anode.

Many of the process crucibles used for the high-temperature operations of distillation and casting are graphite crucibles with castable ceramic liners such as zirconia, yttria, and alumina, depending on the application as previously discussed. These coatings degrade over time and the crucibles must be either relined or disposed of. The high-temperature furnaces have various components, liners, and heatshields made of stainless steel, molybdenum, and tantalum that are subject to corrosion over time.

4.8 Reference Electrodes

Reference electrodes (RE) are used in OR and ER cells as datum from which to measure the potentials of other electrodes in the cell. A RE can distinguish between stainless steel, uranium, and lithium in the OR cell, and between stainless steel, cadmium, zirconium, and uranium in the ER cell. This information is used for process control.

Suitable REs are the Ni/NiO in the OR cell, and the Ag/AgCl in the ER cell. The Ni/NiO RE is comprised of a magnesia tube with a porous frit on the bottom. Inside is a nickel wire packed in a bed of NiO powder. When the RE is submerged, the molten salt permeates the frit and the NiO powder. A pseudo-equilibrium is established between the nickel wire and Ni^{2+} cations in the salt. However, because of the porous frit, this RE is not stable over time from mixing of the reference salt and the bulk salt through the frit. The Ag/AgCl RE is comprised of a mullite closed-bottom-tube. Inside is a silver wire packed in a bed of LiCl-KCl eutectic salt with a nominal concentration of AgCl. Alternatively, the salt can be AgCl. An equilibrium is established between the silver wire and Ag^{+} cations in the salt. The reference salt and the bulk salt communicate through the mullite tube. Because the mullite tube is a closed tube, there is no mixing between the reference salt and the bulk salt. This type of RE has shown to be stable in ER salt during years of service.

4.9 Process Equipment Scaleup

There are important caveats, but aqueous reprocessing is largely thought of as a “continuous operation,” while pyroprocessing is largely thought of as a “batch operation.” This is because it is difficult to envision how high-temperature operations such as oxide reduction, electrorefining, distillation, and casting can be performed with actinide materials in a continuous manner, although efforts have been made. However, even batch operations, if orchestrated properly, can at least mimic continuous operations.

When inherent engineering constraints limit the size of a particular unit operation, and there are such constraints, the solution to increase the throughput rate is often to simply duplicate the unit operation. For example, if the size of the anode basket for electrorefining is constrained by criticality limits, then have more anode baskets. If the size of the salt mass in an ER vessel is constrained by criticality limits, then have more ERs. Based on the nature of reprocessing spent fuels, it may often be the case that the size of a unit operation is constrained by criticality limits, or the ability to maintain the requirements of MC&A.

4.10 Planar Electrode and Scraped Cathode Designs

Planar electrode designs incorporate rows of alternating anode and cathode electrodes in a rectangular geometry. The purpose is an attempt to provide design options that 1) efficiently utilize the available space and minimize the salt volume, 2) accommodate automated remote system hot cell operations, and 3) accommodate equipment modularity and redundancy for scaleup. The baskets holding solid materials tend to be thin and rectangular.

Scraped cathodes are for ER applications. As the uranium dendrites form on the cathode rods, a scraping mechanism is actuated that disengages (scrapes) the dendrites from the cathode rods. The dendrites fall through the salt by gravity into a product collector (receiver crucible) underneath the cathode rods. Some designs allow the scraping mechanism to also serve as a compactor for the purpose of increasing the amount of electrorefined uranium contained in the product collector upon removal. Electrorefined uranium is recovered by removing and emptying the product collector. A conceptual ER cell with planar anode baskets (four assemblies) and scraped cathodes (five assemblies) is shown in Figure 11. The surface of the salt (not shown) would be below the tops of the cathode rods and anode baskets. The product collectors (not shown) would be underneath the cathode rods.

In OR applications, the oxide fuel is loaded into similar rectangular baskets as shown in Figure 11. However, the scraped cathode rods are replaced with a series of semi-inert or consumable anodes.

The SFT Program does not use planar electrode designs or scraped cathodes. Here, chopped EBR-II fuel elements are loaded into a cruciform anode basket with four compartments, and electrorefined uranium is collected on a plain-carbon-steel cathode mandrel. In this arrangement, electrorefined uranium is recovered by removing the cathode mandrel from the ER vessel and scraping the uranium from the cathode mandrel externally to the ER vessel. Cladding hulls are recovered by removing the anode basket from the ER vessel, opening the doors of the four individual compartments, and removing the hulls. Photographs of an anode basket being emptied of hulls, bare cathode mandrel, and cathode mandrel with electrorefined uranium are shown in Figure 12. The SFT Program is in the process of testing a scraped cathode design for uranium electrorefining. Trials with depleted uranium are expected to begin in 2024.

The JFCS Program does use planar electrode designs and scraped cathodes. Here, oxide fuel elements are declad, the oxide material is sized and loaded into rectangular baskets that serve as the cathodes during oxide reduction, and the same baskets serve as the anodes during uranium electrorefining. In the OR, the anodes evolve O_2(g) and are spaced between a series of cathode baskets. In the ER, the cathodes collect electrorefined uranium deposits and are spaced between a series of anode baskets. The electrorefined uranium is scraped into a product collector with compaction. As described earlier, the batch sizes used for the JFCS Program are in the order of a few kilograms.

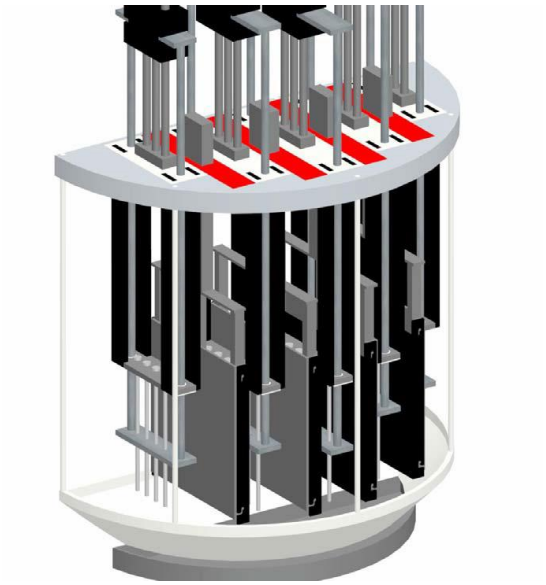

Figure 11. Conceptual electrorefiner with planar anode baskets and scaped cathodes.

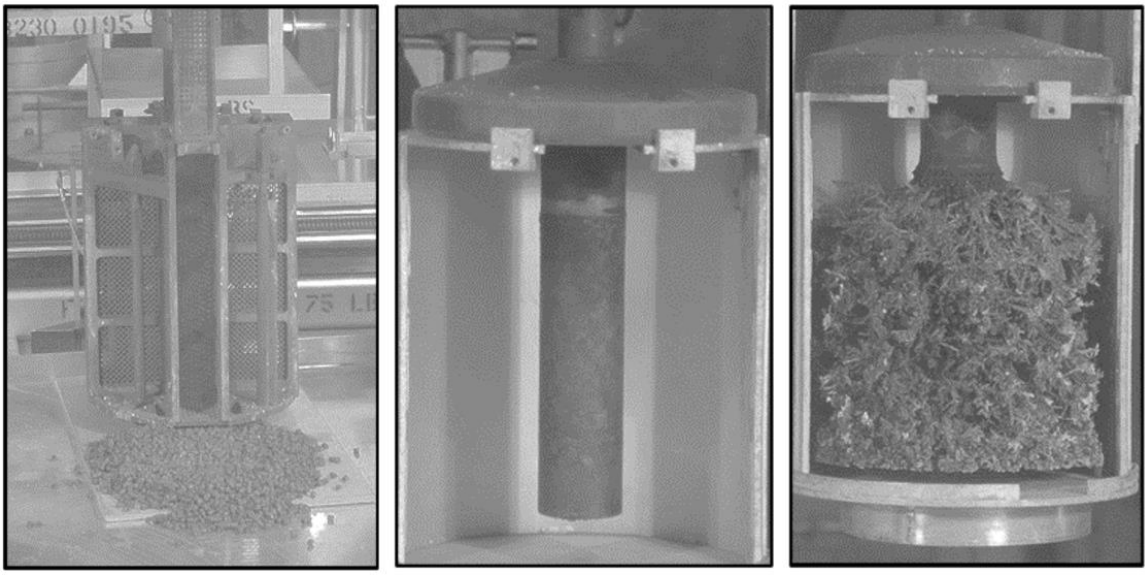

Figure 12. From left to right, photographs of an anode basket, bare cathode mandrel, and cathode mandrel with electrorefined uranium deposit.

Determination of whether planar electrodes and scraped cathodes are an appropriate design choice is entirely application specific. The type of fuel to be processed and the fuel cycle goals must be considered. The intent is to develop equipment designs that are more amenable to automated operations.

4.11 Manual versus Automated Process Operations

The pyroprocessing equipment associated with the SFT and JFCS Programs are operated manually. Some of the unit operations have mechanized components that are controlled by system software, but these are limited to simple tasks that are overseen by staff. Most of the work is performed by staff using mechanical telemanipulators. It is generally accepted that this degree of manual operation and human involvement in the process would not be practical for a commercial scale pyroprocessing facility. Consequently, efforts to scale-up the equipment designs are synonymous with efforts to automate the equipment designs.

4.12 Process Equipment Holdup

Process equipment holdup includes the accumulation of unaccounted materials in process equipment. Identifying and tracking holdup is a MC&A issue with consequences for process operations and criticality safety. Examples of holdup include oxide sludge in the OR and ER vessels, uranium metal and transition metal fission products in the ER vessel, salt in the distillation furnace heat shields and vacuum system, fuel residue in the decladding and chopping operations, and casting dross in the casting furnace crucibles. Cross contamination is the contamination of a batch by materials from previous batches. Cross contamination often occurs as the result of holdup. Cross contamination may not be detrimental to operations, but it makes MC&A more challenging.

Strategies to manage holdup and cross contamination include equipment disassembly, cleaning, and inspection. Individual equipment components can be weighed to determine if they have gained or lost weight. Oxide sludge in the OR and ER vessels can be chlorinated into salt. And uranium metal in the ER vessel can be chlorinated into the salt or recovered by electrorefining from the vessel to the cathode mandrel. Holdup is addressed in much greater detail in Section 6.

4.13 Material At Risk

“Material at Risk” is a term used at INL to describe material within the hot cells that would adversely contribute to an accident scenario involving either the loss of the inert atmosphere within the hot cells or the loss of containment of the hot cells. Materials of concern include pyrophoric material, combustible material, and radiological material. The consequences of an accident involving radiological material are mitigated by imposed limits on the quantity of exposed pyrophoric material allowed in the hot cells and by imposed limits on the quantity of radioactive materials in the hot cells.

Conservatively, the pyrophoricity of all process materials and process streams must be considered under normal operating conditions and off-normal operating conditions as unique situations may arise. Table 25 provides a summary of materials contributing to “material at risk”.

Table 25. Summary of the Materials Contributing to “Material at Risk.”

Name	Description
Breached SFR Metal Fuel	Sodium-bonded metal fuel that has breached cladding exposing the sodium and the fuel to the atmosphere.
Air Oxidized SFR Metal Fuel	Sodium-bonded metal fuel that has been oxidized by exposure to air or oxygen in the hot cell.
Water Oxidized SFR Metal Fuel	Sodium-bonded metal fuel that has been oxidized by exposure to water or moisture in the hot cell.
ER Uranium Dendrite (Salt Coated)	Electrorefined uranium recovered as a cathode deposit. The uranium exhibits the dendritic morphology associated with a very high surface area. As recovered, the material is approximately 10 wt% salt, which may provide some protection against pyrophoricity.

Name	Description
ER Uranium Dendrite (Salt Free)	Same as above but the salt has been removed by distillation rendering the material more susceptible to pyrophoricity.
ER Anode Residue (Salt Coated)	Includes the cladding hulls, transition metal fission products, and unoxidized fuel residue. As recovered, the material is approximately 27 wt% salt, which may provide some protection against pyrophoricity.
ER Anode Residue (Salt Free)	Same as above but the salt has been removed by distillation rendering the material more susceptible to pyrophoricity.
Uranium Ingots	The SFT Program generates HALEU ingots between approximately 3 and 50 kg. Although these ingots have a low surface area compared to the dendritic form of uranium, they could potentially contribute as combustible material in the event of a fire.
Uranium Casting Dross	Uranium casting dross is produced in both the zirconia- and yttria-lined process crucibles used in the distillation and casting furnaces. These drosses can contain finely divided uranium metal making them potentially reactive to oxygen, moisture, and water.
Metal Waste Ingots	The SFT Program generates metal waste ingots that are approximately 50 kg. Because these ingots have radiological content, they could potentially contribute to a radiological release.
Process Samples	The SFT Program collects process samples of the chopped EBR-II driver fuel and uranium pin samples from the casting operations. Because these samples have radiological content, they could potentially contribute to a radiological release.
OR and ER Salts	OR and ER salts are not pyrophoric or combustible, but they do have radiological content. Upon solidification, particulate could become airborne and contribute to a radiological release.
OR and ER Salt Sludge	This includes solid materials lost to the OR and ER salts that report as a sludge on the bottom of the vessels. The sludge can be recovered mechanically. Like casting dross, the sludges can contain finely divided uranium metal making them potentially reactive to oxygen, moisture, and water.
OR Reduced Metal (Salt Coated)	Oxide fuel is reduced to metal in the OR cathode basket. Like electrorefined uranium that has the dendritic morphology, the reduced metal in the OR cathode basket will also have a high surface area. As recovered, the material is approximately 10 wt% salt, which may provide some protection against pyrophoricity.
OR Reduced Metal (Salt Free)	Same as above but the salt has been removed by distillation rendering the material more susceptible to pyrophoricity.
Graphite Process Crucibles	Graphite crucibles are used in the distillation and casting operations. Because these crucibles have radiological content, they could potentially contribute to a radiological release.

"Material at risk" applies to materials that are exposed to the hot cell atmosphere. Once the materials are contained within an approved "closed metal confinement (CMC)" container within the hot cell, then the materials are no longer considered "material at risk". These containers must provide a "confinement boundary" that provides a high likelihood of protecting the contained materials from air. CMC containers are engineered for specific materials and storage locations.

4.14 Hydrogen Release

Many of the metals in spent nuclear fuel are highly reactive with moisture and water. The release of $H_2(g)$ will occur under some conditions when a metal is oxidized by water.

$$xMe + yH_2O = Me_xO_y + yH_2(g)$$

Such reactions can occur rapidly and produce a great amount of thermal energy, as in the case of sodium metal reacting with water. Or the reactions can occur slowly, as in the case of breached SFR fuel reacting with moisture in the argon atmosphere within the hot cell. Materials such as casting drosses, OR salts, ER salts, and process crucibles can also contain finely divided metals that can react with water as shown above.

4.15 Decay Heat Load

Decay heat is the thermal energy emitted by spent fuel as the fission products decay to other isotopes until a stable isotope is reached. Decay heat is a function of fuel composition, neutronics history in the core, and age since removed from the core. The decay heat load of a mass of material is measured in watts. During pyroprocessing, much of the decay heat load is transferred to the OR salt in the forms of Group 1 and Group 2 fission products, to the ER salt in the form of Group 1, Group 2, and lanthanide fission products, and to the ER anode sludge in the form of transition metal fission products. Decay heat load is certainly higher in new spent fuel compared to old spent fuel. The cooling curves for EBR-II driver fuels are shown in Figure 13. These data were modeled using ORIGEN code[1] and include many different fuel types and burn-up histories. After about 5 years the decay heat load has decreased by approximately two orders of magnitude, and the rate of cooling has significantly slowed.

For example, a typical EBR-II Mk-III (U-10Zr) fuel assembly with 61 fuel elements, had a decay heat load of approximately 1,500 W when initially removed from the reactor, and approximately 500 W after about 100 days of cooling. The electrorefiner anode baskets designed for the IFR Program could accommodate chopped fuel from three assemblies, bringing the decay heat load to 1,500 W per batch if this 100-days-old spent fuel were being processed. Although decay heat poses no issues with the salt chemistry inside the OR and ER cells, there is a practical limit that will require the fuel to cool for years before being processed.

Most of what makes spent fuel radioactive is concentrated into the OR and ER salts. These locations become sources of extremely high radiation levels which has consequences on the electronic equipment supporting these operations.

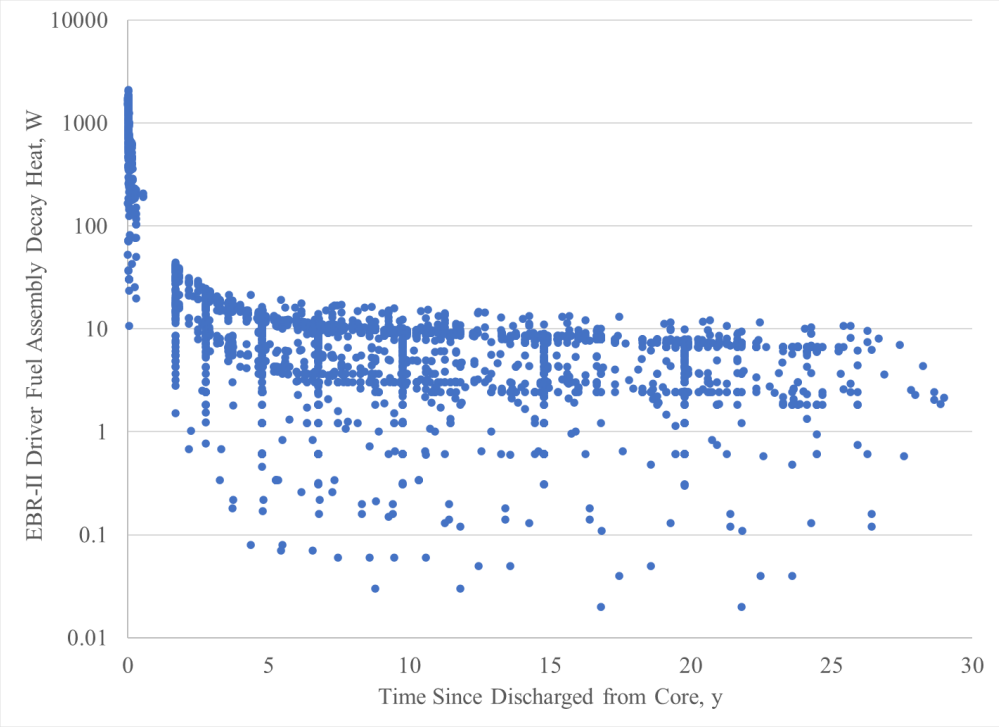

Figure 13. EBR-II driver fuel cooling curve.

4.16 Criticality Limits

Aqueous reprocessing and pyroprocessing are different with regards to criticality engineering. In an aqueous system, the actinides are dissolved in either water or organic solvents. Both hydrogen and carbon are strong neutron moderators. Consequently, there are strict limits with regards to solution concentrations and the geometric configurations of piping and tankage. By comparison, in pyroprocessing actinides are dissolved in molten chloride salts. Chlorine is not a neutron moderator. Therefore, compared to aqueous reprocessing, pyroprocessing is much less encumbered by limitations of solution concentrations and geometric configurations. For example, ER salts containing 10 wt% HEU and 10 wt% TRU as metal chlorides dissolved in LiCl-KCl eutectic, in a cylindrical vessel 1-m in diameter and 0.5-m deep, is possible. In addition, in the FCF and HFEF hot cells, great care is taken to minimize the amount of neutron moderators in the hot cells. This difference in criticality engineering between aqueous reprocessing and pyroprocessing is the main reason for the claim that a pyroprocessing facility will have a smaller facility footprint than an aqueous reprocessing facility.

4.17 Service Life of OR and ER Salts

As fission products accumulate in the OR and ER salts, there comes a limit where the salts must be managed by some combination of chemical processing and waste disposal. There are competing factors that will cause this limit. These include liquidus temperature, decay heat load, excess volume, and administrative limitations based on safety considerations. The safety considerations are based on assessments of catastrophic events such as earthquakes and loss of the hot cell environment and radiation containment. Typically, to add conservatism to the safety basis, the OR and ER salts are considered as point sources of high concentrations of actinides and fission products.

4.18 Loss of Power Event

Interruptions to facility-wide utility power can be mitigated by backup power systems such as batteries and diesel generators. Pyroprocessing flowsheets utilize several different high temperature unit operations such as OR and ER cells containing molten salt, distillation furnaces, and casting furnaces. Loss of power to the process equipment can lead to possible equipment damage. Equipment designs must tolerate loss of power at any point in the process cycle and tolerate the recovery of operations once power is restored.

The OR and ER cells are meant to be constantly maintained at their operating temperatures keeping the salts molten. Conceptually, one cell can have a salt inventory on the order of 1 MT or more. An extended loss of power will eventually lead to the salt freezing inside its containment vessel. Liquid salt is less dense than solidified salt. Therefore, freezing results in volume contraction, and melting results in volume expansion. Both volume contraction and expansion can result in mechanical stresses on the containment vessel and any equipment inside the containment vessel. Therefore, damage to the containment vessel can occur during freezing, but damage is potentially more likely to occur during reheating as the expanding salt presses against the vessel walls. In some design concepts, the primary containment vessel is surrounded by a secondary containment vessel, and the space between the two vessels is monitored for salt intrusion that would indicate the failure of the primary containment vessel.

Salt in an OR or ER cell is a complex chemical system. Phase separation will occur as the salt cools between the liquidus (the onset of solidification) and solidus (the completion of solidification) temperatures. A consequence of such phase separation is that fission products and actinides become concentrated in a smaller volume of molten salt as solidification progresses. This can have consequences on factors such as the decay heat load limits with respect to fission product concentrations, and the criticality limits with respect to actinide concentrations.

Distillation and casting furnaces will contain molten salt and molten metal at different times within the process cycles. These molten materials will be contained in process crucibles or, in the case of distillation furnaces, condensing on heat shields as the vapors are migrating from the hot zone to the cold zone. Loss of power during a process cycle can potentially damage the equipment and crucibles by the same mechanical stresses described above for the OR and ER vessels. However, following a loss of power event the subsequent recovery is more complex for a distillation furnace with salt than it is for a casting furnace with no salt. The distillation furnace has the added complexity of remelting the salt throughout the system between the hot zone and the cold zone.

In general terms, loss of power to high-temperature process equipment can result in cooling rates greater than those encountered during normal operations. Or interruptions to the processes that are more difficult to recover from than simply reenergizing the equipment, such as remelting solidified salts and metals. All of these off-normal conditions may lead to mechanical stresses that can damage equipment. However, this does not necessarily pose a safety risk.

4.19 Exposure of Salts to Oxygen and Moisture

LiCl is a highly hygroscopic salt, meaning that it is a powerful desiccant capable of absorbing moisture from the atmosphere. In a study performed at INL, a 40-g sample of LiCl collected 63 g of water from an air atmosphere at 32°C and 40% relative humidity, effectively turning the LiCl into a pool of salt water. KCl and NaCl are not nearly as hygroscopic as LiCl. Some aqueous brines can be returned to metal chlorides by simple drying in air under elevated temperatures. However, many of the more reactive metal chlorides will form oxychlorides during simple drying. These more reactive metal chlorides require the presence of a chlorine chemical potential in the form of $Cl_2(g)$ or HCl(g) to prevent the formation of oxychlorides and return the salts to chlorides.

Lanthanide and actinide chlorides are highly reactive with oxygen and moisture. The exposure of high-temperature salts containing lanthanide and actinide chlorides to ambient air will result in the oxidation of these metals, and in certain cases, the vapor transport of materials to cooler locations where they recondense as solids. This facet of molten salt chemistry has not been well studied.

OR and ER salts exposed to air cannot be recovered by simple drying processes. Exposure to air will oxidize many of the metal constituents in these salts, and the salts can only be fully recovered by processes of repurification and chlorination.

Pyroprocessing facilities are generally envisioned as a hot cell facility containing the pyroprocessing equipment. The atmosphere within the hot cell is maintained as dry argon with low concentrations of oxygen and moisture. Within the hot cell there is strict control of materials that moderate neutrons. In an event where the hot cell loses its argon atmosphere and ambient air enters the hot cell, the absorption of water by hygroscopic salts will act as a mechanism to introduce moderator into the hot cell environment. The consequences of this should be considered from the standpoint of criticality safety.

There are similar safety considerations for pyroprocessing salts that are stored in steel containers. Exposure to air will cause the salt to deliquesce into a pool of salt water. This will accelerate the corrosion of the steel container and introduce moderator into the storage area.

INL performed an exposure test of a typical ER salt. A salt mixture of LiCl-KCl eutectic and approximately 4 wt% UCl_3 was prepared and melted at 500°C in a purified argon atmosphere with oxygen and moisture levels below a few ppm. A photograph of the resulting sample is shown in Figure 14 (left). Solidified LiCl-KCl eutectic salt would be white and the dark color, almost black, is characteristic of LiCl-KCl eutectic salt with some UCl_3. This sample was then reheated to 500°C in an unpurified air atmosphere for 24 hr and allowed to cool for 24 hr. A photograph of the resulting sample is shown in Figure 14 (right). The yellow color indicates that some of the UCl_3 was oxidized.

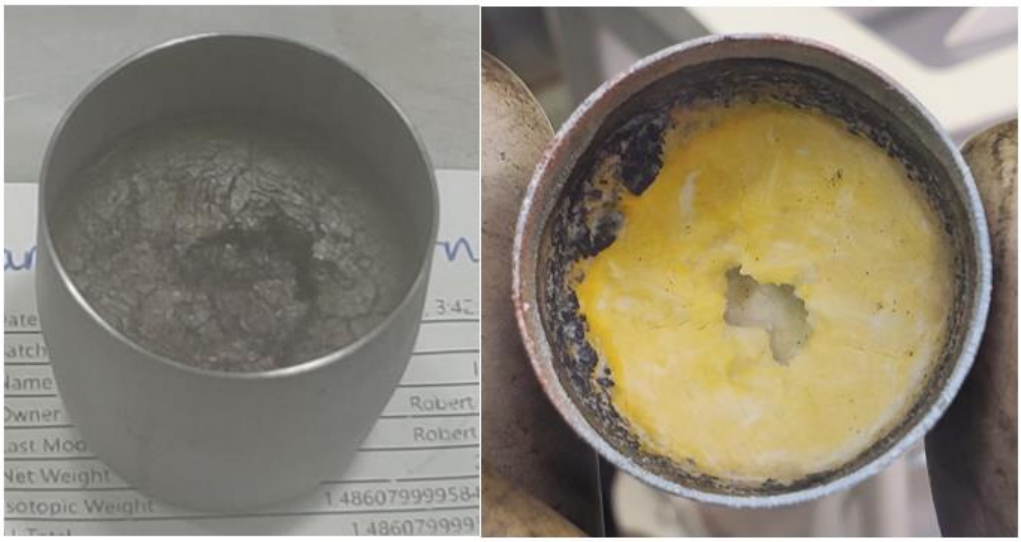

Figure 14. Photographs of LiCl-KCl-UCl_3 salt before (left) and after (right) exposure to air at 500°C.

INL performed an exposure test of LiCl-KCl eutectic salt. A 40-g puck of salt was exposed to air in an atmospheric oven at 32°C and 40% relative humidity for 1,150 hr. Afterwards, there was a mass gain of approximately 19 g due to the absorption of water from the air. Nearly all the mass gain occurred in the first 350 hr, with little additional gain until the test was ended at 1,150 hr. Photographs of the resulting sample are shown in Figure 15. Figure 15 (left) is the salt at the beginning of the test, and Figure 15 (right) is the salt at the end of the test. At the end of the test, the puck is surrounded by a pool of salt water.

Figure 15. Photographs of LiCl-KCl salt before (left) and after (right) exposure to air at 32°C.

4.20 Casting Crucible Failure

In the SFT Program, graphite crucibles are used in distillation and casting furnaces as previously described. Three different castable liners are used. Zirconia is used when the contents are uranium and salt. Yttria is used when the content is salt-free uranium. And alumina is used when the contents are cladding hulls and salt. Crucible failure generally means that the ceramic lining materials failed in some way to expose the graphite. When this occurs, the crucible is disposed of. Generally, crucibles last from between 15 to 20 batches before failure on average. However, variance is large; crucibles have been known to fail during the first batch, and crucibles have been known to last over 30 batches.

Failure of the crucible lining materials does not necessarily lead to leakage. However, leakage has occurred in instances when crucibles have cracked, leading to the spillage of molten metal and salt into the process equipment. None of the high-temperature process equipment used for the SFT and JFCS Programs employs active liquid cooling. Therefore, a steam explosion, or its equivalent with other fluids, is not possible. The leakage can damage process equipment, but this does not necessarily pose a safety risk.

There is a well-known damage mechanism involving molten metals. A molten metal must be contained in materials that are compatible with the molten metal. When this containment is lost, the molten metal can contact materials that are incompatible with the molten metal. In some cases, molten metal can dissolve other metals by the process of alloying at temperatures below the melting temperatures of the other metals. For example, in many instances the melting temperature of a binary alloy is lower than the melting temperature of either pure metal. These factors must be considered when assessing the consequences of the loss of containment of a batch of molten metal. Pyroprocessing salts do not exhibit this type of alloying behavior with metals, Pyroprocessing salts will solidify without dissolving metals.

4.21 Furnace Overtemperature

As described earlier, pyroprocessing flowsheets utilize several high-temperature furnace operations. The heat is provided by either electrical resistance heating elements, or by induction coupled to a receptor material such as a graphite crucible. Table 26 provides a summary of the capabilities of different furnace technologies.

Table 26. Summary of Furnace Limitations

Heating Mechanism	Heating Element Material	Heating Element Atmosphere	Approximate Maximum Temperature, °C
Resistance	Nickel-Chromium Alloy	Air, Inert, Vacuum	1,200
	Silicon Carbide	Air, Inert	1,550
	Silicon Carbide	Vacuum	1,000
	Molybdenum Disilicide	Air	1,750
	Graphite	Inert, Vacuum	>2,000
Induction	Copper or Graphite Receptor	Air, Inert, Vacuum	>2,000

The furnaces are expected to be engineered with safety systems that prevent overtemperature conditions. These are called overtemperature controllers. The rigor of these overtemperature safety systems must be proportional to the consequences of an overtemperature condition. The furnace applications include the OR cells, ER cells, distillation furnaces, and casting furnaces. Table 27 provides a summary of the furnace capabilities historically used for these operations in the SFT and JFCS Programs. However, there are many options available to design engineers.

Table 27. Summary of Furnace Types Used in Pyroprocessing

Unit Operation	Typical Operating Temperature, °C	Typical Heating Element Type
OR Cell	650	Nickel-Chromium Alloy
ER Cell	500	Nickel-Chromium Alloy
Distillation	Up to 1,200	Silicon Carbide
Distillation	Up to 1,550	Copper or Graphite Receptor
Metal Casting	Up to 1,200	Silicon Carbide
Metal Casting	Up to 1,650	Copper or Graphite Receptor

Construction materials such as ferrous steel alloys lose their mechanical properties at elevated temperatures. Standard ferrous steel alloys begin to significantly lose mechanical properties around 500°C. Specialty ferrous steel alloys can push this limit to about 800°C. The OR and ER vessels operate at about 650°C and 500°C, respectively. These are ferrous steel alloy vessels surrounded by resistance heaters and thermal insulation. These operating conditions are already against the mechanical limits of ferrous alloys. Nevertheless, these alloys have melting temperatures above approximately 1,400°C.

Distillation and casting furnaces that use silicon carbide heating elements are similar to the OR and ER vessels, in that the furnace vessels are surrounded by heaters and insulation. Distillation and casting furnaces that use induction heating are different in that the heat is resonated from the graphite receptor crucible. The steel components of this type of furnace are not directly exposed to the high temperatures.

4.22 Loss of Process Signals

The OR and ER electrochemical cells are powered by external DC power supplies. Control of the OR and ER operations requires monitoring a series of amperage and voltage signals relative to the power supplies, anodes, cathodes, and REs. The power supplies provide current to the anode-to-cathode circuits, and the current is regulated based on the voltages that develop between the anode-to-RE and the cathode-to-RE signals. Loss of these process signals may result in the following.

- Loss of OR cathode-to-RE signal: excess lithium metal generation.

- Loss of OR anode-to-RE signal: oxidation of the anode materials or the generation of $Cl_2(g)$ if a graphite anode is in service.
- Loss of ER cathode-to-RE signal: deposition of the more electropositive metals with uranium.
- Loss of the ER anode-to-RE signal: oxidation of the steel anode basket (in the case of direct transport or anodic dissolution) or the steel vessel (in the case of deposition) or the cathode (in the case of cathodic stripping).

Robust process signals are provided by proper engineering design, but there should always be a way of verifying that the process signals are correct. This can be done by redundancy such as having two REs present for comparison.

4.23 Radiation Damage and Dry Argon

As discussed earlier, the OR and ER salts will become sources of very high radiation as fission products accumulate in these salts. Materials in these high radiation areas are susceptible to radiation damage. Electrical insulating materials and electronic components are particularly susceptible to radiation damage and embrittlement. Hot cell operations often design equipment such that the electronic components are, as much as possible, outside the hot cell.

The breakdown voltage of dry argon is significantly less than that of air: 6 versus 36 kV cm^{-1}, respectively. And the heat capacity of argon is significantly less than that of air: 0.52 versus 1.01 kJ kg^{-1} K^{-1}, respectively. These differences can result in electronics failures by electrical arcing and overheating. And some materials require an oxygen atmosphere to work properly. For example, due to the low oxygen level in the hot cells, standard graphite brushes in electrical motors have failed prematurely in dry argon service. To improve the service lives of these motors, the standard graphite materials are replaced with silver-doped graphite.

4.24 Excessing Equipment from Hot Cells

Any pyroprocessing flowsheet will have waste streams that are more-or-less anticipated as part of the process. However, the mechanical systems associated with the operation of the hot cells, and the operation of the process equipment inside the hot cells, are very complex. Equipment malfunction, failure, modification, and obsolescence are inherent aspects of normal operations. The environment inside a hot cell hosting pyroprocessing will be highly contaminated. The FCF and HFEF hot cells at INL are each equipped with a water wash station (WWS), a suited entry repair area (SERA), and a hot repair area (HRA). The purpose of the WWS is to lower the surface contamination of articles leaving the shielded hot cell. The purpose of the SERA is to provide an area where a worker, wearing the proper protective equipment, can work hands-on with articles decontaminated and removed from the shielded hot cell. The articles in question are subject to radiological surveys before a worker enters the SERA.

Equipment excessed from the hot cells comes in all shapes and sizes. Size reduction of the excess equipment is achieved by disassembly and cutting. The scrap is loaded into containers inside that hot cell, which are then loaded into drums or boxes for transportation outside the hot cell. Again, radiological surveys are performed before the drums or boxes leave the facility.

At INL, the FCF and HFEF each have two hot cells, one with an air environment, and one with an argon environment. Workers do not enter these hot cells. The radiation levels inside the hot cells are much too high to allow worker entry. Historically, when FCF transitioned from its mission as a post irradiation examination (PIE) facility, to a facility supporting the IFR Program, the FCF hot cells were decontaminated and refurbished. This work progressed from the late 1980's to the early 1990's. Following the decontamination efforts, workers did make entries into the FCF air cell and argon cell. However, the FCF hot cell decontamination efforts included removing and disposing of all process equipment from the hot cells. The decontamination efforts required significant resources.

4.25 Emissions from Hot Cells

At INL, the atmospheres within the FCF and HFEF hot cells are maintained at slightly negative pressures relative to the ambient atmosphere. In the event of a leak, this design feature draws the ambient atmosphere into the hot cell and prevents the hot cell atmosphere from leaking out. The argon atmospheres are circulated through an internal conditioning system that includes high efficiency particulate air (HEPA) filters, a palladium-based oxygen absorber, a diatomaceous-earth-based moisture absorber, and temperature control. When the air and argon hot cell atmospheres are vented to the ambient atmosphere, the discharge gases pass through HEPA filters and an array of detection and monitoring equipment to verify that the emissions are withing the environmental discharge requirements. These atmospheric control systems were not designed specifically to support pyroprocessing operations, they were features of the hot cells before the pyroprocessing activities.

4.26 Fuel Fabrication

The U.S. commercial nuclear reactor fleet is comprised of about 60 PWRs and 30 BWRs. Fuels for these reactors are fabricated from LEU that has been obtained from natural uranium. The uranium is mined, milled, purified to yellowcake, calcined to UO_2, converted to UF_6, enriched, and converted back to UO_2 as a feedstock to fuel fabrication. There are two important characteristics of fuels fabricated by this route: radiation shielding is not required to handle these materials, and there is no TRU present.

Aqueous reprocessing can recover uranium that essentially has these same characteristics. This is because of the high separation factors discussed earlier. However, this is not the case with pyroprocessing. Uranium recovered by pyroprocessing contains residual fission products and transuranics and, therefore, may require shielding. Therefore, if electrorefined uranium from pyroprocessing is to be used for fuel fabrication, these facilities will need ways of managing the associated radiation and residual transuranics.

4.27 Molten Salt Reactors

This topic is outside the purview of this report, but a few words are warranted. In the 1950s and 1960s, a significant amount of research was performed at the Oak Ridge National Laboratory (ORNL) on molten salt reactors utilizing the ^{232}Th/^{233}U fuel cycle. In this fuel cycle, ^{232}Th is the fertile isotope that is transmutated to ^{233}Pa, which decays to ^{233}U. It is analogous to the ^{238}U/^{239}Pu fuel cycle. The transmutation reactions are shown below.

$$^{232}_{90}Th + n \rightarrow {}^{233}_{90}Th\ (21.8\ min) \rightarrow {}^{233}_{91}Pa + {}^{0}_{-1}\beta\ (27.0\ d) \rightarrow {}^{233}_{92}U + {}^{0}_{-1}\beta$$

$$^{238}_{92}U + n \rightarrow {}^{239}_{92}U\ (23.4\ min) \rightarrow {}^{239}_{93}Np + {}^{0}_{-1}\beta\ (2.4\ d) \rightarrow {}^{239}_{94}Pu + {}^{0}_{-1}\beta$$

The ^{232}Th/^{233}U fuel cycle requires management of the ^{233}Pa (27 d), particularly if the reactor is a breeder reactor. Because of the relatively long half-life of ^{233}Pa, its presence adversely affects the breeding ratio by adsorbing neutrons. The early reactor concepts had two molten salt streams flowing through the reactor core: a blanket salt containing ^{232}Th, and a fuel salt containing ^{233}U. Later reactor concepts combined blanket and fuel into a single molten salt stream flowing through the reactor core. In each case, the ^{233}Pa was managed by chemical process of the molten salt to remove and isolate the ^{233}Pa, allow it to decay to ^{233}U outside the reactor, recover the ^{233}U, and return the ^{233}U to the fuel salt. To accomplish this, the chemical processing flowsheets conceptualized were complicated with numerous high-temperature unit operations. Fredrickson, Cao, et al. (2018)[2] provides a summary of this early work at ORNL.

There is renewed interest and development in molten salt reactor technologies. One way to divide the technologies is into two groups, 1) those that use molten salt as a coolant only, and 2) those that use molten salt as a fuel and coolant. Important properties of these molten salts include the following:

- Radiochemical behavior in the reactor core.
- Chemical compatibility with the materials of construction.
- Thermophysical property compatibility with the engineered systems.
- Salt management from headend to backend.

The strongest overlap between pyroprocessing and molten salt reactor technologies arguably has to do with the latter bullet, salt management from headend to backend. Common issues include salt synthesis, fission product management, and salt waste disposal.

4.28 Resources Required for Pyroprocessing Research

Pyroprocessing research generally involves the handling of hygroscopic salts and reactive metals that are potentially pyrophoric. Therefore, experiments are often performed in inert argon-atmosphere gloveboxes where the oxygen and moisture are maintained at low levels. High-temperature furnaces are used for handling molten salts and metals, and for distillation operations. Potentiostats and DC power supplies are used for electrochemical measurements and electrochemical cell operations, and a suite of capabilities is required for materials characterization such as analytical chemistry, microscopy, and thermo-physical measurements.

Much useful research can be performed with non-radiological materials, making this subject a popular research area for academic institutions. Working with uranium requires more work control and greater resources but is still within the realm of work that can be performed at academic institutions. Working with transuranics requires significant resources and a highly trained staff. Therefore, work with transuranics is generally not possible at academic institutions and is relegated to National Laboratories. Working with irradiated spent nuclear fuels requires facilities with highly specialized infrastructures and staff that are only available within the DOE complex.

5. SUMMARY OF RECENT R&D PUBLISHED IN THE OPEN LITERATURE

Recent research activities in the U.S., ROK, and Japan have mostly focused on ways to improve upon the three flowsheets described for the IFR, SFT, and JFCS Programs. Other countries are pursuing pyroprocessing research in support of their nuclear energy ambitions, most notably are increased numbers of publications from China and India. This literature summary focused on the more recent publications of particular interest to pyroprocessing and generally those published within the last 10 years.

5.1 Review Papers

Recent review papers are summarized in Table 28. These cover a variety of topics and are written by authors familiar with pyroprocessing technologies.

Table 28. Summary of Recent Review Papers

Author	Year	Primary Subject
Mirza [3]	2023	Reprocessing of oxide fuels.
Fredrickson [4]	2022	IFR Program history and SFT Program status.
Riley [5]	2022	Phosphate conversion of OR and ER salts.
Carlson [6]	2021	Treatment and immobilization of OR and ER salts.
Fredrickson [7]	2021	Summary of fuel types and reprocessing technologies.
Galashev [8]	2021	Actinide and fission product recovery technologies.
Moyer [9]	2021	Nuclear fuel cycle research directions.
Williams [10]	2021	Electrochemical concentration measurement techniques.
DelCul [11]	2021	Fuel reprocessing technologies.
Riley [12]	2020	Treatment and immobilization of OR and ER salts.
Willett [13]	2020	Fission gas measurements.
Baron [14]	2019	Technology readiness level assessment of separations technologies.
Fredrickson [15]	2019	Electrochemical experimental techniques.
Park [16]	2019	Waste treatment developments in ROK.
Riley [17]	2018	Treatment and immobilization of ER salts.
Zhou [18]	2018	Modeling of electrochemical operations.
Frank [19]	2015	Waste treatment and waste form fabrication.
Soelberg [20]	2013	Iodine and krypton control.
Inoue [21]	2011	Technology developments in Japan.

5.2 Salt Management

Salt management is a key issue for pyroprocessing. The goals are mostly related to improving the retention of actinides in the fuel cycle or improving the condition of salt wastes by minimizing the actinide content, minimizing the volume, or increasing the durability. Research in these areas have pursued many avenues including:

- Recovery of transuranics from ER salts to keep them in the fuel cycle.
- Recovery of actinides from ER salts prior to treatment of salt for disposal.
- Recovery of lanthanide fission products from ER salts to minimize salt waste.

- Recovery of Group 1 and 2 fission products from OR and ER salts to minimize salt waste.
- Limiting the amount of bond-sodium reporting to the ER salt to minimize salt waste.
- UCl_3 oxidant synthesis for ER operations.
- Processing of salt into waste forms suitable for interim storage or geologic repositories.
- Processing of fission products into waste forms suitable for geologic repositories.
- Processing of bond-sodium into waste forms suitable for geologic repositories.

Research on reactive liquid metal electrodes for the recovery of fission products and actinides are summarized in Table 29. In principle, the mechanisms driving separations rely on the alloying behaviors between the solute cations and the liquid metal electrodes. For example, when a cation is reduced to a metal on an electrode that is otherwise inert to the reducing metal (e.g., uranium onto a tungsten electrode), then reduction occurs at a particular cathode potential relative to the RE selected. For illustrative purposes, call this the "*normal cathode potential*." When alloy systems are selected that are not inert to the reducing metal, then reduction occurs at a cathode potential less negative than the normal cathode potential. This process is called "*under potential deposition*." Cations that would not deposit together onto an inert cathode, will deposit together onto a reactive cathode due to underpotential deposition. This mechanism is exploited to remove Group 1, Group 2, and lanthanide fission products from the ER salt. The reduced metals are collected in the liquid metal alloy, which can either be the waste product or can be subject to further processing such as distillation, depending on the application.

In each of these process scenarios, there must be a corresponding anode reaction. Often this is the evolution of Cl_2(g) on a graphite electrode. And Cl_2(g), like any other process stream, requires a disposition path. Unfortunately, Cl_2(g) is difficult to manage because it is highly reactive and, consequently, its generation increases the chlorine chemical potential of the salt thereby making the salt more corrosive to its containment vessel. Chlorine management is not a trivial problem. Representative anode and cathode reactions are shown below.

$$xCl^- = \frac{x}{2}Cl_2(g) + xe^-$$

$$Me^{x+} + xe^- = Me^0$$

Where,

Cl^- is the halide that is oxidized to a gas.

Me is the cation that is reduced to a metal.

Table 29. Summary of Research on Reactive Metal Electrodes.

Author	Year	Solvent Salt	Solute Salt	Liquid Metal
Ding [22]	2023	LiCl-KCl	$NdCl_3$	Ga-Al
Yang [23]	2023	LiCl-KCl	UCl_3	Al
			$LaCl_3$	Ga
			$CeCl_3$	Ga-Al
			$PrCl_3$	
			$NdCl_3$	
Zhang [24]	2023	LiCl-KCl	$SmCl_3$	Bi
Im [25]	2022	LiCl-KCl	$NdCl_3$	Bi
				Sn

Author	Year	Solvent Salt	Solute Salt	Liquid Metal
Novoselova [26]	2022	LiCl-KCl-CsCl	$DyCl_3$	Ga
				Cd
Jang [27]	2022	LiCl-KCl	CsCl	Zn
			$SrCl_2$	Bi
				Cd
				Pb
Volkovich [28]	2021	LiCl-KCl	UCl_3	Ga
			$ZrCl_4$	Zn
				Ga-Zn
				Ga-Sn
				Ga-In
Liu [29]	2021	LiCl-KCl	$LaCl_3$	Al
			UCl_3	Ga
				In
				Zn
				Cd
				Hg
				Sn
				Pb
				Bi
Liu [30]	2021	LiCl-KCl	UCl_3	Ga
			$LaCl_3$	
			$CeCl_3$	
			$PrCl_3$	
			$NdCl_3$	
			$SmCl_3$	
Smolenski [31]	2021	LiCl-KCl	UCl_3	Ga
			$DyCl_3$	Ga-Al
Yang [32]	2021	LiCl-KCl	$LaCl_3$	Al
				Ga
				Ga-Al
Lichtenstein [33]	2020	LiCl-KCl	$SrCl_2$	Bi
			$BaCl_2$	
Nigl [34]	2020	LiCl-KCl	$BaCl_2$	Sb
			$SrCl_2$	Bi
				Sn
				Pb
				Bi-Sb
Novoselova [35]	2020	LiCl-KCl	$DyCl_3$	Ga
Han [36]	2020	LiCl-KCl	YCl3	Zn
				Cu

Author	Year	Solvent Salt	Solute Salt	Liquid Metal
Fredrickson [37]	2020	LiCl-KCl	UCl_3	Cd
			$PuCl_3$	
Woods [38]	2020	LiCl-KCl	CsCl	Bi
			$SrCl_2$	
			$BaCl_2$	
Yang [39]	2020	LiCl-KCl	UCl_3	Ga-Al
			$CeCl_3$	
Yin [40]	2020	LiCl-KCl	$LaCl_3$	Bi
			$CeCl_3$	
			$PrCl_3$	
			$NdCl_3$	
Fredrickson [41]	2018	LiCl-KCl	UCl_3	Cd
			$PuCl_3$	
Novoselova [42]	2019	LiCl-KCl	UCl_3	Ga-In
			$LaCl_3$	
Lichtenstein [43]	2018	LiCl-KCl	$BaCl_2$	Bi
			$SrCl_2$	Bi
Fredrickson [44]	2018	LiCl-KCl	UCl_3	Cd
			$PuCl_3$	
Novoselova [45]	2018	LiCl-KCl	UCl_3	Ga-In
			$NdCl_3$	
Yin [46]	2018	LiCl-KCl	UCl_3	Bi
Yin [47]	2018	LiCl-KCl	$PrCl_3$	Bi
Liu [48]	2017	LiCl-KCl	$CeCl_3$	Ga
			$NdCl_3$	
Luo [49]	2016	LiCl-KCl	$NdCl_3$	Zn
Liu [50]	2014	LiCl-KCl	$SmCl_2$	Zn

Research on reactive metal drawdown is summarized in Table 30. In these processes, a reductant is introduced to the salt to reduce metal cations that are less reactive than the reductant itself. The chemical reaction is as follows:

$$Me + \frac{y}{x} Me'Cl_x = MeCl_y + \frac{y}{x} Me'$$

Where,

Me is the reductant that is oxidized to a cation.

Me' is the cation that is reduced to a metal.

For example, lithium is a powerful reductant because LiCl is a stable metal chloride. Lithium will reduce all lanthanide and actinide chlorides. Recovery of the reduced metals requires separation by salt distillation and metal consolidation.

Table 30. Summary of Research on Reactive Metal Drawdown.

Author	Year	Solvent Salt	Solute Salt	Reductant
Wang [51]	2022	LiCl-KCl	$LaCl_3$	Li
			$SmCl_3$	
Yoon [52]	2020	LiCl-KCl	UCl_3	La
			$MgCl_2$	Ce
			$DyCl_3$	Y
			$CeCl_3$	
			$LaCl_3$	
			$NdCl_3$	
Bagri [53]	2018	LiCl-KCl	UCl_3	Gd
			$MgCl_2$	
			$LaCl_3$	
			$NdCl_3$	
			$CeCl_3$	
Bagri [54]	2017	LiCl-KCl	UCl_3	Gd
Perumal [55]	2015	LiCl-KCl	UCl_3	Li-Cd
			$CeCl_3$	
Simpson [56]	2012	LiCl-KCl	CsCl	Li
			$LaCl_3$	
			$CeCl_3$	
			$NdCl_3$	

Research on drawdown based on conversion and precipitation is summarized in Table 31. In these processes, a precipitant is added to chemically convert the fission product chlorides to a waste form that is chlorine-free and more durable than the chlorine-containing salt waste forms. Consequently, these processes are often called dechlorination or dehalogenization processes. Recovery of the precipitate requires salt distillation. However, the chlorine needs to be accounted for and in these processes the chlorine is often released as Cl_2(g) or HCl(g). As discussed earlier, chlorine management is not a trivial problem. Furthermore, the recovered precipitate requires further processing to place it into a durable waste form suitable for a geologic repository.

Table 31. Summary of Research on Precipitation-Based Drawdown for Salt Wastes.

Author	Year	Solvent Salt	Solute Salt	Reagent	Precipitate
Han [57]	2023	LiCl-KCl	CsCl	Na_3PO_4	$LaPO_4$
			$SrCl_2$	K_2CO_3	$SmPO_4$
			$BaCl_2$		$NdPO_4$
			$LaCl_3$		$DyPO_4$
			$SmCl_3$		Cs_3PO_4
			$NdCl_3$		$SrCO_3$
			$DyCl_3$		$BaCO_3$

Author	Year	Solvent Salt	Solute Salt	Reagent	Precipitate
Bailey [58]	2022	LiCl-KCl	$LaCl_3$	La_2O_3	Na_2O
				Na_2CO_3	Fe_2O_3
				Fe_2O_3	P_2O_5
				$NH_4H_2PO_4$	La_2O_3
Dong [59]	2022	LiCl-KCl	NaCl	$H_2C_2O_4$	$Li_2C_2O_4$
			CsI		$K_2C_2O_4$
			$SrCl_2$		$Na_2C_2O_4$
			$CeCl_3$		$Ce_2C_2O_4$
			$NdCl_3$		SrC_2O_4
					$Nd_2[C_2O_4]_3$
Harrison [60]	2022	LiCl-KCl	YCl_3	Li_3PO_4	YPO_4
			$LaCl_3$	K_3PO_4	$LaPO_4$
			$CeCl_3$		$CePO_4$
			$PrCl_3$		$PrPO_4$
			$NdCl_3$		$NdPO_4$
			$SmCl_3$		$SmPO_4$
			$SrCl_2$		$SrCO_3$
			$BaCl_2$		$BaCO_3$
Qu [61]	2022	LiCl-KCl	$NdCl_3$	K_2S	Nd_2S_3
			$CeCl_3$	$Na_2S•xH_2O$	Ce_2S_3
			$SmCl_3$		Sm_2S_3
			$GdCl_3$		Gd_2S_3
Han [62]	2021	LiCl-KCl	CsCl	Na_3PO_4	$LaPO_4$
			$SrCl_2$	K_2CO_3	$SmPO_4$
			$BaCl_2$	Li_2CO_3	$NdPO_4$
			$LaCl_3$		$DyPO_4$
			$SmCl_3$		Cs_3PO_4
			$NdCl_3$		$SrCO_3$
			$DyCl_3$		$BaCO_3$
Uozumi [63]	2021	LiCl-KCl	$CeCl_3$	Li_2O	Ce_2O_3/CeO_2
			$SmCl_3$	Li_2CO_3	$Sm_2O_3/SmOCl$
			$EuCl_3$		Eu_2O_3
			$GdCl_3$		$Gd_2O_3/GdOCl$

Author	Year	Solvent Salt	Solute Salt	Reagent	Precipitate
Gardner [64]	2021	LiCl-KCl	NaCl	$H(SiO_2)_{2.6}(AlO_2)$	$Li(SiO_2)_{2.6}(AlO_2)$
			CsCl		$K(SiO_2)_{2.6}(AlO_2)$
			$NdCl_3$		$Na(SiO_2)_{2.6}(AlO_2)$
			$CeCl_3$		$Cs(SiO_2)_{2.6}(AlO_2)$
			$SrCl_2$		$Nd[(SiO_2)_{2.6}(AlO_2)]_3$
			YCl_3		$Ce[(SiO_2)_{2.6}(AlO_2)]_3$
			KI		$Sr[(SiO_2)_{2.6}(AlO_2)]_2$
					$Y[(SiO_2)_{2.6}(AlO_2)]_3$
Yang [65]	2021	LiCl-KCl	CsCl	$SnCl_4•5H_2O$	Cs_2SnCl_6
Gardner [66]	2020	LiCl-KCl	NaCl	$H(SiO_2)_{2.6}(AlO_2)$	K_2O
			CsCl	Fe_2O_3	Li_2O
			$NdCl_3$		Na_2O
			$CeCl_3$		Cs_2O
			$SrCl_2$		Nd_2O_3
			YCl_3		Ce_2O_3
Manson [67]	2020	NaCl-KCl	$CeCl_3$	ZrO_2	$Ca_{0.9}Zr_{0.9}Ce_{0.2}Ti_2O_7$
				TiO_2	
				CaO	
Riley [68]	2020	LiCl-KCl	NaCl	$NH_4H_2PO_4$	$Me_2O•P_2O_5$
			CsCl	Fe_2O_3	$MeO•P_2O_5$
			CsI		$Me_2O_3•P_2O_5$
			KI		
			$SrCl_2$		
			YCl_2		
			$LaCl_3$		
			$CeCl_3$		
			$NdCl_3$		
Wasnik [69]	2019	LiCl-KCl	NaCl	$H(SiO_2)_{2.6}(AlO_2)$	$Li(SiO_2)_{2.6}(AlO_2)$
			CsCl		$K(SiO_2)_{2.6}(AlO_2)$
			$NdCl_3$		$Na(SiO_2)_{2.6}(AlO_2)$
			$CeCl_3$		$Cs(SiO_2)_{2.6}(AlO_2)$
			$SrCl_2$		$Nd[(SiO_2)_{2.6}(AlO_2)]_3$
			YCl_3		$Ce[(SiO_2)_{2.6}(AlO_2)]_3$
					$Sr[(SiO_2)_{2.6}(AlO_2)]_2$
					$Y[(SiO_2)_{2.6}(AlO_2)]_3$
Eun [70]	2017	LiCl-KCl	$SrCl_2$	Li_2CO_3	$SrCO_3$
		LiCl	$BaCl_2$	K_2CO_3	$BaCO_3$

Author	Year	Solvent Salt	Solute Salt	Reagent	Precipitate
Riley [71]	2017	LiCl-KCl	$SrCl_2$	TeO_2	TeO_2, PbO_2
		$LiCl-Li_2O$	CsCl	PbO_2	
			NaCl		
			$NdCl_3$		
			YCl_3		

Research on salt purification by crystallization are summarized in Table 32. This technique is commonly called zone refining and it is applied in many industries to purify such materials as silicon, gallium, germanium, aluminum, and a variety of chemicals. The separations rely on the partitioning of impurities ahead of the solidification front from the solid phase into the liquid phase. The phenomena are governed by thermodynamic phase diagram behavior, but these interpretations are limited to two or three component systems. Empirical experimentation is required to understand the behavior of multicomponent systems because of the chemical complexity. For pyroprocessing applications, its niche is for the fission products that form stable chlorides and are not amenable to recovery by reactive metal electrodes, reactive metal drawdown, and precipitation drawdown techniques. Much of the research has focused on the Group 1 and Group 2 fission products.

Table 32. Summary of Research on Salt Purification by Crystallization.

Author	Year	Solvent Salt	Solute Salt
Choi [72]	2020	LiCl	CsCl
			$SrCl_2$
			$BaCl_2$
			$NdCl_3$
			$EuCl_3$
Choi [73]	2018	LiCl	CsCl
			$SrCl_2$
			$BaCl_2$
Shim [74]	2017	LiCl-KCl	CsCl
			$SrCl_2$
Shim [75]	2016	LiCl	CsCl
			$SrCl_2$
Williams [76]	2015	LiCl-KCl	CsCl
			$SrCl_2$
Versey [77]	2014	LiCl	CsCl
Choi [78]	2013	LiCl	CsCl
			$SrCl_2$
			$BaCl_2$
Williams [79]	2013	LiCl-KCl	CsCl

5.3 Oxide Reduction

Research on oxide reduction is summarized in Table 33. The basic chemistry of oxide reduction was described earlier.

Table 33. Summary of Research on Oxide Reduction

Author	Year	Salt	Oxide	Notes
Chamberlain [80]	2022	LiCl	UO_2	Materials Corrosion
Horvath [81]	2022	LiCl	NiO	Equipment Study
Kim [82]	2022	LiCl	UO_2	Modeling Study
Shishkin [83]	2022	LiCl	La_2O_3	
			Nd_2O_3	
			CeO_2	
Yao [84]	2022	LiCl	UO_2	
		LiCl-KCl		
		LiCl-LiF		
Yoo [85]	2021	LiCl	UO_2	Modeling Study
Kim [86]	2021	LiCl	NiO	Chemical Reduction
Burak [87]	2020	LiCl	UO_2	
Burak [88]	2020	LiCl	UO_2	
Herrmann [89]	2019	LiCl	UO_2	Pt Anode
				Ir Anode
Choi [90]	2017	LiCl	UO_2	
Kim [91]	2017	LiCl	UO_2	C Anode
Park [92]	2013	LiCl	UO_2	
Herrmann [93]	2012	LiCl	Spent MOX Fuel	Pt Anode
			UO_2	
			PuO_2	
Phongikaroon [94]	2011	LiCl	UO_2	Modeling Study
Herrmann [95]	2010	LiCl	Spent LWR Fuel	Pt Anode
			UO_2	
			PuO_2	
Herrmann [96]	2006	LiCl	Spent LWR Fuel	Pt Anode
			UO_2	
			PuO_2	

5.4 Chemical Decladding

Research on the chemical decladding of zirconium clad LWR fuels is summarized in Table 34. The basic separations process is to expose the fuel to a reactant that chlorinates the zirconium to $ZrCl_4$, which has a high vapor pressure. Recycling the zirconium would involve the Kroll Process, in which the $ZrCl_4$ is reduced to zirconium metal by reaction with magnesium.

Table 34. Summary of Research on Chemical Decladding of Zirconium-Clad Fuels

Author	Year	Reactant	Product
Vestal [97]	2023	SCl_2	$ZrCl_4$
Conrad [98]	2023	S_2Cl_2	$ZrCl_4$
		$SOCl_2$	
Bruffey [99]	2021	S_2Cl_2	$ZrCl_4$
		$SOCl_2$	
Nevarez [100]	2021	Cl_2	$ZrCl_4$
Collins [101]	2017	Cl_2	$ZrCl_4$
Collins [102]	2016	Cl_2	$ZrCl_4$
Collins [103]	2012	Cl_2	$ZrCl_4$

5.5 Uranium Electrorefining

Research on uranium electrorefining is summarized in Table 35. The works of Gardner and Harward loosely fit into this category because they address interim storage of ER salts.

Table 35. Summary of Research on Uranium Electrorefining

Author	Year	Subject
Zhao [104]	2023	Modeling of uranium dendrite morphologies.
Hege [105]	2023	Uranium electrochemistry review paper.
Gardner [106]	2022	Stabilization of ER salts for interim storage.
Harward [107]	2022	Stabilization of ER salts for interim storage.
Swain [108]	2022	Effect of moisture in LiCl-KCl salts.
Swain [109]	2022	Effect of moisture in LiCl-KCl salts.
Xiong [110]	2022	Fundamental modeling of salt chemistry.
Zhao [111]	2022	Modeling of uranium electrorefining.
Swain [112]	2021	Effect of moisture in LiCl-KCl salts.
Westphal [113]	2020	Bond-sodium management to reduce ER salt waste.
Lee [114]	2017	Effect of cathode materials on uranium electrorefining.

5.6 Chlorination Chemistries

Research on the chlorination of metal and oxide fuels is summarized in Table 36. Chlorination is used for several applications including production of UCl_3 oxidant for ER operations, and chlorinating oxide fuels or oxide sludge into ER salts.

Table 36. Summary of Research on Chlorination of Actinides

Author	Year	Salt	Reactant	Oxidant
Chamberlain [115]	2022	LiCl-KCl	UO_2	$ZrCl_4$
Herrmann [116]	2022	LiCl-KCl	Spent MOX Fuel	Electrochemical
			Spent LWR Fuel	UCl_3
Herrmann [117]	2022	LiCl-KCl	U	NH_4Cl
		NaCl	UH_3	
Meng [118]	2022	LiCl-KCl	UO_2	CCl_4
			PuO_2	$COCl_2$
				Cl_2
				$ZrCl_4$
				$AlCl_3$
Perhach [119]	2022	$NaCl-CaCl_2$	U	HCl
Samanta [120]	2022	LiCl-KCl	UO_2	$AlCl_3$
Yoon [121]	2022		U	NH_4Cl
Yoon [122]	2022	LiCl-KCl	U_3O_8	NH_4Cl
			CeO_2	
			NdO_2	
			SrO_2	
Zhong[123]	2021	$NaCl-AlCl_3$	U	$AlCl_3$
Kitawaki[124]	2013		U_3O_8	CCl_4

5.7 Reprocessing Facility Investigations

Research related to reprocessing facilities are summarized in Table 37. These include cost estimates, equipment design, and flowsheet developments.

Table 37. Summary of Research on Reprocessing Facility Considerations

Author	Year	Subject
Kim[125]	2023	Cost analysis.
Kim[126]	2022	Cost analysis.
Kim[127]	2020	Hardware disassembly.
Chang[128]	2019	Conceptual design of a pyroprocessing facility.
Simpson[129]	2018	Conceptual flowsheet for reduced ER salt waste.
Chang[130]	2018	Conceptual design of a pyroprocessing facility.
Moon[131]	2015	Facility safety controls.
Williamson[132]	2011	Conceptual designs of a pyroprocessing flowsheet.

6. PYROPROCESSING FACILITY SAFEGUARDS

This chapter discusses the issues, challenges, and opportunities associated with nuclear material measurement and fissile materials inventory management in pyroprocessing facilities. Due to the extreme processing environments involving inert atmospheres, high temperature materials, concentrated radioactivity, and corrosivity of the molten salts used in pyroprocessing, traditional safeguards and materials accounting techniques used in aqueous reprocessing facilities are not directly applicable. Holdup, the estimate of unaccounted nuclear materials retention in unknown locations, is a significant challenge in pyroprocessing, where large amounts of fissile materials are maintained as in-process inventory. The operating characteristics of pyroprocessing facilities, such as their batch nature and electrochemical processes, provide unique opportunities for inventory assessment. The development of reliable low-latency inventory measurement and estimation techniques considering these unique characteristics is essential to ensure the safe, secure, and uninterrupted operation of pyroprocessing facilities.

The safeguards and MC&A at nuclear fuel handling facilities are designed to deter the diversion of nuclear materials. While all commercial nuclear fuel reprocessing facilities currently use aqueous reprocessing methods, molten salt electrochemical reprocessing, also known as pyroprocessing, can be an alternative method for extracting fissile materials for recycling. This process is not amenable to producing high-purity fissile isotope products, making it less attractive for illicit proliferation attempts.[133,134,135,136,137]

The currently envisioned pyroprocessing facility designs present challenges for adopting MC&A and process monitoring techniques developed for aqueous reprocessing directly because of its batch process nature, harsh hot-cell inert atmosphere environments, and significant in-process material inventory.[134,136,137,138,139,140,141] In response to this challenge, novel measurement and monitoring techniques have been developed for pyroprocessing facilities. The latter part of this report reviews existing and proposed measurement and monitoring techniques for pyroprocessing facilities, highlighting their measurement latency, performance, and targets. The following sections outline the challenges in MC&A and safeguards for pyroprocessing facilities and provides insights for future research and development efforts.

6.1 Safeguards Challenges and Opportunities

The primary unit operations of the pyroprocessing facility are housed within a small footprint, highly radioactive, and inert atmosphere hot cell environments. This design feature limits physical access to the main facilities and simplifies physical security measures. In addition, remote manipulators and heavy equipment are utilized to access unit cells and materials. However, this restricted facility access creates challenges for safeguards and MC&A. A recent report, “The MPACT 2020 Milestone: Safeguards and Security by Design of Future Nuclear Fuel Cycle Facilities,” offers an overview on this topic.[142]

The design process for a safeguards and security system regarding a new reprocessing facility requires regulatory confirmation. The International Atomic Energy Agency (IAEA) safeguards regulations can also be referenced for large throughput reprocessing facilities. The IAEA timeliness goal is to detect the loss of 8 kg of fissile materials within 1 month, with 95% detection probability and 5% false alarm probability.[142]

In the U.S., the Code of Federal Regulations (CFR) outlines physical protection of plants and materials in 10 CFR Part 73, and MC&A of special nuclear material in 10 CFR Part 74. The Nuclear Regulatory Commission (NRC) has a stringent goal, which is to detect 2 kg of fissile materials within 7 days, with 95% detection probability and 5% false alarm probability.

Safeguard design process and simulation-based validation efforts are outlined in reports.[142,143,144] The primary component of safeguard design includes facility MC&A, process monitoring, and containment and surveillance.

The cornerstone of facility safeguards is the evaluation of holdup, which represents the amount of unaccounted material in the facility. This holdup is an inevitable byproduct of uncertainties (such as random error from measurements) or unknown physical and chemical factors that arise during facility operation. Holdup accounting serves as a means of assessing facility misuse or attempts to divert materials, making it an essential safeguard tool. Essentially, evaluating facility holdup involves attempting to perform a mass balance and determine associated uncertainties. Let us define $i_{fissile}(j)$ as the mass of fissile materials in the j^{th} incoming batch to the processing facility. Then, the total input of fissile materials is equal to the sum of all instances of fissile materials across all processed incoming batches. That is,

$$I_{fissile}(n) = \sum_{j=1}^{n} i_{fissile}(j)$$

Similarly, denote $o_{fissile}(j)$ as the mass of fissile materials exiting from the processing facility between processing j-1th and jth incoming batches. Then, the total fissile material output is the summation of $o_{fissile}(j)$ up to n^{th} incoming batch. That is,

$$O_{fissile}(n) = \sum_{j=1}^{n} o_{fissile}(j)$$

Then, we can set the following mass balance equation,

$$I_{fissile}(n) = O_{fissile}(n) + P_{fissile}(n) + H_{fissile}(n)$$

Where,

- $I_{fissile}(n)$ represents the total inventory of fissile materials input at time step *n*. This term includes the fuel feed stream to the processing facility.
- $O_{fissile}(n)$ represents the total inventory of fissile materials output at time step *n*. This term encompasses the product and waste streams that exit the processing facility.
- $P_{fissile}(n)$ represents the in-process fissile materials inventory at time step *n*. This term takes into account the fissile materials inventory present in the unit processes, such as electrorefiners, distillation furnaces, and so on.
- $H_{fissile}(n)$ represents the inventory of fissile materials associated with the holdup at time step *n*. It serves to explain any mass imbalances that may exist.

In turn, we have the equation explaining the holdup.

$$H_{fissile}(n) = I_{fissile}(n) - O_{fissile}(n) - P_{fissile}(n)$$

Usually, the holdup cannot be directly measured, and thus, it needs to be inferred from measurements of the other terms. Facilities may incur holdups due to various reasons, with measurement uncertainty being a primary cause that can result in positive or negative holdups. Typically, $I_{fissile}(n)$and $O_{fissile}(n)$ increase with respect to *n*, while $P_{fissile}(n)$ is bounded. As a result, once the facility has processed a sufficient amount of material, the holdup can be approximated using the following equation:

$$H_{fissile}(n) \approx I_{fissile}(n) - O_{fissile}(n)$$

This equation indicates that in-process fissile materials inventory becomes irrelevant for explaining holdup.

However, nuclear regulations have strict requirements for material loss, and maintaining a fissile inventory of around 50 kg at any given time in scaled pyroprocessing facilities would not be uncommon. Even with accurate input and output accountancy, not having a way to assess the fissile materials inventory in the facility means that the holdup, $H_{fissile}(n)$, is likely to be around 50 kg, as it is the only way to reconcile the input and output fissile materials inventories. This implies that around 50 kg of fissile materials are likely to be unaccounted for most of the time, which would trigger frequent safeguard events.

If the facility has a low-resolution measurement tool, such as one with a 20% standard deviation on in-process fissile materials, the standard deviation of the holdup will be:

$$std\left(H_{fissle}(n)\right) = std\left(I_{fissile}(n) - O_{fissile}(n) - P_{fissile}(n)\right) \geq 10kg.$$

Two methods for avoiding frequent safeguard events are precision measurement tools for assessing in-process fissile materials inventory or designing unit processes with minimum in-process fissile materials inventory to tolerate high uncertainty in measurement. While the latter is beyond the scope of this report, this report will focus on the issue of measurement quality. To provide an example of holdup assessment and its associated uncertainty, consider the following:

> Suppose the facility operates by maintaining in-process fissile materials at 50 kg, while the daily input and output both have 50 kg of fissile material, measured in one batch per day, with a standard deviation of 1% (0.5 kg) for each measurement. The yearly fissile throughput is estimated to be 18.25 MT. A 1,000 MW thermal reactor is known to consume 1 kg of fissile materials daily. With optimistic throughput assumptions, a pyroprocessing facility operating efficiently at the recommended scale could support 50 reactors of 1,000 MW capacity. Then, two or three of these facilities could process the spent fuel generated by all nuclear power plants in the US, totaling approximately 100,000 MW capacity. With a yearly fissile throughput of 18.25 MT, the variance of the total fissile materials input becomes:
>
> $$var\left(I_{fissile}(n)\right) = \sum_{j=1}^{n} var\left(i_{fissile}(j)\right) = 0.25n$$
>
> The standard deviation of the total fissile materials becomes:
>
> $$std\left(I_{fissile}(n)\right) = \sqrt{\sum_{j=1}^{n} var\left(i_{fissile}(j)\right)} = \sqrt{n * 0.5^2} = 0.5\sqrt{n}$$
>
> Following one year of nominal operation, the standard deviation on the input fissile materials stream becomes:
>
> $$std\left(I_{fissile}(365)\right) = 0.5\sqrt{365} \approx 9.5525\ kg$$
>
> The simplest and most conservative approach to evaluating in-process fissile materials involves relying solely on the most recent measurement. If we assume that the in-process fissile materials are held at 50 kg with a relative standard deviation of 2%, or 1 kg, then the variance of the in-process fissile material is $var\left(P_{fissile}(n)\right) = 1$. As a result, the variance of the hold-up becomes:

$$var\left(H_{fissile}(n)\right) = var\left(I_{fissile}(n)\right) + var\left(O_{fissile}(n)\right) + var\left(P_{fissile}(n)\right) = 0.5n + 1.$$

Then, the standard deviation of the hold-up becomes:

$$std\left(H_{fissile}(n)\right) = \sqrt{0.5n + 1}\ (kg).$$

Following 1 year of continuous operation, the standard deviation on the holdup becomes:

$$std\left(H_{fissile}(365)\right) = \sqrt{183.5} \approx 13.55kg.$$

The degree of uncertainty accumulation on the hold-up inventory outlined above is likely to result in frequent false alarms of safeguard events. One potential solution to this issue involves implementing an accountancy strategy that divides and measures the daily inventory, as opposed to relying on a single measurement. For instance, if 1 kg of fissile material is measured, daily inventory will result in 50 measurements taken each day with a similar level of relative measurement uncertainty. This would lead to a standard deviation of 0.01 kg per measurement. Then:

$$var\left(I_{fissile}(n)\right) = \sum_{j=1}^{n} 50 * var\left(\frac{i_{fissile}(j)}{50}\right) = 50 * 0.0001n = 0.005n$$

$$std\left(I_{fissile}(n)\right) = \sqrt{0.005n} = 0.0707\sqrt{n}$$

Given the same level of uncertainty in the estimation of in-process fissile material inventory, the implementation of a finely divided input and output measurement accountancy strategy would lead to holdup uncertainty following one year of nominal operation as outlined below:

$$std\left(H_{fissile}(365)\right) = 2 * 0.0707\sqrt{365} + 1 \approx 3.7kg$$

Based on the calculations provided above, using non-destructive measurement tools with a finely divided materials streams could lead to more precise inventory accounting and minimize holdup uncertainty. However, one drawback is that this strategy would require more handling and sampling of materials. In addition, there may be a lower limit on the amount of input feed that can be divided, as measurement tools may require a certain quantity of materials to warrant accuracy. Each accountancy term is discussed in more detail below.

6.2 Input Accountancy

Aqueous processing involves dissolving both fuel and clad, and sampling from a well-mixed liquid solution to establish input accountancy. On the other hand, pyroprocessing usually separates the majority of fuel materials from the cladding, resulting in fuel-stripped cladding as an independent waste stream with a fractional fuel phase partition. While this has been proposed as a way to minimize the waste stream, it poses a challenge for accountancy due to incomplete fuel phase segregation from the cladding.

Recent advances in mechanical and chemical decladding processes for oxide fuels have resulted in nearly complete recovery of fuel materials from the fuel pins.[145,146,147,148,149,150,151,152,153,154,155] Additionally, promising solutions have emerged for addressing the sampling issue in oxide fuel feeds, such as the use of representative sampling methods like the riffler[156,157] and decrepitation with voloxidation followed by powder sampling.[158]

Compared to oxide fuel, establishing input accountancy for metal fuel in pyroprocessing facilities poses an additional challenge. As present, there is currently no agreeable means of obtaining representative samples from metal fuel feeds. Consequently, current accounting practices rely on reactor physics calculations and confirmatory sample analysis, resulting in high uncertainty regarding input inventory, which cannot be quantified accurately. While these methods may be adequate for pilot-scale exercises, they are unsuitable for high-throughput facilities. Therefore, there is a need to focus on developing new methods to establish accurate input accountancy for metal fuels. One proposal for establishing input accountancy for metal fuel input feed is to credit the electrorefiner operation, which dissolves most actinides, lanthanides, alkali, and alkali earth elements into the salt. A small fraction of actinides may remain associated with the cladding and end up in the metal waste stream. However, since this amount is small, typically less than 5% of the entire fissile inventory, conservative holdup assessment using mass measurement data may absorb it without triggering safeguard events, as demonstrated below:

$$var\left(I_{fissile}^{interim}(n)\right) = var\left(I_{fissile}^{ER}(n-1)\right) + var\left(i_{fissile}^{MW,low\ latency}(n)\right)$$

The variance term $var\left(i_{fissile}^{MW,low\ latency}(n)\right)$ cam be obtained with mass measurement data and moderately liberal assumptions about the partitioning of fissile materials inventory. Subsequently, consolidation and sampling efforts can help determine the fissile quantity present in the waste stream, thus completing the input accountancy, albeit with some delay. That is:

$$var\left(I_{fissile}(n)\right) = var\left(I_{fissile}^{ER}(n-1)\right) + var\left(i_{fissile}^{MW,high\ quality}(n)\right)$$

Establishing input accountancy in pyroprocessing facilities poses unique challenges that require tailored approaches to account for the inhomogeneous nature of the fuel and the absence of a complete inventory dissolver for input accountancy.

Candidate measurement techniques may employ a combination of the approaches summarized in the later part of this subsection. Low-latency techniques can provide an interim estimate of the fissile inventory in the input stream, while high-latency and high-accuracy techniques can establish a low-uncertainty input accountancy with a delay.

6.3 Output Accountancy

The primary output streams from a pyroprocessing facility typically include uranium metals, group actinide metals, discharged salt, and cladding waste. Miscellaneous outputs include wasted casting crucibles and dross. The standard method for establishing accountancy is based on the analysis of liquid metal and salt samples. During consolidation operations, each batch provides an opportunity to obtain a homogenized liquid sample. Analyzing this sample can enable output accountancy, albeit with a delay. With a similar accountancy strategy combining low-latency and high-latency techniques surveyed in Section 3, it may be possible to operate a high-throughput facility minimizing safeguards event triggers in the following manner:

$$var\left(O_{fissile}^{interim}(n)\right) = var\left(O_{fissile}(n-1)\right) + var\left(o_{fissile}^{low\ latancy}(n)\right)$$

Subsequently, with high-latency and high-accuracy techniques, it is possible to update and minimize the output fissile materials inventory variance, as shown below:

$$var\left(O_{fissile}(n)\right) = var\left(O_{fissile}(n-1)\right) + var\left(o_{fissile}^{high\ quality}(n)\right)$$

Candidate measurement techniques may employ a combination of the approaches summarized in the later part of this subsection. Low-latency techniques can provide an interim estimate of the fissile inventory in the output stream, while high-latency and high-accuracy techniques can establish a low-uncertainty output accountancy with a delay.

6.4 In-Process Material Accountancy

It is crucial to have in-situ measurement tools for in-process material accountancy that do not require time-consuming sample retrieval and preparation. This is because the lack of measurement or high latency can result in significant uncertainty and increase in the holdup, which may render the facility inoperable. Various technologies, such as bubbler, voltammetry, and spectroscopy, have been developed to aid in measuring in-process materials in molten salts.

An alternative approach to address the issue of safeguard improvement is to minimize the fissile inventory within the facility. However, this may limit the cell size and reduce the overall throughput of the facility. From a processing technology perspective, there is a need for research to aid in this area.

In order to achieve a reliable in-process fissile materials inventory assessment, a high-quality salt sample is necessary. However, the presence of inhomogeneities, such as incomplete mixing or solid phase precipitates, can pose a challenge for accurate sampling. Non-homogenized multiphase conditions may introduce uncertainty to the sampling-based estimation approach. To address this challenge, the liquid can be vigorously mixed prior to sampling and any undissolved phases can be filtered out before analysis. This presents an engineering challenge that needs to be addressed.

Recently, a significant advancement in sampling is the development of a microfluidic sampler that can generate uniform salt samples for analysis. This development addresses the challenge of obtaining representative salt samples in real-time, which has been identified as a potential breakthrough for electrochemical safeguards. Furthermore, automated sample collection could be beneficial for commercial scale plants. The new tools include a sampling loop platform for sample extraction, on-line optical analysis, and electrochemical tools for in-situ salt characterization. The sampling loop platform has undergone preliminary testing, and the electrochemical tools have demonstrated stable and accurate measurements over extended periods in engineering-scale process equipment.[159]

6.5 Accountancy Tools

Table 38 outlines various promising techniques that can be utilized individually or in combination for establishing fissile materials accountancy in pyroprocessing facilities. The latter section of this report reviews the relevant measurement technologies including all techniques listed below.

Table 38. List of prospective measurement technologies applicable to pyroprocessing facilities.

Technique	Estimated Quantity	Locations	Uncertainty	Latency
Load cell	Clad mass, Salt mass	Facility Floor	Low	Low
Bubbler	Liquid density	Molten salt	Low	Low
Bubbler	Liquid level	Molten salt	Low	Low
Static Electroanalyses	Elemental concentration	Molten salt	High	Low
Dynamic Electroanalyses	Elemental concentration	Molten salt	Medium	Low
Thermogram	Elemental concentration	Molten metal	Medium	Low
LIBS	Elemental concentration	Ubiquitous	Medium	Low
Gamma spectroscopy	Gamma signature	Ubiquitous	Medium	Low
Microcalorimetry	Photon energy signatures	Ubiquitous	Low	High
Hybrid k-Edge Densitometry	Photon energy signatures	Molten salt	Low	High
Optical Spectroscopies (UV-Vis, Near-IR)	Photon energy absorption	Molten salt	Low	High
Raman Spectroscopy	Photon energy shift	Molten salt	Low	High

Technique	Estimated Quantity	Locations	Uncertainty	Latency
Tracer Dilution Method	Salt inventory	Molten salt	Low	High
ICP-OES/ICP-MS	Isotopic/elemental composition	Analytical site	Low	High
Thermal Ionization Mass Spectrometry	Isotopic/elemental composition	Analytical site	Low	High

In addition to measurement technologies, it is crucial to identify and manage factors that contribute to holdup beyond measurement uncertainty. Understanding the sources and managing their impact is essential for effective holdup management. Experience from processing operations can aid in developing a strategy. For instance, some issues to consider are:

- Material loss due to handling, such as materials lost on the cell floor.
- Unexpected byproducts not reporting to output streams, such as oxidation products from reactions with oxygen and moisture.
- Inability to recover materials completely from containers, such as unrecoverable products from containers or salt hold-up in distillation furnace components.
- In-cell holdup resulting from imperfect cell operation, such as unaccounted metallic uranium phase in the electrorefiner.

The identification of holdup location and phases can offer a solution to reduce and resolve holdup inventory. Systematic techniques such as those described in "A new inventory tracking method for Mark-V electrorefiner are available to identify materials lost to an unidentified phase, and these techniques warrant further attention.[160] They have the potential to support regulatory compliance, material accountancy, and safeguards.

6.6 Inventory Resetting

Pyroprocessing facilities adopt liquid metal cathode technologies for group actinide recovery in a fractional manner, which is different from the once-through production process used in aqueous reprocessing facilities. In pyroprocessing, fissile materials accumulate in the salt and are recovered in fractional groups, resulting in a steady presence of significant quantities of fissile transuranics in the salt. This steady-state characteristic makes completely cleaning out the system to reconcile fissile material inventory wasteful. Furthermore, high temperature, high radioactivity, high corrosivity, and low accessibility present challenges for inventory interrogation via transferring the salt for plant cleanout to reset inventory.

Traditional materials accounting techniques used in aqueous reprocessing plants, such as uranium and plutonium measurements of the input accounting minus those of the product and the waste streams, are adequate as instantaneous in-process fissile materials are not significant with diluted solutions. High throughput of aqueous reprocessing facilities comes from rapid flow and contactor design. This may not be suitable for pyroprocessing facilities as in-process fissile materials are likely to be significantly higher than those of aqueous reprocessing facilities. Instead, reliable in-process inventory estimation techniques that consider the unique operating characteristics of the pyroprocessing process are necessary. The batch processing nature of the pyroprocessing allows for interim inventory assessments, which is not possible in continuous production processes that require operation halts for assessment. Furthermore, the electrochemical nature of the pyroprocessing process, based on the ionic nature of the molten salt, provides an opportunity to interrogate the melt's inventory using electrochemical means.[159,161,162,163,164,165,166,167,168] Hence, electrochemical means can be a unique in-situ tool for building a reliable safeguard system in pyroprocessing facilities.

There are many promising developments in the field outlined in the following section, and synergistically joining these efforts would be necessary to construct a reliable MC&A and safeguard strategy. Developing reliable inventory estimation techniques that consider the unique characteristics of pyroprocessing facilities is essential to ensure the safe and secure management of fissile materials.

6.7 Applicable Measurement Technologies Review

In pyroprocessing systems, various measurement methods have been proposed for deployment. These methods can be classified based on their measurement target, the latency period, potential deployment locations, and the estimated uncertainty. This report primarily categorizes the methods according to their latency period. The importance of low latency techniques cannot be overstated, as they play a crucial role in improving the timeliness of MC&A procedures, enabling facility safeguards, and allowing uninterrupted facility operation. Meanwhile, high latency techniques also have a significant role to play, as they can provide more accurate measurement results, a deeper understanding of the nature of safeguards incidents, and can help assess the situation in a post-incident manner.

Following the methodology outlined in "Review of Candidate Techniques for Material Accountancy Measurements in Electrochemical Separations Facilities," the evaluation of candidate measurement technologies considers four factors: 1) measurement latency, 2) information that can be obtained from the measurement, 3) potential deployment locations, and 4) estimated measurement uncertainty.[169] Latency is judged based on the entire process of making a single measurement, including sample retrieval and preparation, and measurement execution. Measurements that are taken in situ and are nearly instantaneous (taking minutes or less) are considered low latency, while those that take longer than a few hours due to sampling requirements and subsequent preparations, onsite testing, and/or offsite analysis are considered high latency. This latency evaluation is based on the available literature and authors' own assessment, which may change with future developments. The references and technologies provided may not be exhaustive.

6.7.1 Low Latency Measurement Technologies

- Load Cell[170]: Load cell measurements of mass are based on electrical signals that respond to compressive forces. This is a basic but very precise mass measurement, but it only shows the overall mass that is moving through the system. However, this information is valuable in determining the complete mass inventory of the pyroprocessing system and detecting possible diversion attempts. Measurement devices can be placed at various areas within the pyroprocessing facility. In principle, the facility must ensure that these measurements are taken for any material movement in the facility. The uncertainty associated with load cell measurements is typically low with proper calibrations. The material mass information can provide important insights into facility operation when used in conjunction with other measurement technologies.[160]
- Bubbler[171,172,173,174,175]: The evaluation of the molten salt level and density provides information on the mass of salt in the vessel when the level has been calibrated against volume. Therefore, knowledge of density and molten salt level enables the assessment of the overall mass of salt in the vessel, but not its composition. Moreover, unexpected changes in the molten salt level can indicate the presence of gross diversion or material addition in specific areas, while changes in density can indicate potential alterations in composition with possible material substitutions. These measurements can serve as a valuable safeguard tool. These measurements can be taken in-situ from the molten salts in processing units of the pyroprocessing facility using bubbler systems.[171,172,173,174,175] This approach leverages the linear relationship between pressure and the depth and density of the liquid. Associated research has shown that the use of a bubbler system can provide accurate measurements for both density and level below 1%.

- Static Electroanalyses[161,162,163,164]: Static electroanalytical techniques measure the potential of one electrode relative to a reference electrode with a very small amount of current flow and associated reactions. Typically, two electrodes are employed using various electrolyte configurations, and finding compatible material combinations is key to extracting the desired information from the electrolyte. For pyroprocessing applications, these techniques are commonly used to determine the concentration of specific species within molten salts. The sensitivity of this measurement is high, and it is likely to vary as electrode conditions change over time. Therefore, even though high accuracy and precision may be obtainable in a laboratory setting, as done for thermodynamics quantity measurement experiments, the best use of this technique is qualitative in in-situ field applications.
- Dynamic Electroanalyses[159,165,166,167,168]: Dynamic electroanalytical techniques deal with time-dependent phenomena at electrode/electrolyte interfaces. Depending on which process variables to control, techniques are divided into controlled potential and controlled current methods. Controlled potential techniques use potentiostats to regulate the potential in a specific manner, with the current being monitored as the response to the potential. This type of technique is referred to as voltammetry. Alternatively, galvanostats can be used to control the current, with the potential of the working electrode being examined as the response to the current. The dynamic nature of this technique requires careful control of operation parameters such as electrode surface area, signal sweep rate, and response signal interpretation experience to extract information with better accuracy and precision. The techniques can be used for quantitative assessment with moderate measurement uncertainties of less than 10%.
- Thermogram[176,177]: This technique is based on the cooling behavior of alloy systems and can be used for in-situ monitoring of plutonium content in actinide alloys. The process involves heating the alloy, primarily composed of uranium and plutonium, to a liquid state in an inert or reducing atmosphere, and then cooling it to a solid state in the same environment. The temperature of the U-Pu alloy during the cooling process is monitored to determine a solidification temperature signature, which is used to calculate the amounts of uranium and plutonium present in the alloy. This method can be applied to the consolidation of group actinide metals. Although no formal uncertainty analysis has been performed, typical thermogram approaches have moderate uncertainty. Therefore, this can be considered a low-latency tool for providing interim composition information prior to executing low-uncertainty analysis.
- Laser-Induced Breakdown Spectroscopy[178,179,180,181,182,183]: Laser-induced breakdown spectroscopy (LIBS) is a fast and non-destructive technique for elemental analysis. LIBS uses a pulsed laser to vaporize small samples of subject materials, creating a transient plasma. With the relaxation of the plasma, each element emits photons at characteristic frequencies, allowing for identification of the sample's composition. If isotope specific photon information is available, this technique can also be used to determine the sample's isotope composition. LIBS can be widely used throughout a facility because it can be implemented remotely from the target and deal with various material forms, making its installation more manageable and versatile. However, moderate to high uncertainties, with an estimated deviation of up to 10%, are anticipated. Therefore, this can be considered a low-latency tool for providing interim composition information prior to executing low-uncertainty analysis.
- Gamma Spectroscopy[184,185,186]: Gamma spectroscopy has a suitable role in assessing gamma-bearing radioactive materials in a facility. It can identify specific isotopes with distinctive highly penetrating gamma signatures, such as ^{137}Cs, ^{134}Cs, and ^{154}Eu. Passive gamma measurements can monitor the location of gamma-emitting fission products in the facility, providing information on the accumulation of gamma-emitting fission products and serving as an indicator for any diversion scenarios. The accuracy of the techniques used to measure the quantity of gamma sources has a moderate level of uncertainty, usually aimed to approach 1%, when employing spectroscopy or total counting methods under optimized measurement conditions. Additionally, these signatures are related to the burnup of the fuel, its cooling time, and enrichment, which can then be used to estimate the

input inventory with the conjunction of depletion codes, at the expense of elevated uncertainty reaching 10%. The best independent use of this technique in low-latency applications for pyroprocessing facilities is qualitative radioactive material signature detection.

- Neutron Counter[187,188,189,190,191,192,193,194]: The total neutron counting method is a tool for measuring neutrons. This technique can be useful in tracking the presence of neutron-emitting actinides, such as ^{244}Cm, and determining the location of associated transuranics in a pyroprocessing facility. However, while it can accurately measure neutron-emitting actinides with an error rate of around 1%, it is not a direct method for establishing the overall actinide inventory. To determine the inventory of other actinides, additional assumptions are necessary which can result in much higher uncertainty and potentially hinder the accuracy of the assessment. The best independent use of this technique in low-latency applications for pyroprocessing facilities is qualitative transuranic material signature detection.
- Alpha Spectrometry[195,196,197]: With alpha decay, plutonium and other minor actinide isotopes release unique and distinguishable alpha particles. The unique energy release from these heavy isotopes during alpha decay can be used for isotopic analysis determining relative isotopic distributions. While alpha spectrometry can be accurate and provide direct measurement of alpha signatures of actinide isotopes, with uncertainty values approaching 1% in controlled environments, further research is needed to determine its applicability and sustainability in a highly radioactive pyroprocessing facility. Recent advancement in silicon carbide (SiC) alpha detectors offer a direction for exploration.

Table 39 summarizes the low latency measurement technologies with measured quantity, possible locations in pyroprocessing facilities, respective perceived uncertainties.

Table 39. Summary of low latency measurement technologies.

Technique	Measured Quantity	Locations	Uncertainty	Reference
Load cell	Mass	Facility Floor	Low	170
Bubbler	Liquid density	Molten salt	Low	171, 172, 173, 174, 175
Bubbler	Liquid level	Molten salt	Low	171, 172, 173, 174, 175
Static Electroanalyses	Elemental concentration	Molten salt	High	161, 162, 163, 164
Dynamic Electroanalyses	Elemental concentration	Molten salt	Medium	159, 165, 166, 167, 168
Thermogram	Elemental concentration	Molten metal	Medium	176, 177
LIBS	Elemental concentration	Ubiquitous	Medium	178, 179, 180, 181, 182
Gamma spectroscopy	Gamma signature	Ubiquitous	Medium	184, 185, 186
Neutron counter	Neutron signature	Ubiquitous	High	187, 188, 189, 190, 191
Alpha spectrometry	Alpha signature	Ubiquitous	N/A	195, 196, 197

6.7.2 High Latency Measurement Technologies

- Calorimetry[198]: Calorimetry is a non-destructive method that utilizes a thermocouple-type device to analyze heat-generating materials. As this technique requires neither homogenization nor special sample preparation, it can be useful in assessing heterogeneous bulk materials in pyroprocessing facilities. The method isolates subject heat-generating materials in a sealed chamber connected to a heat sink and measures the change in electrical potential proportional to the temperature gradient. Prior knowledge of heat-generating isotopes can be used to extract information from materials containing them. However, there may be a delay of several hours as the system reaches thermal equilibrium with materials, and uncertainty is typically high. Compositional resolution of heat-generating isotopes relies on independent isotopic analysis with other analytical means or compositional assumptions. Although the extracted information may be crude, the technique is effective for non-destructively analyzing heterogeneous bulk materials with arbitrary geometry and matrix that cannot be directly interrogated.
- Microcalorimetry[199,200,201,202,203,204]: The microcalorimetry method can detect single-photon heating with superconducting transition-edge sensors (TESs). This technique is known to resolve crowded energy features and can be applied in pyroprocessing facilities when subject materials are homogenized and the attenuation of emitted energy from the materials is minimal. Under a controlled environment, uncertainty of actinide isotopes quantity estimation, such as 238Pu, 239Pu, 240Pu, and 241Am characterized with crowded energy signature, can be less than 1%. Accuracy comes with latency cost as the small size and low count rate efficiency of TES-based microcalorimetry systems can require longer measurement times for reliable statistics. In addition, constructing a large scale microcalorimeter system is known to be constrained by real-time handling/processing capability of data stream from large TES pixel arrays. To overcome this constraint, advancements in efficient real-time processing of large-size data are desired to improve the feasibility of large-scale microcalorimetry systems.
- Hybrid k-Edge Densitometry[184,205,206,207,208,209]: X-ray fluorescence (XRF) estimates elemental ratios in the subject materials by measuring emitted fluorescence X-rays from the subject materials when it is excited by an X-ray source. K-edge densitometry (KED) infers the concentration of dominant species in the subject materials using X-ray beam attenuation at the K-edge energy. As both techniques use X-ray source, these techniques can be combined to create hybrid K-edge densitometry (HKED) for quantifying species concentration of interest. Onsite instrumentation may provide moderate latency measurements for XRF and KED, with an expected latency of several hours. Homogenized solid or liquid subject materials can be analyzed for compositions with this hybrid X-ray technique. Studies have reported a low uncertainty of less than 1%, making it a promising technology for future development.
- Optical (UV-Vis, Near-IR) Spectroscopies[210,211,212,213,214,215,216,217,218,219,220,221,222,223,224]: UV-Vis and Near-IR spectroscopies utilize photons from the ultraviolet and infrared regions of the spectrum to identify specific species, respectively. The absorbed photon excites an electron to higher energy molecular orbitals, giving rise to an excited state. It causes certain wave lengths of light beams to become attenuated. A spectrophotometer can be used to determine the concentration of species in the subject materials through optical transmission measurements, thus providing the elemental concentrations of the subject materials, typically liquids in an optically transparent container. With a clever sampler design for bulk liquid and careful calibration, it is envisioned to be performed in situ for determining concentrations of species responding to these techniques. Studies have reported a low uncertainty of less than 1% for species responding to the ultraviolet and infrared regions, making it a promising area for future development.

- Raman Spectroscopy[211,224,225,226,227,228,229]: Raman spectroscopy utilizes light of various wavelengths, including ultraviolet, infrared, and visible light, to direct photons onto a substance and then measure the energy shift of the scattered light. The energy shift is a result of vibrational shifts in the molecules of the material and each molecule gives a different corresponding shift, allowing for elemental identification. One noted advantage of Raman spectroscopy is the ability to measure from a distance at the expense of elevated uncertainty, likely over 10%. It can also complement UV-Vis, Near-IR spectroscopies for detecting species not responding to photons of the ultraviolet and infrared regions and is readily applicable to solid subject materials. It is expected to perform similarly to other optical spectroscopy techniques under controlled experimental conditions.
- Tracer Dilution Method[156,157,158,230,231]: The tracer dilution method is a method for determining the mass of liquid in arbitrarily shaped containers. This is useful as the internal shape of electrolyte containers in pyroprocessing systems changes over time with deposits and/or byproduct accumulation, which makes it unreliable to estimate inventory based upon liquid level measurement. This method involves the use of radioactive sources with a known activity or exogeneous element, which can be dissolved into the bulk liquid. After complete mixing, a small sample of the liquid is taken and its elemental mass and/or radioactivity of injected radioactive sources are measured, which can lead into the bulk liquid mass estimate in the bulk liquid container. The trace dilution method is a relatively simple and straightforward way to determine the mass of molten salt in pyroprocessing systems with accuracy but latency at present.
- Inductively Coupled Plasma Mass Spectrometry and Optical Emission Spectroscopy[232,233,234]: Inductively coupled plasma mass spectrometry (ICP-MS) and optical emission spectroscopy (ICP-OES) are techniques that can be used for quantifying isotopic and elemental concentrations, typically used in a combined manner to obtain the overall composition of the sample. To achieve this, a laser of inductively coupled plasma ionizes the sample. ICP-MS measures an atom's mass by mass spectrometry (MS) while ICP-OES quantitation is based on measurement of excited atoms and ions at the wavelength characteristics for the specific elements being measured. These are widely adopted reference techniques that analytical laboratories use for estimating composition. However, these techniques require laborious sample preparation, making it less attractive as a real-time measurement method. Properly performed ICP-MS and ICP-OES measurements have among the highest precision of available techniques, capable of quantifying individual isotopes and elements with typical uncertainties of no greater than 2% and usually lower than 1%, but in-situ application is unlikely.
- Thermal Ionization Mass Spectrometry[235,236,237,238,239]: The technique known as thermal ionization mass spectrometry (TIMS) measures isotope ratios of elements that can be ionized thermally. A chemically purified liquid sample is heated to evaporate the solvent. Further heating removes a single electron and ionizes the atoms of the sample. Then, TIMS uses a magnetic sector mass analyzer to separate the ions based on their mass to charge ratio. These separated ions are directed into collectors, where they are converted into voltage. By comparing the voltages corresponding to each separated ion beam, precise isotope ratios can be determined. By spiking tracer isotopes in a manner that is similar to the tracer dilution technique, absolute concentrations of isotopes are estimated with TIMS. This highly precise spectroscopy technique is often used as a reference tool for establishing MC&A in pyroprocessing facilities at INL.
- Active Neutron Interrogation and Neutron Coincidence Counting[240,241,242,243,244,245,246,247,248,249]: Active neutron interrogation (ANI) is a technique bombarding a sample with neutrons to induce fission. The induced fission neutrons are then analyzed using appropriate neutron-sensitive detectors combined with timing information to identify their location. Explosives detection has been the primary application for this technique but the possible application to pyroprocessing facility is also noted. ANI is typically known to have high uncertainty and latency for estimating isotopic concentrations. The best application for this technology is likely to be a qualitative detection tool rather than quantification device.

Table 40 summarizes the high latency measurement technologies with measured quantity, possible locations in pyroprocessing facilities, respective perceived uncertainties.

Table 40. Summary of high (hour or more) latency measurement technologies.

Technique	Measured Quantity	Likely Locations	Uncertainty	Reference
Calorimetry	Heat	Facility Floor	High	198
Microcalorimetry	Photon heat	Ubiquitous	Low	199, 200, 201, 202, 203
Hybrid k-Edge Densitometry	Photon energy signatures	Molten salt	Low	184, 205, 206, 207, 208, 209
Optical Spectroscopies (UV-Vis, Near-IR)	Photon energy absorption	Molten salt	Low	210, 211, 212, 213, 214, 215, 216, 217, 218, 219, 220, 221, 222, 223, 224
Raman Spectroscopy	Photon energy shift	Molten salt	Low	211, 224, 225, 226, 227, 228, 229
Tracer Dilution Method	Salt inventory	Molten salt	Low	156, 157, 230
ICP-OES/ICP-MS	Isotopic/elemental composition	Analytical site	Low	232, 233, 234
TIMS	Isotopic/elemental composition	Analytical site	Low	235, 236, 237, 238, 239
ANI	Fissile isotope concentration	Facility Floor	High	240, 241, 242, 243, 244, 245, 246, 247, 248, 249

6.8 Summary and Recommendations

Pyroprocessing incorporates a family of technologies that can be applied to reprocessing a variety of spent nuclear fuel types. Pyroprocessing has been most extensively studied for sodium-bonded metallic HEU fuels used in EBR-II and the FFTF Reactor (the IFR and SFT Programs) and uranium oxide fuels used in light water reactors (JFCS Program). Considerable research has been carried out in the US and many other countries, notably the Republic of Korea, Japan, and Russia, where the technologies have been demonstrated at both laboratory and pilot scales.

Although pyroprocessing holds significant promise for future nuclear fuel recycling efforts, particularly in applications involving metallic fuels, it is currently not used in commercial nuclear fuel reprocessing facilities. In order to commercialize this technology, there are still significant challenges associated with pyroprocessing to address, especially with regards to scaleup, automation, salt management, waste management, and nuclear materials accountancy. Further research and development are needed to address these challenges and fully realize the potential of these technologies. The engineering design requirements of a pyroprocessing facility are based upon the needs of the fuel cycle scenario the facility is meant to serve. Once a specific fuel cycle scenario is selected, pyroprocessing research and development efforts become more focused.

Scaleup of process equipment such as the OR and ER cells, and the distillation and casting furnaces, are influenced by criticality limitations and the requirements of nuclear materials accountancy. In turn, the criticality limitations are influenced by the type of fuel to be processed which, for example, may include HEU/Zr metallic fuels, DU/TRU/Zr metallic fuels, MOX oxide fuels, and LEU oxide fuels. As the unit operations reach their maximum sizes, throughput is increased by running parallel unit operations.

Automation to some degree is a requirement of a commercial reprocessing facility. The SFT and JFCS Programs do not include many aspects of automation with regards to the movement of materials from one unit of operation to the next. These activities are largely performed manually by operators with mechanical systems such as overhead cranes and telemanipulators inside the hot cells. A commercial reprocessing facility will require integrated unit operations that can accommodate automated remote systems operations.

Salt management is at the center of pyroprocessing development. Salt management is related to all aspects of the process, including separations chemistries, actinide management, fission product management, decay heat management, waste management, and nuclear materials accountancy. The more complex salt management becomes, the greater the number of unit operations involved in the process, and the greater the complexity of the process.

Waste management requirements are dictated by the acceptance criteria for both transportation and disposition into geologic repositories. These acceptance criteria will address topics such as waste composition, packaging, and chemical stability. Without known standards for transportation and disposition, the requirements of pyroprocessing wastes cannot be determined accurately.

Nuclear materials accountancy requires strategy with respect to facility design, process measurement, and statistical rigor. It is a design requirement of every unit operation and process stream. Nuclear materials accountancy is important for safeguards and security, and for criticality safety. Facility operations will be impacted by the requirement for periodic closeout and inventory analysis.

Pyroprocessing operations have several notable safety implications related to high temperature operations. These include chemical reactivity with air and moisture, corrosion, loss of electrical power, loss of control signals, and spilling of molten salt or molten metal. None of the aforementioned stand out as inherently dangerous as all can be mitigated by administrative and engineering controls.

Chemical reactivity will need to be considered in situations where process salts and metals that are meant to be maintained within a dry argon atmosphere are inadvertently exposed to oxygen and moisture by a process upset. Many factors influence the consequences of such exposures. The more extreme events can lead to rapid oxidation and the pyrophoricity of metals under the correct conditions, and reactions of high temperature salts and metals can release H_2(g), HCl(g), and Cl_2(g).

Corrosion of the materials of construction is related to high chemical potentials of chlorine and oxygen in forms such as $Cl_2(g)$ and $O_2(g)$, respectively. Based on experience at INL, corrosion within the uranium electrorefiner has been mitigated by the presence of uranium metal and zirconium metal in the ER cell, which has greatly suppressed the chlorine and oxygen chemical potentials in that environment. Greater corrosion has been observed in oxide reduction operations in the OR cell where $O_2(g)$ is liberated at the anode. Salt management strategies that rely on the liberation of the chlorine as $HCl(g)$ or $Cl_2(g)$ will have to mitigate the corrosion effects of these processes.

Loss of electrical power must be anticipated because it will inevitably occur. Loss of power can lead to rapid cooling of the high temperature process equipment and the solidification of process liquids such as molten salts and metals. Equipment designs must both tolerate loss of power and provide a means of recovery from loss of power.

Loss of control signals must also be anticipated because this too will inevitably occur. The process equipment will be controlled based on feedback between process signals and computer control logic. Process signals will voltage or amperage signals that are related to engineering units such as temperatures, voltages, amperages, pressure, masses, etc. When these signals are lost or lose calibration (drift), then loss of control or misinterpretation of the process can occur. Such events are mitigated by system redundancies and control logic. Strategies for troubleshooting, verifying, and repairing the control systems should be addressed during equipment design.

Spillage of molten salt or molten metal is one more event that should be anticipated. Based on experience at INL, spillage of these materials has occurred when process crucibles have failed while in service. The molten materials have spilled into distillation and casting furnaces. Damage to the process equipment has been minimal but does require extensive disassembly and cleanout of the process equipment.

There are marked differences between pyroprocessing and aqueous reprocessing technologies. Pyroprocessing has lower separations factors, incorporates many batch processing operations, greatly limits the exposure of nuclear materials to moderators in the hot cells, lacks accountancy tanks to track nuclear materials inventories, and recovers actinide products as metals.

Separation factors for pyroprocessing technologies are significantly lower than for aqueous technologies. While pyroprocessing can recovery purified uranium and TRU as U/TRU alloys, pyroprocessing is not intended to recovery individual actinide metals as high purity products, something that aqueous technologies are well suited for with respect to actinide oxides. This disparity between the two routes has largely to do with the enhanced valence chemistry of the metal ions during aqueous separations. More valence states are available in the aqueous chemistry route than the molten salt chemistry route, allowing these properties to be exploited for enhanced separations.

Batch processing is an inherent feature of pyroprocessing. Materials are discretely advanced in containers from one unit operation to the next. Research efforts have been made to design equipment that better approximates a continuous flow process for the purpose of aiding mechanical automation. Aqueous reprocessing is seen as much more of a continuous flow process once the fuels are dissolved into the acid media.

Moderators are expressly removed from pyroprocessing operations. These moderators include sources such as water for process equipment cooling and hydraulic fluids for process equipment mechanical functions.

Nuclear materials inventories are fundamentally different between pyroprocessing and aqueous technologies. The lack of moderators allows for much greater actinide concentrations in molten salts than in aqueous solutions. Consequently, the in-process actinide inventory in a pyroprocessing facility can be markedly greater than the in-process inventory in an aqueous facility, all other things being equal.

Metal products are produced by pyroprocessing. Aqueous reprocessing recovers actinides as purified oxides. This is the basis for suggesting that pyroprocessing may be better suited for a metallic fuel cycle application, which aqueous reprocessing may be better suited for an oxide fuel cycle application. The fundamental reason is that actinide metals can be recovered from halide molten salts, while actinide metals are too chemically reactive with water to be recovered as anything other than oxides from aqueous solutions. An exception to this rule is the Salt Cycle Process, which is a molten salt process designed to reprocess MOX fuels.

Review papers were categorized separately. These cover several different aspects of pyroprocessing development from perspectives that are broader than those found in technical papers related to discretized research topics. These review papers were selected because the authors are known to be familiar with pyroprocessing technologies.

The recent journal publications related to salt management chemistries have been categorized into topical areas of reactive metal electrodes, reactive metal drawdown, precipitation-based drawdown, and salt purification by crystallization. These topics are important for waste management with regards to rejecting fission products to the waste streams and retaining actinides in the fuel cycle.

Reactive metal electrodes exploit the thermodynamics of metal alloy system to selectively collect metal cations from the ER salt. Actinide metal cations are typically targeted for the purpose of retaining the actinides in the fuel cycle. After the actinides are removed and recovered from the ER salt, the salt can be further processed in preparation for fission product disposal.

Reactive metal drawdown serves the same purpose as reactive metal electrodes but is functionally different. The metal serving as the reductant must be more electropositive than the metal to be drawn down from the salt. An example is the use of lithium metal as the reductant to drawdown uranium metal from the salt. The metals that are drawn down can effectively precipitate from the salt or, in a more controlled manner, be collected on a cathode.

Precipitation-based drawdown is focused on the removal of fission products from the OR and ER salts by chemical conversion of the fission product chlorides to mineral forms such as oxides, phosphates, carbonates, and sulfides.

Salt purification by crystallization is also focused on the removal of fission products from the OR and ER salts. This technique exploits the portioning of impurities in the molten salt ahead of a solidification front. Effectively, as solidification occurs, the solidified phase is cleaner than the molten phase, but only up to a point. The technique provides a means of concentrating the fission products into a smaller volume of waste salt.

The recent journal publications related to process chemistries of unit operations have been categorized into topical areas of oxide reduction, chemical decladding, uranium electrorefining, chlorination chemistry, and facility investigations.

Oxide reduction is the process of converting spent oxide fuels to metals in preparation for uranium electrorefining. Oxide reduction technologies are significantly less mature than uranium electrorefining technologies. Compared to uranium electrorefining, oxide reduction require more time due to the kinetic limitations of mass transfer between the solid and liquid phases of the reduction process.

Chemical decladding is focused on the removal of zirconium alloy cladding from LWR oxide fuels. The reaction of the cladding with chlorinating chemicals converts the zirconium metal to $ZrCl_4(g)$ which is recovered separately. The oxide fuel is unaffected by the process. Consideration is given to converting the $ZrCl_4$ back to zirconium metal as a means of recycling the zirconium.

Uranium electrorefining is where most of the chemical separations occur. All but the transition metal fission products are partitioned to the salt while uranium is electrorefined from the anode to the cathode. The electrorefined uranium accumulates on the cathode as a highly dendritic, high surface area, deposit. This uranium is harvested and consolidated into an ingot as the salt is distilled and collected for return to the ER cell. Much experience has been gained on uranium electrorefining through the SFT Program.

Chlorination chemistry is important for several aspects of pyroprocessing and MSR development. For pyroprocessing, chlorination provides a means of replenishing the ER salt with UCl_3, which is consumed as fission products and TRU accumulate in the ER salt. Chlorination also provides a means of dispositioning oxidized materials that are not candidates for electrorefining such as corroded metallic fuels and casting dross. For MSRs, chlorination provides a means of preparing fuel salts from uranium oxide materials.

Facility investigations provide means of assessing the cost models and technology readiness levels of the various aspects of pyroprocessing. Compared to aqueous reprocessing, pyroprocessing technologies are at their infancy. The total amount of spent fuel processed by pyroprocessing is measured in terms of a few metric tons resulting from the SFT Program. The JFCS Program processed a total of approximately 26 kg of oxide fuels.

Safeguards and accountancy technologies for pyroprocessing facilities are under development. Much work is being performed in these areas under the JFCS Program. The safeguards challenges are strikingly different between aqueous reprocessing and pyroprocessing. Research efforts have focused on input accountancy, in-process inventory management, and minimizing fissile inventories.

Input accountancy for pyroprocessing is an area that deserves regulatory attention and innovation. Input accountancy at an aqueous reprocessing facility is achieved by dissolving a batch of fuel in an acidic solution and transferring the solution into an accountancy tank. The volume, density, and composition of the fluid in the accountancy tank provide the mass of nuclear materials entering the process. Pyroprocessing is not amenable to an accountancy tank. While there has been some progress in oxide fuel accountancy with solid particle sampling, metallic fuel input accountancy is an area that needs to be explored further.

In-process inventory management becomes increasingly important as the scale of pyroprocessing processes increases. Pyroprocessing readily handles many forms of fissile materials including spend fuels, molten salts, and molten metals. Current pyroprocessing concepts tend to maintain significant in-process fissile inventories. This means that it is important to develop appropriate safeguards and accountancy tools to ensure that the fissile inventories are maintained in an accurate and appropriate manner. Inventory management is complicated by the batch-wise processing and material transfers associated with pyroprocessing.

Minimizing fissile inventories while increasing throughput is likely to be a tradeoff in the design of a commercial scale pyroprocessing facility. However, future process development, particularly development aimed at scaling up pyroprocessing, will need to pay attention to this aspect to alleviate the burdens associated with safeguards and inventory management.

7. ACKNOWLEDGEMENTS

This report was prepared for the United States Nuclear Regulatory Commission by the Idaho National Laboratory. Many researchers have been involved in the development of pyroprocessing technologies both nationally and internationally. This report is merely a summary of experiences related to a portion of that work.

8. AUTHORS

Guy L. Fredrickson, Ph.D.

Dr. Fredrickson is a Distinguished Research Scientist in the Pyrochemistry and Molten Salt Systems Department at the Idaho National Laboratory. He received his Ph.D. in Metallurgical and Materials Engineering from the Colorado School of Mines, Golden, CO.

guy.fredrickson@inl.gov

ORCID: 000000018711338X

Tae-Sic Yoo, Ph.D.

Dr. Yoo is a Distinguished Research Scientist in the Advanced Technology of Molten Salts Department at the Idaho National Laboratory. He received his Ph.D. in Electrical Engineering from the University of Michigan, Ann Arbor, MI.

tae-sic.yoo@inl.gov

ORCID: 0000000222445700

9. REFERENCES

1. Bell, M. J. 1973. “ORIGEN — The ORNL Isotope Generation and Depletion Code.” Oak Ridge National Laboratory, ORNL, 4628.
2. Fredrickson, G., G. Cao, R. Gakhar, and Yoo, T. S. 2018. “Molten Salt Reactor Salt Processing – Technology Status.” INL/EXT-18-51033, Idaho National Laboratory.
3. Mirza, M., et. al. 2023. “Electrochemical Processing in Molten Salts – A Nuclear Perspective.” Energy & Environmental Science. DOI: 10.1039/D2EE02010F.
4. Fredrickson, G. L., et. al. 2022. “History and Status of Spent Fuel Treatment at the INL Fuel Conditioning Facility.” Progress in Nuclear Energy, 143. 104037.
5. Riley, B. J., and S. Chong. 2022. “Dehalogenation Reactions Between Halides Salts and Phosphate Compounds.” Frontiers in Chemistry. DOI: 10.3389/fchem202.976781.
6. Carlson, K., et. al. 2021. “Molten Salt Reactors and Electrochemical Reprocessing: Synthesis and Chemical Durability of Potential Waste Forms for Metal and Salt Waste Streams.” International Materials Reviews, 66: 339-363.
7. Fredrickson, G. L., and T. S. Yoo. 2021. “Nuclear Fuels and Reprocessing Technologies: A U.S. Perspective.” INL/EXT-20-69106, Idaho National Laboratory.
8. Galashev, A. Y. 2022. “Recovery of Actinides and Fission Products from Spent Nuclear Fuel via Electrolytic Reduction: Thematic Overview.” International Journal of Energy Research, 46: 3891-3905.
9. Moyer, B. A., et. al. 2021. “Report for the US Department of Energy, Office of Nuclear Energy, Innovative Separations R&D Needs for Advanced Fuel Cycles Workshop.” August 30 to September 1, 2021.
10. Williams, T., R. Shum, D. Rappleye. 2021. “Review – Concentration Measurements in Molten Chloride Salts Using Electrochemical Methods.” Journal of the Electrochemical Society: 168.
11. DelCul, G. D., and B. B. Spencer. 2020. “12 – Reprocessing and Recycling.” Advances in Nuclear Fuel Chemistry, Woodhead Publishing Series in Energy.
12. Riley, B. J. 2020. “Electrochemical Salt Wasteform Development: A Review of Salt Treatment and Immobilization Options.” Industrial Engineering and Chemical Research, 59: 9760-9774.
13. Willett, C. D., S. R. Kimmig, W. S. Cassata, B. H. Isselhardt, M. Liezers, G. C. Eiden, and J. F. Wacker. 2020. “Fission Gas Measurements in Spent Fuel: Literature Review.” LLNL-TR-815309, Lawrence Livermore National Laboratory.
14. Baron, P. et. al. 2019. “A Review of Separations Processes Proposed for Advanced Fuel Cycles Based on Technology Readiness Level Assessments.” Progress in Nuclear Energy, 177: 103091.
15. Fredrickson, G. L., et. al. 2019. “Review – Electrochemical Measurements in Molten Salt Systems: A Guide and Perspective.” Journal of the Electrochemistry Society, 166: D645-D659.
16. Park, G. I. et. al. 2019. “Recent Progress in Waste Treatment Technology for Pyroprocessing at KAERI.” JNFCWT, 17: 279-298.
17. Riley, B. J., D. A. Pierce, J. V. Crum, B. D. Williams, M. M. V. Snyder, and J. A. Peterson. 2018. “Waste Form Evaluation for $RECl_3$ and REO_x Fission Products Separated from Used Electrochemical Salt.” Progress in Nuclear Energy, 104: 102-108.

18. Zhou, W., J. Zhang, and Y. Wang. 2018. “Review – Modeling Electrochemical Processing for Applications in Pyroprocessing.” Journal of the Electrochemical Society, 165: E712-E724.

19. Frank, S. et. al. 2015. “Waste Stream Treatment and Waste Form Fabrication for Pyroprocessing of Used Nuclear Fuel.” INL/EXT-14-34014, Idaho National Laboratory.

20. Soelberg, N. R., T. G. Garn, M. R. Greenhalgh, J. D. Law, R. Jubin, D. M. Strachan, and P. K. Thallapally. “Radioactive Iodine and Krypton Control for Nuclear Fuel Reprocessing Facilities.” Science and Technology of Nuclear Installations. DOI: 10.1155/2013/702496.

21. Inoue, T, T. Koyama, and Y. Arai. 2011. “State of the Art Pyroprocessing Technology in Japan.” Energy Procedia, 7: 405-413.

22. Ding, L., et. al. 2023. “Electroextraction of Neodymium from LiCl-KCl Using Binary Liquid Ga-Al Cathode.” Journal of Rare Earths.

23. Yang, D. W., et. al. “Kinetic Properties and Electro0Separation of U on Binary Liquid Ga-Al Eutectic Alloy Cathode.” Journal of Radioanalytical and Nuclear Chemistry. DOI: 10.1007/s10967-023-08782-y.

24. Zhang, H., Q. Du, X. Du, Z. Xu, S. Guo, and W. Zhou. 2023. “Selective Extraction of Sm from LiCl-KCl Molten Salt into Wasteforms via Liquid Bismuth.” Separations and Purification Technology, 313: 123441.

25. Im, S., N. D. Smith, S. C. Baldivieso, J. Gesualdi, and Z. K. Liu. 2022. “Electrochemical Recovery of Nd Using Liquid Metals (Bi and Sn) in LiCl-KCl-NdCl3.” Electrochimica Acta, 425: 140655.

26. Novoselova, A., et. al. 2022. “Electrode Processes and Electrochemical Formation of Dy-Ga and Dy-Cd Alloys in Molten LiCl-KCl-CsCl Eutectic.” Journal of Electroanalytical Chemistry, 906: 116012.

27. Jang, J., M. Lee, G. Y. Kim, and S. C. Jeon. 2022. “Cesium and Strontium Recovery from LiCl-KCl Eutectic Salt Using Electrolysis with Liquid Cathode.” Nuclear Engineering and Technology, 54: 3957-3961.

28. Volkovich, V.A., D. S. Maltsev, M. N. Soldatova, A. A. Ryzhov, and A. B. Ivanov. 2021. “Application of Low Melting Metals for Separation of Uranium and Zirconium in a “Fused Chloride – Liquid Alloy” System.” Metals, 11.

29. Liu, K., Z. F. Chai, and W. Q. Shi. 2021. “Liquid Electrodes for An/Ln Separation in Pyroprocessing.” Journal of the Electrochemical Society, 168: 032507.

30. Liu, K., Y. L. Liu, Z. F. Chai, and W. Q. Shi. 2021. “Electroseparation of Uranium from Lanthanides (La, Ce, Pr, Nd, and Sm) on Liquid Gallium Electrode.” Separation and Purification Technology, 265: 118524.

31. Smolenski, V., and A. Novoselova. 2021. “Electrochemical Separation of Uranium from Dysprosium in Molten Salt/Liquid Metal Extraction System.” Journal of the Electrochemical Society, 168: 062505.

32. Yang, D. W., et. al. 2021. “Electrodeposition Mechanism of La3+ on Al, Ga, and Al-Ga Alloy Cathodes in LiCl-KCl Eutectic Salt.” Journal of the Electrochemical Society, 168: 062511.

33. Lichtenstein, T., T. P. Nigl, and H. Kim. 2020. “Recovery of Alkaline-Earths into Liquid Bi in Ternary LiCl-KCl-$SrCl_2$/$BaCl_2$ Electrolytes at 500°C.” Journal of the Electrochemical Society, 167: 102501.

34. Nigl, T. P., T. Lichtenstein, Y. Kong, and H. Kim. 2020. “Electrochemical Separation of Alkaline-Earth Elements from Molten Salts Using Liquid Metal Electrodes.” ACS Sustainable Chemical Engineering, 8: 14818-14824.

35. Novoselova, A., V. Smolenski, and V. A. Volkovich. 2020. “Electrochemical Behavior of Dysprosium in Fused LiCl-KCl Eutectic at Solid Inert Mo and Liquid Active Ga Electrodes.” Journal of the Electrochemical Society, 167: 112510.

36. Han, W., et al. 2020. “Electrochemical Extraction of Metallic Y Using Solid and Liquid Double Cathodes.” Electrochimica Acta, 346: 136233.

37. Fredrickson, G. L., and T. S. Yoo. 2020. “Liquid Cadmium Cathode Performance Model Based on the Equilibrium Behaviors of U and Pu in Molten LiCl-KCl/Cd System at 500°C.” Journal of Nuclear Materials, 528: 151883.

38. Woods, M. E., and S. Phongikaroon. 2020. “Assessment on Recovery of Cesium, Strontium, and Barium from Eutectic LiCl-KCl Salt with Liquid Bismuth System.” JNFCWT, 18: 421-437.

39. Yang, D. W., et. al. 2020. “Application of Binary Ga-Al Alloy Cathode in U Separation from Ce: The Possibility in Pyroprocessing of Spent Nuclear Fuel.” Electrochimica Acta, 353: 136449.

40. Yin, T., Y. Liu, D. Yang, Y. Yan, G. Wang, Z. Chao, and W. Shi. 2020. “Thermodynamic and Kinetics Properties of Lanthanides (La, Ce, Pr, Nd) on Liquid Bismuth Electrode in LiCl-KCl Molten Salt.” Journal of the Electrochemical Society, 167: 122507.

41. Fredrickson, G. L., and T. S. Yoo. 2018. “Analysis and Modeling of the Equilibrium Behaviors of U and Pu in Molten LiCl-KCl/Cd System at 500°C.” Journal of Nuclear Materials, 508: 51-62.

42. Novoselova, A., V. Smolenski, V. A. Volkovich, and Y. Luk’yanova. 2019. “Thermodynamic Properties of Ternary Me-Ga-In (Me = La, U) Alloys in a Fused Ga-In/LiCl-KCl System.” Journal of Chemical Thermodynamics, 130: 228-234.

43. Lichtenstein, T., T. P. Nigl, N. D. Smith, and H. Kim. 2018. “Electrochemical Deposition of Alkaline-Earth Elements (Sr and Ba) from LiCl-KCl-$SrCl_2$-$BaCl_2$ Solution Using a Liquid Bismuth Electrode.” Electrochimica Acta, 281: 810-815.

44. Fredrickson, G. L., and T. S. Yoo. 2018. “Analysis and Modeling of the Equilibrium Behaviors of U and Pu in Molten LiCl-KCl/Cd System at 500°C.” Journal of Nuclear Materials, 508: 51-62.

45. Novoselova, A., and V. Smolenski. 2018. “The Influence of the Temperature and Ga-In Alloy Composition on the Separation of Uranium from Neodymium in Molten Ga-In/3LiCl-2KCl System During the Recycling of High-Level Waste.” Journal of Nuclear Materials, 509: 313-317.

46. Yin, T., K. Liu, Y. Liu, Y. Yan, G. Wang, Z. Chai, and W. Shi. 2018. “Electrochemical and Thermodynamic Properties of Uranium on the Liquid Bismuth Electrode in LiCl-KCl Eutectic.” Journal of the Electrochemical Society, 165: D722-D730.

47. Yin, T., K. Liu, Y. Liu, Y. Yan, G. Wang, Z. Chai, and W. Shi. 2018. “Electrochemical and Thermodynamic Properties of Pr on the Liquid Bismuth Electrode in LiCl-KCl Eutectic.” Journal of the Electrochemical Society, 165: D452-D460.

48. Liu, K., Y. L. Liu, Z. F. Chai, and W. Q. Shi. 2017. “Evaluation of the Electroextraction of Ce and Nd from LiCl-KCl Molten Salt Using Liquid Ga Electrode.” Journal of the Electrochemical Society, 164: D169-D178.

49. Luo, L. X., Y. L. Liu, N. Liu, L. Wang, L. Y. Yuan, Z. F. Chai, and W. Q. Shi. 2016. "Electrochemical and Thermodynamic Properties of Nd (III)/Nd (0) Couple at Liquid Electrode in LiCl-KCl Melt." Electrochimica Acta, 191: 1026-1036.

50. Liu, Y. L., et. al. 2014. "Electrochemical Extraction of Samarium from LiCl0KCl Melt by Forming Sm-Zn Alloys." Electrochimica Acta, 120: 369-378.

51. Wang, D. D., et. al. 2022. "Separation of Uranium from Lanthanides (La, Sm) with Sacrificial Li Anode in LiCl-KCl Eutectic Salt." Separation and Purification Technology, 292: 121025.

52. Yoon, D., S. Paek, J. H. Jang, J. Shim, and S. J. Lee. 2020. "Actinide Drawdown from LiCl-KCl Eutectic Salt via Galvanic/Chemical Reactions Using Rare Earth Metals." JNFCWT, 18: 373-382.

53. Bagri, P., J. Ong, C. Zhang, and M. F. Simpson. 2018. "Optimization of UCl_3 and $MgCl_2$ Separation from Molten LiCl-KCl Eutectic Salt via Galvanic Drawdown with Sacrificial Gd Anode." Journal of Nuclear Materials, 505: 149-158.

54. Bagri, P., C. Zhang, and M. F. Simpson. 2017. "Galvanic Reduction of Uranium (III) Chloride from LiCl-KCl Eutectic Salt Using Gadolinium Metal." Journal of Nuclear Materials, 492: 120-123.

55. Perumal, S. V., B. P. Reddy, G. Ravisankar, and K. Nagarajan. 2015. "Actinides Draw Down Process for Pyrochemical Reprocessing of Spent Nuclear Fuel." Radiochimica Acta, 103: 287-292.

56. Simpson, M. F., T. S. Yoo, D. LaBrier, M. Lineberry, M. Shaltry, and S. Phongikaroon. 2012. "Selective Reduction of Active Metal Chlorides from Molten LiCl-KCl Using Lithium Drawdown," Nuclear Engineering and Technology, 44: 767-772.

57. Han, W., Y. Zhang, R. Liu, Y. Sun, and M. Li. 2023. "Removal of RE^{3+}, Cs^{+}, Sr^{2+}, Ba^{2+} from Molten Salt Electrolyte by Precipitation and Solidification of Glass-Ceramics." Journal of Non-Crystalline Solids, 606: 122208.

58. Bailey, D. J., L. J. Gardner, M. T. Harrison, D. McKendrick, and N. C. Hyatt. 2022. "Development of Monazite Glass-Ceramic Wasteforms for the Immobilization of Pyroprocessing Wastes." MRS Advances, 7: 81-85.

59. Dong, Y., K. Xu, Z. Jia, C. Niu, and D. Xu. 2022. "Dechlorination and Vitrification of Electrochemical Processing Salt Waste." Journal of Nuclear Materials, 567: 153833.

60. Harrison, M. T., and D. McKendrick. 2022. "Treatment of Waste Salt Arising from the Pyrochemical Treatment of Used Nuclear Fuel Using Precipitation Methods," MRS Advances, 7: 117-121.

61. Qu, Y., M. Chang, Y. Luo, Y. Niu, H. Fu, and Q. Dou. 2022. "Removal of Rare Earth Fission Products from LiCl-KCl Molten Salt by Sulfide Precipitation." Journal of Radioanalytical and Nuclear Chemistry, 331: 4011-4019.

62. Han, W., Y. Zhang, R. Liu, Y. Sun, and M. Li. 2021. "Purification of Spent Electrolyte by Sequential Precipitation Method and Its On-Line Monitoring," Ionics, 27: 4829-4838.

63. Uozumi, K., M. Iizuka, and T. Omori. 2021. "Removal of Rare-Earth Fission Products from Molten Chloride Salt Used in Pyroprocessing by Precipitation for Consolidation into Glass-Bonded Sodalite Waste Form." Journal of Nuclear Materials, 547: 152784.

64. Gardner, L., M. Wasnik, B. Riley, M. Simpson, and K. Carlson. 2021. “Effect of Reduced Dehalogenation on the Performance of Y Zeolite-Based Sintered Waste Forms.” Journal of Nuclear Materials, 545: 152753.

65. Yang, K., W. Zhu, B. J. Riley, J. D. Vienna, D. Zhao, and J. Lian. 2021. “Perovskite-Derived Cs_2ScCl_6-Silica Composites as Advanced Waste Forms for Chloride Salt Wastes.” Environmental Science and Technology, 55: 7605-7614.

66. Gardner, L. D., M. S. Wasnik, B. J. Riley, S. Chong, M. F. Simpson, and K. L. Carlson. 2020. “Synthesis and Characterization of Sintered H-Y Zeolite-Derived Waste Forms for Dehalogenated Electrorefiner Salt.” Ceramics International, 46: 17707-17716.

67. Mason, A. R., F. Y. Tocino, M. C. Stennett, and N. C. Hyatt. 2020. “Molten Salt Synthesis of Ce Doped Zirconolite for the Immobilization of Pyroprocessing Wastes and Separated Plutonium.” Ceramics International, 46: 29080-29089.

68. Riley, B. J., J. A. Peterson, J. D. Vienna, W. L. Ebert, and S. M. Frank. 2020. “Dehalogenation of Electrochemical Processing Salt Simulants with Ammonium Phosphates and Immobilization of Salt Cations in an Iron Phosphate Glass Waste Form.” Journal of Nuclear Materials, 529: 151949.

69. Wasnik, M. S., A. K. Grant, K. Carlson, and M. F. Simpson. 2019. “Dechlorination of Molten Chloride Waste Salt from Electrorefining via Ion-Exchange Using Pelletized Ultra-Stable H-Y Zeolite in a Fluidized Particle Reactor.” Journal of Radioanalytical and Nuclear Chemistry, 320: 309-322.

70. Eun, H. C., et. al. 2017. “A Study of Separation and Solidification of Group II Nuclides in Waste Salt Delivered from the Pyrochemical Process of Used Nuclear Fuel.” Journal of Nuclear Materials, 491: 149-153.

71. Riley, B. J., et. al. 2017. “Assessment of Lead Tellurite Glass for Immobilizing Electrochemical Salt Wastes from Used Nuclear Fuel Reprocessing.” Journal of Nuclear Materials, 495: 405-420.

72. Choi, J. H., K. R. Lee, H. W. Kang, and H. S. Park. 2020. “Reactive-Crystallization Method for Purification of LiCl Salt Waste.” Journal of Radioanalytical and Nuclear Chemistry, 325: 485-492.

73. Choi, J. H., et. al. 2018. “Melt-Crystallization Monitoring System for the Purification of 10 kg-Scale LiCl Salt Waste.” Nuclear Engineering and Design, 326: 1-6.

74. Shim, M., H. G. Choi, J. H. Choi, K. W. Yi, and J. H. Lee. 2017. “Separation of Cs and Sr from LiCl-KCl Eutectic Salt via a Zone-Refining Process for Pyroprocessing Waste Salt Minimization.” Journal of Nuclear Materials, 491: 9-17.

75. Shim, M., H. G. Choi, K. W. Yi, I. S. Hwang, and J. H. Lee. 2016. “Separation of CsCl and SrCl2 from a Ternary CsCl-SrCl2-LiCl via a Zone Refining Process for Waste Salt Minimization of Pyroprocessing.” Journal of Nuclear Materials, 480: 403-410.

76. Williams, A. N., M. Pack, and S. Phongikaroon. 2015. “Separation of Strontium and Cesium from Ternary and Quaternary Lithium Chloride – Potassium Chloride Salt via Melt Crystallization.” Nuclear Engineering Technology, 47: 867-874.

77. Versey, J. R., S. Phongikaroon, and M. F. Simpson. 2014. “Separation of CsCl from LiCl-CsCl Molten Salt by Cold Finger Melt Crystallization.” Nuclear Engineering and Technology, 46: 395-406.

78. Choi, J. H., et. al. 2013. “Inclusion Behavior of Cs, Sr, and Ba Impurities in LiCl Crystal Formed by Layer-Melt Crystallization: Combined First-Principles Calculation and Experimental Study.” Journal of Crystal Growth, 371: 84-89.

79. Williams, A. N., S. Phongikaroon, and M. F. Simpson. 2013. “Separation of CsCl from a Ternary CsCl-LiCl-KCl Salt via a Melt Crystallization Technique for Pyroprocessing Waste Minimization.” Chemical Engineering Science, 89: 258-263.

80. Chamberlain, J., and M. F. Simpson. 2022. “Corrosion of Anode Materials During Direct Electrolytic Reduction of Uranium Oxide in Molten LiCl-Li_2O.” Journal of Nuclear Materials, 564: 153680.

81. Horvath, D., J. King, R. Hoover, S. Warman, K. Marsden, D. Yoon, and S. Herrmann. 2022. “Experimental Observations for Anode Optimization of Oxide Reduction Equipment.” JNFCWT, 20: 383-398.

82. Kim, J. W., S. J. Yoon, T. S. Yoo, and E. S. Kim. 2022. “Modelling and Preliminary Analysis of Salt Convection Effect on Electrochemical Reduction for Uranium Oxides Using Smoothed Particle Hydrodynamics.” NTHAS12: The 12th Japan-Korea Symposium on Nuclear Thermal Hydraulics and Safety, Miyazaki, Japan.

83. Shishkin, A. V., V. Y. Shishkin, A. A. Pankratov, A. A. Burdina, and Y. P. Zaikov. 2022. “Electrochemical Reduction of La_2O_3, Nd_2O_3, and CeO_2 in LiCl-Li_2O Melt.” Materials, 15: 3963.

84. Yao, B., Y. Xiao, Y. Jia, S. Wu, M. Yang, and H. He. 2022. “Diffusion Behavior of Oxygen in the Electro-Deoxidation of Uranium Oxide in LiCl-Rich Melt.” Journal of Nuclear Materials, 562: 153582.

85. Yoo, T. S., S. D. Herrmann, S. J. Yoon, and K. C. Marsden. 2021. “Analysis and Modeling of Oxide Reduction Processes for Uranium Oxides.” Journal of Nuclear Materials, 545: 15625.

86. Kim, S. W., S. Y. Han, J. Jang, M. K. Jeon, and E. Y. Choi. 2021. “Mechanochemical Approach for Oxide Reduction of Spent Nuclear Fuels for Pyroprocessing,” JNFCWT, 19: 255-266.

87. Burak, A., J. Chamberlain, and M. F. Simpson. 2020. “Li_2O Entrainment During UO_2 Reduction in Molten LiCl-Li_2O: Part II. Effect of Cathode Reduction Mechanism.” Journal of the Electrochemical Society, 167: 166513.

88. Burak, A., J. Chamberlain, and M. F. Simpson. 2020. “Study of Entrainment of Li_2O in Product from Direct Electrolytic Reduction of UO_2 in Molten LiCl-Li_2O. Part 1: Post-Processing and Analysis Technique.” Journal of Nuclear Materials, 529: 151913.

89. Herrmann, S. D., P. K. Tripathy, S. M. Frank, and J. A. King. 2019. “Comparative Study of Monolithic Platinum and Iridium as Oxygen-Evolving Anodes During the Electrolytic Reduction of Uranium Oxide in a Molten LiCl-Li_2O Electrolyte.” Journal of Applied Electrochemistry, 49: 379-388.

90. Choi, E. Y., et. al. 2017. “Electrolytic Reduction Runs of 0.6 kg Scale – Simulated Oxide Fuel in a Li_2O-LiCl Molten Salt Using Metal Anode Shrouds.” Journal of Nuclear Materials, 489: 1-8.

91. Kim, S. W., et. al. 2017. “A Preliminary Study of Pilot-Scale Electrolytic Reduction of UO_2 Using a Graphite Anode.” Nuclear Engineering and Technology, 49: 1451-1456.

92. Park, W., J. M. Hur, S. S. Hong, E. Y. Choi, H. S. Im, S. C. Oh, and J. W. Lee. 2013. “An Experimental Study for Li Recycling in an Electrolytic Reduction Process for UO_2 with a Li_2O-LiCl Molten Salt.” Journal of Nuclear Materials, 441: 232-239.

93. Herrmann, S. D., S. X. Li, and B. R. Westphal. 2012. “Separation and Recovery of Uranium and Group Actinide Products from Irradiated Fast Reactor MOX Fuel via Electrolytic Reduction and Electrorefining.” Separation Science and Technology, 47.

94. Phongikaroon, S., S. D. Herrmann, and M. F. Simpson. 2011. “Diffusion Model for Electrolytic Reduction of Uranium Oxides in a Molten LiCl-Li_2O Salt.” Nuclear Technology, 174: 85-93.

95. Herrmann, S. D., and S. X. Li. 2010. “Separation and Recovery of Uranium Metal from Spent Light Water Reactor Fuel via Electrolytic Reduction and Electrorefining.” Nuclear Technology, 171.

96. Herrmann, S. D., S. X. Li, M. F. Simpson, and S. Phongikaroon. 2006. “Electrolytic Reduction of Spent Nuclear Oxide Fuel as Part of an Integrated Process to Separate and Recover Actinides from Fission Products.” Separation Science and Technology, 41.

97. Vestal, B. K., J. Travis, A. Albert, S. Bruffey, J. McFarlane, E. D. Collins, R. D. Hunt, and C. E. Barnes. 2023. “A Novel Protocol to Recycle Zirconium from Zirconium Alloy Cladding from Used Nuclear Fuel Rods.” Journal of Nuclear Materials, 154339.

98. Conrad, J. K., M. E. Woods, and G. P. Horne. 2023. “Radiolytic Evaluation of Select Sulfur Chlorides (S_2Cl_2 and $SOCl_2$) for Advanced Low Temperature Chlorination of Zirconium-Based Used Nuclear Fuel Cladding.” Radiation Physics and Chemistry, 20: 110732.

99. Bruffy, S. H., R. D. Hunt, B. K. Vestal, and C. E. Barnes. 2021. “Advanced Low-Temperature Chlorination of Zirconium.” ORNL/SPR-2021/2135, Oak Ridge National Laboratory, (August).

100. Nevarez, R. B., B. McNamara, and F. Poineau. 2021. “Recovery of Zirconium from Zircaloys Using a Hydrochlorination Process.” Nuclear Technology, 207: 263-269.

101. Collins, E. D., T. D. Hylton, G. D. Del Cul, B. B. Spencer, R. D. Hunt, and J. A. Johnson. 2017. “Completion of a Chlorination Test Using 250 grams of High-Burn-Up Used Fuel Cladding from a North Anna Pressurized Water Reactor.” ORNL/LTR-2017/327, Oak Ridge National Laboratory, (June).

102. Collins, E. D., J. A. Johnson, T. D. Hylton, R. R. Brunson, R. D. Hunt, G. D. DelCul, E. C. Bradley, and B. B. Spencer. 2016. “Complete Non-Radioactive Operability Tests for Cladding Hull Chlorination.” U.S. Department of Energy, Fuel Cycle Research and Development, FCDR-MRWFD-ORNL/ LTR-2016/172.

103. Collins, E. D., G. D. DelCul, B. B. Spencer, R. R. Brunson, J. A. Johnson, D. S. Terekhov, and N. V. Emmanuel. 2012. “Process Development Studies for Zirconium Recovery/Recycle from Used Nuclear Fuel Cladding.” Procedia Chemistry, 7: 72-76.

104. Zhao, D., L. Yan, T. Jiang, S. Peng, and B. Yue. 2023. “Phase-Field Modeling and Morphological Classification of Uranium Dendrites for the Electrorefining of Used Nuclear Fuel.” Journal of the Electrochemical Society. 170: 022502.

105. Hege, N., J. Jackson, and J. Shafer. 2023. “Review – Fundamental Uranium Electrochemistry and Spectroscopy in Molten Salt Systems.” Journal of the Electrochemical Society, 170: 016503.

106. Gardner, L., A. Harward, J. Howard, G. Fredrickson, T. S. Yoo, M. Simpson, and K. Carlson. 2022. “Deliquescence of Eutectic LiCl-KCl Diluted with NaCl for Interim Waste Salt Storage.” Nuclear Technology, 208: 310-317.

107. Harward, A., L. Gardner, C. M. Decker Oldham, K. Carlson, T. S. Yoo, G. Fredrickson, M. Patterson, and M. F. Simpson. 2022. “Water Sorption/Desorption Characteristics of Eutectic LiCl-KCl Salt-Occluded Zeolites.” JNFCWT, 20: 259-268.

108. Swain, L., G. Pakhui, A. Jain, and S. Ghosh. 2022. “Electrochemical Behavior of LiCl-KCl Eutectic Melts Containing Moisture as Impurity. Part II: Uranium Electrode.” Journal of Electroanalytical Chemistry, 907: 115969.

109. Swain, L., G. Pakhui, A. Jain, and S. Ghosh. 2022. “Electrochemical Behavior of LiCl-KCl Eutectic Melts Containing Moisture as Impurity. Part I: Inert Tungsten Electrode.” Journal of Electroanalytical Chemistry, 910: 116125.

110. Xiong, W., and L. Hao. 2022. “Fundamental Issues Identified for Thermodynamic Description of Molten Salt System.” Journal of Phase Equilibrium and Diffusion, 43: 894-902.

111. Zhao, D., L. Yan, T. Jiang, S. Peng, and B. Yue. 2022. “Multiphysics Simulation Study of the Electrorefining Process of Spent Nuclear Fuel from LiCl-KCl Eutectic Molten Salt.” Journal of the Electrochemical Society, 169: 072501.

112. Swain, L., S. Ghosh, G. Pakhui, and B. P. Reddy. 2021. “Redox Behavior of Moisture in LiCl-KCl Eutectic Melts: A Cyclic Voltammetry Study.” Nuclear Technology, 207: 119-146.

113. Westphal, B., D. Tolman, K. Tolman, S. Frank, S. Herrmann, and S. Warmann. 2020. “Options Study for the Neutralization of Elemental Sodium During the Pyroprocessing of Used Nuclear Fuel.” JNFCWT, 18: 113-118.

114. Lee, C. H., T. J. Kim, S. Park, S. J. Lee, S. W. Paek, D. H. Ahn, and S. K. Cho. 2017. “Effect of Cathode Material on the Electrorefining of U in LiCl-KCl Molten Salts.” Journal of Nuclear Materials, 488: 210-214.

115. Chamberlain, J., and M. F. Simpson. 2022. “Development of a Scalable Method to Chlorinate UO_2 to UCl_3 Using $ZrCl_4$.” Journal of Radioanalytical and Nuclear Chemistry, 331: 4983-4996.

116. Herrmann, S. D., B. R. Westphal, S. X. Li, and H. Zhao. 2022. “Parametric Study of Used Nuclear Oxide Fuel Constituent Dissolution in Molten LiCl-KCl-UCl3.” Nuclear Technology, 208: 871-891.

117. Herrmann, S. D., H. Zhao, K. K. Bawane, L. He, K. R. Tolman, and X. Pu. 2022. “Synthesis and Characterization of Uranium Trichloride in Alkali-Metal Chloride Melt.” Journal of Nuclear Materials, 565: 153728.

118. Meng, Z. K., R. S. Lin, H. Chen, W. C. Song, C. S. Wang, H. He, and G. A. Ye. 2022. “Progress in Chlorination and Dissolution Technology of Oxide of Uranium and Plutonium.” Journal of Nuclear and Radiochemistry, 44: 313-325.

119. Perhach, C., J. Chamberlain, N. Rood, E. Hamilton, and M. F. Simpson. 2022. “Chlorination of Uranium Metal in Molten NaCl-$CaCl_2$ via Bubbling HCl.” Journal of Radioanalytical and Nuclear Chemistry, 331: 2303-2309.

120. Samanta, N., S. Kumar, S. Maji, M. Chandra, P. Venkatesh, and A. Jain. 2022. “Electrochemical and Spectroscopic Analysis of Thermochemical Conversion of UO_2 to UCl_3 Using $AlCl_3$ and Al in LiCl-KCl Eutectic.” Progress in Nuclear Energy, 153: 104429.

121. Yoon, D., S. Peak, and C. Lee. 2022. “Chlorination of Uranium Metal to Uranium Trichloride Using Ammonium Chloride.” Journal of Radioanalytical and Nuclear Chemistry, 331: 2209-2216.

122. Yoon, D., S. Peak, S. K. Lee, J. H. Lee, and C. H. Lee. 2022. “Chlorination of TRU/RE/SrO_x in Oxide Spent Nuclear Fuel Using Ammonium Chloride as a Chlorinating Agent.” JNFCWT, 20: 193-207.

123. Zhong, Y. K., et. al. 2021. “In-Situ Anodic Precipitation Process for Highly Efficient Separation of Aluminum Alloys.” Nature Communications, 12: 5777.

124. Kitawaki, S., T. Nagai, and N. Sato. 2013. “Chlorination of Uranium Oxides with CCl_4 Using a mechanochemical Method.” Journal of Nuclear Materials, 439: 212-216.

125. Kim, S., K. Kim, J. Kim, G. Kim, D. Cho, and S. Bang. 2023. “Pyroprocessing Unit Cost Estimation for a Commercial Facility Using PRIDE Actual Costs in Korea.” Annals of Nuclear Energy, 180: 109501.

126. Kim, S., K. Kim, J. Kim, G. Kim, D. Cho, and S. Bang. 2022. “External Cost Analysis of Nuclear Fuel Cycle Comparing Direct Disposal and Pyroprocessing in Korea,” Progress in Nuclear Energy, 154: 104480.

127. Kim, Y. H., and Y. Z. Cho. 2020. “Analyzing Design Considerations for Disassembly of Spent Nuclear Fuel During Head-End Process of Pyroprocessing.” Science and Technology of Nuclear Installations. https://doi.org/10-1155/2020/8868444.

128. Chang, Y. I., et. al. 2019. “Conceptual Design of a Pilot-Scale Pyroprocessing Facility.” Nuclear Technology, 205: 708-726.

129. Simpson, M. F., and P. Bagri. 2018. “Basis for a Minimalistic Slat Treatment Approach for Pyroprocessing Commercial Nuclear Fuel.” JNFCWT, 18: 1-10.

130. Chang, Y. I., et. al. 2018. “Conceptual Design of a Pilot-Scale Pyroprocessing Facility.” ANL/NE-Landmark-CRADA-12, Rev. 1, Argonne National Laboratory.

131. Moon, S. I., S. J. Seo, W. M. Chong, G. S. You, J. H. Ku, and H. D. Kim. 2015. “Identification of Safety Controls for Engineering-Scale Pyroprocessing Facility.” Nuclear Engineering Technology, 47: 915-923.

132. Williamson, M. A., and J. L. Willit. 2011. “Pyroprocessing Flowsheets for Recycling Used Nuclear Fuel.” Nuclear Engineering and Technology, 43: 329-334.

133. Laidler, J. J., J. E. Battles, W. E. Miller, J. P. Ackerman, and E. L. Carls. 1997. “Development of Pyroprocessing Technology.” Progress in Nuclear Energy. 31: 131–140. https://doi.org/10.1016/0149-1970(96)00007-8.

134. Lee, H., et.al. 2013. “Current Status of Pyroprocessing Development at KAERI.” Science and Technology of Nuclear Installations. https://doi.org/10.1155/2013/343492.

135. Park, S.-H., et. al. 2017. “Status of Development of Pyroprocessing Safeguards at KAERI.” Journal of the Nuclear Fuel Cycle and Waste Technology (JNFCWT), 15. https://doi.org/10.7733/jnfcwt.2017.15.3.191.

136. Inoue, T., T. Koyama, and Y. Arai. 2011. “State of the art of pyroprocessing technology in Japan.” Energy Procedia. 7: 405–413. https://doi.org/10.1016/j.egypro.2011.06.053.

137. Fredrickson, G. L., M. N. Patterson, D. E. Vaden, G. G. Galbreth, T. S. Yoo, J. C. Price, E. J. Flynn, and R. N. Searle. 2022. “History and status of spent fuel treatment at the INL Fuel Conditioning Facility.” Progress in Nuclear Energy. 143. https://doi.org/10.1016/j.pnucene.2021.104037.

138. Williamson, M. A., and J. L. Willit. 2011. “Pyroprocessing flowsheets for recycling used nuclear fuel.” Nuclear Engineering and Technology. 43: 329–334. https://doi.org/10.5516/NET.2011.43.4.329.

139. Nagarajan, K., T. Subramanian, B. Prabhakara Reddy, P. R. Vasudeva Rao, and B. Raj. 2008. “Current status of pyrochemical reprocessing research in India.” Nucl Technol: 259–263. https://doi.org/10.13182/NT08-A3954.

140. Lee, H. J., W. il Ko, S. Y. Choi, S. K. Kim, I. T. Kim, and H. S. Lee. 2014. “An approach to developing an integrated pyroprocessing simulator.” AIP Conf Proc: 9–14. https://doi.org/10.1063/1.4866097.

141. Chang, Y., et. al. 2019. “Conceptual design of a pilot-scale pyroprocessing facility.” Nucl Technol. 205: 708–726. https://doi.org/10.1080/00295450.2018.1513243.

142. Cipiti, B. B., Browne M., and M. Reim. 2021. “The MPACT 2020 Milestone: Safeguards and Security by Design of Future Nuclear Fuel Cycle Facilities.” Journal of Nuclear Materials Management. 49: 5-21.

143. Garcia, H. E., M. F. Simpson, W. Lin, R. B. Carlson, and T. Yoo. 2017. “Application of process monitoring to anomaly detection in nuclear material processing systems via system-centric event interpretation of data from multiple sensors of varying reliability.” Ann Nucl Energy. 103: 60–73. https://doi.org/10.1016/j.anucene.2017.01.006.

144. Cipiti, B. B., N. Shoman, and P. Honnold. 2021. “Safeguards Modeling for Advanced Nuclear Facility Design.” Journal of Nuclear Materials Management. 41.

145. Westphal, B. R., et. al. 2008. “Effect of process variables during the head-end treatment of spent oxide fuel.” Nucl Technol. https://doi.org/10.13182/NT08-A3942.

146. il Park, G., K. H. Cho, J. W. Lee, J. J. Park, and K. C. Song. 2008. “Evaluation of decladding efficiency using high burn-up spent nuclear fuels.” Trans Am Nucl Soc.

147. Kang, K. H., C. H. Lee, M. K. Jeon, S. Y. Han, G. I. Park, and S. M. Hwang. 2015. “Characterization of cladding hull wastes from used nuclear fuels.” Archives of Metallurgy and Materials. 60. https://doi.org/10.1515/amm-2015-0097.

148. Bodine, J. E., I. J. Groce, J. Guon, and L. A. Hanson. 1964. “Oxidative Decladding of Uranium Dioxide Fuels.” Nuclear Science and Engineering. 19. https://doi.org/10.13182/nse64-a19784.

149. Jeon, M. K., J. M. Shin, J. J. Park, and G. il Park. 2012. “Simulation of Cs behavior during the high temperature voloxidation process using the HSC chemistry code.” Journal of Nuclear Materials. 430. https://doi.org/10.1016/j.jnucmat.2012.06.040.

150. You, G. S., W. M. Choung, J. H. Ku, S. I. Moon, and H. D. Kim. 2013. “Pyroprocess facility design for a nuclear fuel cycle.” International Conference on Nuclear Engineering, Proceedings, ICONE. https://doi.org/10.1115/ICONE21-15190.

151. Lee, H., J. M. Hur, J. G. Kim, D. H. Ahn, Y. Z. Cho, and S. W. Paek. 2011. “Korean pyrochemical process R&D activities.” Energy Procedia. https://doi.org/10.1016/j.egypro.2011.06.051.

152. Lee, J. W., D. Y. Lee, Y. S. Lee, J. H. Yang, G. il Park, J. W. Lee, H. M. Kwon, and Y. Z. Cho. 2018. “Estimation on Feeding Portions of Slitting Decladded Fuel Fragments to Electrolytic Reduction Process.” Nucl Technol. 204: 101–109. https://doi.org/10.1080/00295450.2018.1469347.

153. King, J. A., T. J. Malewitz, S. M. James, and B. D. Simmons. 2017. “Mechanical decladding of irradiated FFTF mixed oxide fuel rods.” Trans Am Nucl Soc: 333.

154. Kim, Y., Y. Cho, Y. Lee, and J. Hur. 2019. “Engineering design of a mechanical decladder for spent nuclear rod-cuts.” Science and Technology of Nuclear Installations. https://doi.org/10.1155/2019/9273503.

155. Kim, Y. H., Y. Z. Cho, and J. M. Hur. 2020. “Experimental Approaches for Manufacturing of Simulated Cladding and Simulated Fuel Rod for Mechanical Decladder.” Science and Technology of Nuclear Installations. https://doi.org/10.1155/2020/1905019.

156. Hardtmayer, D., K. Herminghuysen, S. White, A. Kauffman, J. Sanders, S. Li, and L. Cao. 2018. “Determination of molten salt mass using 22Na tracer mixed with 154Eu and 137Cs.” J Radioanal Nucl Chem. 318. https://doi.org/10.1007/s10967-018-5995-x.

157. Cao, L., J. Jarrell, S. White, K. Herminghuysen, A. Kauffman, D.E. Hardtmayer, J. Sanders, and S. Li. 2017. “A radioactive tracer dilution method to determine the mass of molten salt.” J Radioanal Nucl Chem. 314. https://doi.org/10.1007/s10967-017-5417-5.

158. Brainerd, R. J., and G. A. Robbins. 2004. “A tracer dilution method for fracture characterization in bedrock wells.” Ground Water. 42. https://doi.org/10.1111/j.1745-6584.2004.tb02731.x.

159. Zhang, C., D. Rappleye, and M. F. Simpson. 2016. “Development and Optimization of Voltammetry for Real Time Analysis of Multi-Component Electrorefiner Salt.” ECS Trans. 75. https://doi.org/10.1149/07515.0095ecst.

160. Yoo, T., and D. Vaden. 2019. “A new inventory tracking method for Mark-V electrorefiner.” Ann Nucl Energy. 128: 406–413. https://doi.org/10.1016/j.anucene.2019.01.008.

161. Li, S. X., J.-F. Jue, R. S. Herbst, and S. D. Herrmann. 2013. “Actinide-ion sensor.”

162. Cao, G., S. X. L. Li, S. Herrmann, and B. Serrano-Rodriguez. 2019. “Potentiometric sensor.”

163. Cao, G., S. Herrmann, G. L. Fredrickson, and R. Hoover. 2022. “Study of Potentiometry for Monitoring Activity of GdCl3 in Molten LiCl-KCl Salt.” ECS Advances, 1.

164. Cao, G., S. Herrmann, S. Li, R. Hoover, J. King, B. Serrano-Rodriguez, and K. Marsden. 2020. “Development of a Li2O Sensor Based on a Yttria Stabilized Zirconia Membrane for Oxide Reduction in a Molten LiCl-Li2O Electrolyte at 650°C.” Nucl Technol, 206. https://doi.org/10.1080/00295450.2019.1666601.

165. Williams, A. N., G. Cao, and M. R. Shaltry. 2021. “Voltammetry measurements in lithium chloride-lithium oxide (LiCl–Li2O) salt: An evaluation of working electrode materials.” Journal of Nuclear Materials, 546. https://doi.org/10.1016/j.jnucmat.2020.152760.

166. Rakhshan Pouri, S., M. Manic, and S. Phongikaroon. 2018. “A novel framework for intelligent signal detection via artificial neural networks for cyclic voltammetry in pyroprocessing technology.” Ann Nucl Energy, 111. https://doi.org/10.1016/j.anucene.2017.09.002.

167. Jung, Y. E., S. K. Ahn, and M. S. Yim. 2022. “Investigation of neural network-based cathode potential monitoring to support nuclear safeguards of electrorefining in pyroprocessing.” Nuclear Engineering and Technology, 54. https://doi.org/10.1016/j.net.2021.08.020.

168. Rappleye, D., S. Jeong, and M. F. Simpson. 2015. “Application of multivariate analysis techniques to safeguards of the electrochemical treatment of used nuclear fuel.” Ann Nucl Energy. 77: 265-272. https://doi.org/10.1016/j.anucene.2014.11.023.

169. Coble, J. B., S. E. Skutnik, S. N. Gilliam, and M. P. Cooper. 2020. “Review of Candidate Techniques for Material Accountancy Measurements in Electrochemical Separations Facilities.” Nucl Technol, 206. https://doi.org/10.1080/00295450.2020.1724728.

170. Orechwa, Y., and R. G. Bucher. 1997. “Startup calibration and measurement control of the fuel conditioning facility in-cell electronic mass balances.” Journal of Nuclear Materials Management. 25: 12-18.

171. Williams, A. N., A. Shigrekar, G. G. Galbreth, and J. Sanders. 2020. “Application and testing of a triple bubbler sensor in molten salts.” Nuclear Engineering and Technology, 52. https://doi.org/10.1016/j.net.2020.01.002.

172. Williams, A. N., G. G. Galbreth, and J. Sanders. 2018. “Accurate determination of density, surface tension, and vessel depth using a triple bubbler system.” Journal of Industrial and Engineering Chemistry. 63: 149–156. https://doi.org/10.1016/j.jiec.2018.02.011.

173. Williams, A. N., G. G. Galbreth, and J. Sanders. 2018. “Accurate determination of density, surface tension, and vessel depth using a triple bubbler system.” Journal of Industrial and Engineering Chemistry. 63: 149–156. https://doi.org/10.1016/j.jiec.2018.02.011.

174. Shigrekar, A., A. Williams, and G. Galbreth. 2018. “‘Visually determining the thermal expansion of a triple bubbler system in pyroprocessing molten salt.” Trans Am Nucl Soc, 179.

175. Kim, J. Y., S. E. Bae, T. H. Park, S. Paek, T. J. Kim, and S. J. Lee. 2020. “Wireless simultaneous measurement system for liquid level and density using dynamic bubbler technique: Application to KNO3 molten salts.” Journal of Industrial and Engineering Chemistry, 82. https://doi.org/10.1016/j.jiec.2019.09.041.

176. Li, S. X., B. R. Westphal, and S. D. Herrmann. 2015. “Real-time monitoring of plutonium content in uranium-plutonium alloys.”

177. Westphal, B. R., and S. X. Li. 2019. “Evaluation of Experimental Studies in the U-Rich Region of the U-Pu Phase Diagram, Metallurgical and Materials Transactions B: Process Metallurgy and Materials Processing Science.” 50. https://doi.org/10.1007/s11663-019-01525-z.

178. Feng, J., Z. Wang, Z. Li, and W. Ni. 2010. “Study to reduce laser-induced breakdown spectroscopy measurement uncertainty using plasma characteristic parameters.” Spectrochim Acta Part B At Spectrosc, 65. https://doi.org/10.1016/j.sab.2010.05.004.

179. Williams, A., and S. Phongikaroon. 2016. “Optimization of laser-induced breakdown spectroscopy parameters in a novel molten salt aerosol system.” International Conference on Nuclear Engineering, Proceedings, ICONE. https://doi.org/10.1115/ICONE24-60724.

180. Williams, A. N., and S. Phongikaroon. 2017. “Laser-Induced Breakdown Spectroscopy (LIBS) in a Novel Molten Salt Aerosol System.” Appl Spectrosc, 71. https://doi.org/10.1177/0003702816648965.

181. Smith, N. A., J. A. Savina, and M. A. Williamson. 2014. “Application of Laser Induced Breakdown Spectroscopy to Electrochemical Process Monitoring of Molten Chloride Salts.” Symposium on International Safeguards: Linking Strategy, Implementation and People.

182. Williams, A., K. Bryce, and S. Phongikaroon. 2017. “Measurement of Cerium and Gadolinium in Solid Lithium Chloride–Potassium Chloride Salt Using Laser-Induced Breakdown Spectroscopy (LIBS).” Appl Spectrosc, 71. https://doi.org/10.1177/0003702817709298.

183. Hull, G., H. Lambert, K. Haroon, P. Coffey, T. Kerry, E. D. McNaghten, C. A. Sharrad, and P. Martin. 2021. “Quantitative prediction of rare earth concentrations in salt matrices using laser-induced breakdown spectroscopy for application to molten salt reactors and pyroprocessing.” J Anal At Spectrom, 36. https://doi.org/10.1039/d0ja00352b.

184. IAEA. 2004. “Quantifying uncertainty in nuclear analytical measurements.”

185. Dragović, S., A. Onjia, S. Stanković, I. Aničin, G. Bačić. 2005. “Artificial neural network modelling of uncertainty in gamma-ray spectrometry.” Nucl Instrum Methods Phys Res A, 540. https://doi.org/10.1016/j.nima.2004.11.045.

186. Fagan, D. K., S. M. Robinson, and R. C. Runkle. 2012. “Statistical methods applied to gamma-ray spectroscopy algorithms in nuclear security missions.” Applied Radiation and Isotopes, 70. https://doi.org/10.1016/j.apradiso.2012.06.016.

187. Woo, S. M., S. S. Chirayath, and M. Fuhrmann. 2020. “Nuclear fuel reprocessing: Can pyro-processing reduce nuclear proliferation risk?” Energy Policy, 144. https://doi.org/10.1016/j.enpol.2020.111601.

188. Lee, T. H., S. Menlove, H. O. Menlove, H. S. Shin, and H. D. Kim. 2020. “A Direct Nondestructive Assay for the Pu of U/TRU Ingot in Pyroprocessing Using 244Cm Neutron Albedo Reactivity Technique and Its Error.” Nucl Technol, 206. https://doi.org/10.1080/00295450.2020.1743598.

189. Woo, S. M., and S. S. Chirayath. 2019. “Evaluation of nuclear material accountability by the probability of detection for loss of Pu (LOPu) scenarios in pyroprocessing.” Nuclear Engineering and Technology, 51. https://doi.org/10.1016/j.net.2018.08.015.

190. Woo, S. M., S. S. Chirayath, and M. Fratoni. 2018. “Nuclide composition non-uniformity in used nuclear fuel for considerations in pyroprocessing safeguards.” Nuclear Engineering and Technology, 50. https://doi.org/10.1016/j.net.2018.05.011.

191. Seo, H., B. H. Won, S. K. Ahn, S. K. Lee, S. H. Park, G. il Park, and S. H. Menlove. 2016. “Optimization of hybrid-type instrumentation for Pu accountancy of U/TRU ingot in pyroprocessing.” Applied Radiation and Isotopes, 108. https://doi.org/10.1016/j.apradiso.2015.11.109.

192. Borrelli, R. A. 2013. “Potential application of curium neutron detection in the high reliability safeguards approach for remotely handled nuclear facilities.” International Nuclear Fuel Cycle Conference, GLOBAL 2013: Nuclear Energy at a Crossroads.

193. Borrelli, R. A. 2014. “Use of curium neutron flux from head-end pyroprocessing subsystems for the high reliability safeguards methodology.” Nuclear Engineering and Design. 277:166–172. https://doi.org/10.1016/j.nucengdes.2014.06.028.

194. Borrelli, R. A. 2013. “Use of curium spontaneous fission neutrons for safeguardability of remotely-handled nuclear facilities: Fuel fabrication in pyroprocessing.” Nuclear Engineering and Design, 260. https://doi.org/10.1016/j.nucengdes.2013.03.025.

195. Aggarwal, S. K. 2016. “Alpha-particle spectrometry for the determination of alpha emitting isotopes in nuclear, environmental and biological samples: Past, present and future.” Analytical Methods, 8. https://doi.org/10.1039/c6ay00920d.

196. Das, A., and S. P. Duttagupta. 2015. “TCAD simulation for alpha-particle spectroscopy using SIC schottky diode.” Radiat Prot Dosimetry, 167. https://doi.org/10.1093/rpd/ncu369.

197. Garcia, T. R., A. Kumar, B. Reinke, T. E. Blue, and W. Windl. 2013. “Electron-hole pair generation in SiC high-temperature alpha particle detectors.” Appl Phys Lett, 103. https://doi.org/10.1063/1.4824774.

198. Tagziria, H., J. Bagi, B. Pedersen, and P. Schillebeeckx. 2012. “Absolute determination of small samples of Pu and Am by calorimetry.” Nucl Instrum Methods Phys Res A, 691. https://doi.org/10.1016/j.nima.2012.06.062.

199. Hoover, A. S., et. al. 2011. “Large microcalorimeter arrays for high-resolution X- and gamma-rayspectroscopy.” Nucl Instrum Methods Phys Res A. https://doi.org/10.1016/j.nima.2010.09.154.

200. Hoover, A. S., et. al. 2014. “Uncertainty of plutonium isotopic measurements with microcalorimeter and high-purity germanium detectors.” IEEE Trans Nucl Sci, 61. https://doi.org/10.1109/TNS.2014.2332275.

201. Hoover, A. S., et. al. 2013. “Determination of plutonium isotopic content by microcalorimeter gamma-ray spectroscopy.” IEEE Trans Nucl Sci, 60. https://doi.org/10.1109/TNS.2013.2249091.

202. Ullom, J. N., et. al. 2006. “Optimization of transition-edge calorimeter performance.” Nucl Instrum Methods Phys Res A, 559. https://doi.org/10.1016/j.nima.2005.12.173.

203. Ullom, J. N., et. al. 2005. “Optimized transition-edge x-ray microcalorimeter with 2.4 eV energy resolution at 5.9 keV.” Appl Phys Lett, 87. https://doi.org/10.1063/1.2061865.

204. Croce, M., D. Henzlova, H. Menlove, D. Becker, and J. Ullom. “Electrochemical Safeguards Measurement Technology Development at LANL.” Journal of Nuclear Materials Management, 49 (n.d.).

205. Berlizov, A. N., D. A. Sharikov, H. Ottmar, H. Eberle, J. Galy, and K. Luetzenkirchen. 2010. “A quantitative Monte Carlo modelling of the uranium and plutonium X-ray fluorescence (XRF) response from a hybrid K-edge/K-XRF densitometer.” Nucl Instrum Methods Phys Res A, 615. https://doi.org/10.1016/j.nima.2010.01.010.

206. Bootharajan, M., R. Senthilvadivu, K. Sundararajan, and R. Kumar. 2020. “Development and validation of hybrid K-edge/K-XRF densitometer for assay of nuclear fuel from reprocessing plants.” J Radioanal Nucl Chem, 324. https://doi.org/10.1007/s10967-020-07122-8.

207. Cook, M. T., and S. E. Skutnik. 2014. “Evaluation of hybrid K-edge densitometry for pyroprocessing material assay.” Trans Am Nucl Soc.

208. Shizuma, T., R. Hajima, T. Hayakawa, M. Fujiwara, T. Sonoda, and M. Seya. 2011. “Proposal for an advanced hybrid K-edge/XRF densitometry (HKED) using a monochromatic photon beam from laser Compton scattering.” Nucl Instrum Methods Phys Res A, 654. https://doi.org/10.1016/j.nima.2011.05.082.

209. Nicholson, A., S. Croft, and R. D. McElroy. 2016. “K-shell fluorescence yields and their uncertainties for use in hybrid K-edge densitometry.” J Radioanal Nucl Chem, 307. https://doi.org/10.1007/s10967-015-4543-1.

210. Liu, S., et. al. 2017. “Investigation on molecular structure of molten Li2BeF4 (FLiBe) salt by infrared absorption spectra and density functional theory (DFT).” J Mol Liq, 242. https://doi.org/10.1016/j.molliq.2017.07.051.

211. Moon, J., W. C. Phillips, R. Gakhar, and D. Chidambaram. 2020. “Understanding the Structure and Speciation of Molten LiCl-KCl Using Raman and Ultraviolet-Visible-Near IR Spectroscopic Techniques.” ECS Meeting Abstracts. MA2020-02. https://doi.org/10.1149/ma2020-0291185mtgabs.

212. Phillips, W. C., et. al. 2020. “Design and performance of high-temperature furnace and cell holder for in situ spectroscopic, electrochemical, and radiolytic investigations of molten salts.” Review of Scientific Instruments, 91. https://doi.org/10.1063/1.5140463.

213. Kozlowski, T. R. 1968. “Application of High Temperature Infrared Emission Spectroscopy to Molten Salts.” Appl Opt., 7. https://doi.org/10.1364/ao.7.000795.

214. Sun, H., J. Q. Wang, Z. Tang, Y. Liu, and C. Wang. 2020. “Assessment of effects of Mg treatment on corrosivity of molten NaCl-KCl-MgCl2 salt with Raman and Infrared spectra.” Corros Sci., 164. https://doi.org/10.1016/j.corsci.2019.108350.

215. Park, Y. J., S. E. Bae, Y. H. Cho, J. Y. Kim, and K. Song. 2011. “UV-vis absorption spectroscopic study for on-line monitoring of uranium concentration in LiCl-KCl eutectic salt.” Microchemical Journal, 99. https://doi.org/10.1016/j.microc.2011.04.013.

216. Kim, B. Y., and J. il Yun. 2012. “Temperature effect on fluorescence and UV-vis absorption spectroscopic properties of Dy(III) in molten LiCl-KCl eutectic salt.” J Lumin, 132. https://doi.org/10.1016/j.jlumin.2012.06.023.

217. Nagai, T., T. Fujii, O. Shirai, and H. Yamana. 2004. “Study on redox equilibrium of UO22+/U2+ in Molten NaCl-2CsCl by uv-vis spectrophotometry.” J Nucl Sci Technol., 41. https://doi.org/10.1080/18811248.2004.9715534.

218. Nagai, T., A. Uehara, T. Fujii, O. Shirai, N. Sato, and H. Yamana. 2005. “Redox Equilibrium of U 4+ /U 3+ in Molten NaCL-2CsCL by UV-Vis Spectrophotometry and Cyclic Voltammetry.” J Nucl Sci Technol., 42. https://doi.org/10.1080/18811248.2005.9711055.

219. Schroll, C. A., A. M. Lines, W. R. Heineman, and S. A. Bryan. 2016. “Absorption spectroscopy for the quantitative prediction of lanthanide concentrations in the 3LiCl-2CsCl eutectic at 723 K.” Analytical Methods, 8. https://doi.org/10.1039/c6ay01520d.

220. Sooväli, L., E. I. Rõõm, A. Kütt, I. Kaljurand, and I. Leito. 2006. “Uncertainty sources in UV-Vis spectrophotometric measurement.” Accreditation and Quality Assurance, 11. https://doi.org/10.1007/s00769-006-0124-x.

221. Harrington, G., and B. R. Sundheim. 1960. “Absorption Spectra in Molten Salts.” Ann N Y Acad Sci., 79. https://doi.org/10.1111/j.1749-6632.1960.tb42767.x.

222. Sundheim, B. R., and J. Greenberg. 1958. “Absorption spectra of molten salts.” J Chem Phys., 28. https://doi.org/10.1063/1.1744154.

223. Kim, B. Y., and J. il Yun. 2016. “Optical absorption and fluorescence properties of trivalent lanthanide chlorides in high temperature molten LiCl-KCl eutectic.” J Lumin, 178. https://doi.org/10.1016/j.jlumin.2016.06.010.

224. Song, K., and J. W. Yeon. 2015. “Spectroscopic Studies of Lanthanides Ion in High-Temperature Molten Salt.” Appl Spectrosc, 50. https://doi.org/10.1080/05704928.2015.1054498.

225. Park, S., and J. il Yun. 2020. “An in-situ Raman spectroscopic study on potential-pO2- phase diagram of lanthanum in LiCl-KCl eutectic melt.” Journal of Rare Earths, 38. https://doi.org/10.1016/j.jre.2019.06.008.

226. Roy, S., et. al. 2021. “Unraveling Local Structure of Molten Salts via X-ray Scattering, Raman Spectroscopy, and Ab Initio Molecular Dynamics.” Journal of Physical Chemistry B, 125. https://doi.org/10.1021/acs.jpcb.1c03786.

227. Cui, R., and C. Wang. 2021. “In situ high temperature Raman and DFT analysis of cerium fluoride and oxyfluoride structures in molten FLiNaK.” Journal of Raman Spectroscopy, 52. https://doi.org/10.1002/jrs.6093.

228. Salanne, M., C. Simon, P. Turq, and P. A. Madden. 2008. “Calculation of activities of ions in molten salts with potential application to the pyroprocessing of nuclear waste.” Journal of Physical Chemistry B, 112. https://doi.org/10.1021/jp075299n.

229. Iwadate, Y., 2013. “Raman Spectroscopy and Pulsed Neutron Diffraction of Molten Salt Mixtures Containing Rare-Earth Trichlorides: Trial Approaches from Fundamentals to Pyrochemical Reprocessing.” Molten Salts Chemistry. https://doi.org/10.1016/B978-0-12-398538-5.00002-0.

230. Zhang, H., S. X. Li, and M. F. Simpson. 2022. “Testing of an Element Tracer Dilution Method for Measurement of Total Mass of Molten Salt in a Nuclear Fuel Cycle Process or Molten Salt Reactor.” Nucl Technol., 208. https://doi.org/10.1080/00295450.2021.1913031.

231. Michel, C. C., and F. R. E. Curry. 2009. “Glycocalyx volume: A critical review of tracer dilution methods for its measurement.” Microcirculation, 16. https://doi.org/10.1080/10739680802527404.

232. Olesik, J. W. 1996. “Peer Reviewed: Fundamental Research in ICP-OES and ICPMS.” Anal Chem., 68. https://doi.org/10.1021/ac962011+.

233. Tyler, G. 2001. “ICP-OES , ICP-MS and AAS Techniques Compared, Technical Note 05: ICP Optical Spectroscopy.”

234. Olesik, J. W. 1991. “Elemental analysis using ICP-OES and ICP/MS.” Anal Chem., 63. https://doi.org/10.1021/ac00001a001.

235. Bhatia, R. K., et. al. 2021. “Design and development of a compact thermal ionization mass spectrometer for isotope ratio measurement of uranium.” Rapid Communications in Mass Spectrometry, 35. https://doi.org/10.1002/rcm.8963.

236. Kim, J., J. Y. Kim, S. E. Bae, K. Song, and J. H. Park. 2021. “Review of the development in determination of 129I amount and the isotope ratio of 129I/127I using mass spectrometric measurements.” Microchemical Journal, 169. https://doi.org/10.1016/j.microc.2021.106476.

237. Sánchez Hernández, A. M., J. Horta Domenech, D. Wojnowski, and E. Zuleger. 2021. “Improvement of the 241Pu/239Pu isotope ratio measurement by thermal ionisation mass spectrometry - An approach to account for the 241Am in-growth after plutonium purification.” Int J Mass Spectrom, 468. https://doi.org/10.1016/j.ijms.2021.116660.

238. M. Wallenius, K. Mayer, Age determination of plutonium material in nuclear forensics by thermal ionisation mass spectrometry, Fresenius J Anal Chem. 366 (2000). https://doi.org/10.1007/s002160050046.

239. Aggarwal, S. K., 2016. “Thermal ionisation mass spectrometry (TIMS) in nuclear science and technology-a review.” Analytical Methods, 8. https://doi.org/10.1039/c5ay02816g.

240. Lehnert, A. L., E. D. Rothman, and K. J. Kearfott. 2016. “Improvements to an explosives detection algorithm based on active neutron interrogation using statistical modeling” J Radioanal Nucl Chem., 308. https://doi.org/10.1007/s10967-015-4452-3.

241. Whetstone, Z. D., and K. J. Kearfott. 2014. “A review of conventional explosives detection using active neutron interrogation.” J Radioanal Nucl Chem., 301. https://doi.org/10.1007/s10967-014-3260-5.

242. Lehnert, A. L., and K. J. Kearfott. 2016. “Evaluation of a flag-based explosives detection algorithm based on active neutron interrogation for use in sea land cargo containers.” J Radioanal Nucl Chem., 307. https://doi.org/10.1007/s10967-015-4187-1.

243. Whetstone, Z. D., and K. J. Kearfott. 2016. “Layered shielding design for an active neutron interrogation system.” Radiation Physics and Chemistry, 125. https://doi.org/10.1016/j.radphyschem.2016.03.018.

244. Dubi, C., A. Ocherashvilli, G. Varasano, R. Yankovich, T. Bogucarska, and B. Pedersen. 2021. “Active neutron interrogation: Experimental results from the PUNITA device.” Nucl Instrum Methods Phys Res A., 989. https://doi.org/10.1016/j.nima.2020.164933.

245. Bagi, J., L. Szentmiklosi, and Z. Hlavathy. 2012. “Detection of fissile material using cold neutron interrogation combined with neutron coincidence counting.” Nucl Instrum Methods Phys Res B., 291. https://doi.org/10.1016/j.nimb.2012.08.020.

246. Croft, S., A. Favalli, M. T. Swinhoe, B. Goddard, and S. Stewart. 2016. “The effect of deadtime and electronic transients on the predelay bias in neutron coincidence counting.” Nucl Instrum Methods Phys Res A., 814. https://doi.org/10.1016/j.nima.2016.01.022.

247. Bagi, J., et. al. 2009. “Neutron coincidence counting with digital signal processing.” Nucl Instrum Methods Phys Res A., 608. https://doi.org/10.1016/j.nima.2009.07.029.

248. Croft, S., A. Favalli, D. K. Hauck, D. Henzlova, and P. A. Santi. 2012. “Feynman variance-to-mean in the context of passive neutron coincidence counting.” Nucl Instrum Methods Phys Res A, 686. https://doi.org/10.1016/j.nima.2012.05.042.

249. Goddard, B., W. Charlton, and P. Peerani. 2014. “First principle active neutron coincidence counting measurements of uranium oxide.” Nucl Instrum Methods Phys Res A., 739. https://doi.org/10.1016/j.nima.2013.11.101.